

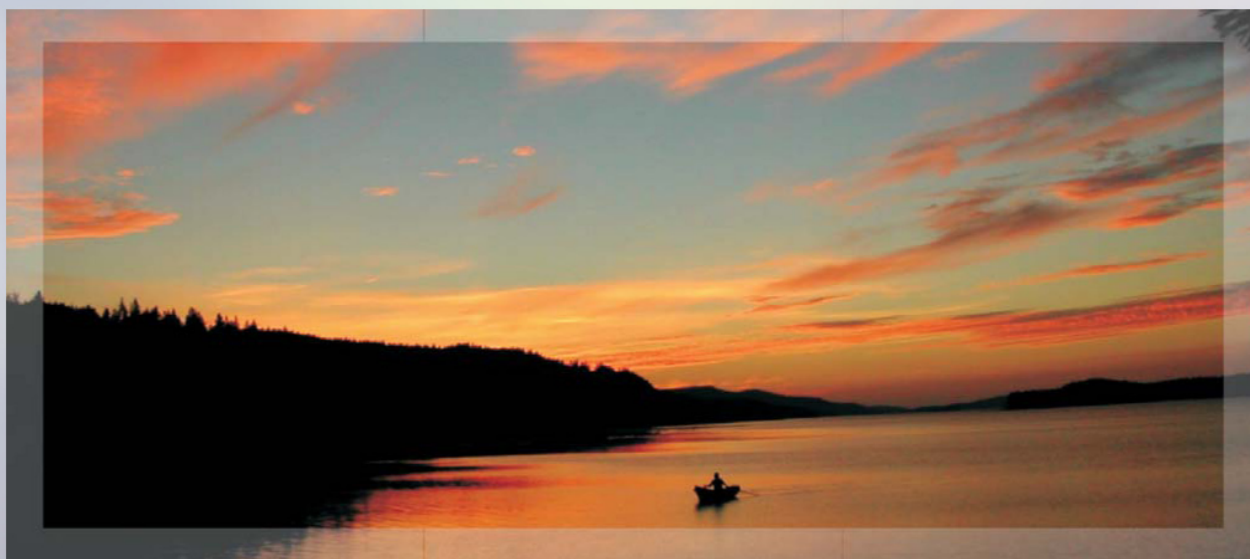
Proceedings



UNIVERSITY OF
EASTERN FINLAND

Eighth International Workshop **Nanocarbon Photonics and Optoelectronics**

31 July - 5 August, 2022, Holiday Centre Huhmari,
Polvijärvi, Finland



Joensuu, 2022

University of Eastern Finland
Institute of Photonics

Proceedings

Eighth International Workshop Nanocarbon Photonics and Optoelectronics

Holiday Centre Huhmari, Polvijärvi, Finland

Editors:
Alexander Obraztsov
Yuri Svirko

Joensuu, Finland

2022

NPO2022 Schedule-at-a-Glance

		Sunday July 31	Monday August 1	Tuesday August 2	Wednesday August 3	Thursday August 4	Friday August 5	
			2D materials	Photonics & Optoelectronics	THz Photonics	Applications & Graphene 3D		
09:	00-15		Opening				DEPARTURE	
	15-30			Shinji Yamashita	Gintaras Valušis	Fedor Jelezko		
	30-45		Andrea Ferrari					
	45-00			Zhipei Sun	Petr Obraztsov	Sergey Malykhin		
10:	00-15		Mikhail Portnoi			Lena Golubewa		
	15-30			Hamza Rehman	Timofei Eremin	Yaraslau Padrez		
10:30-11:00			Coffee Break					
11:	00-15							LEGEND
	15-30		Dmitri Golberg	Albert Nasibulin	Georgy Fedorov	Antonio Mafucci		
	30-45				Dmitry Lyubchenko			
	45-00					Gaia Tomasello		
12:	00-15		Serim Ilday	Geza Mark	Kou Li			
12:15-14:45			Lunch					
14:	45-00	ARRIVAL			Anna Tasolamprou	Rumiana Kotsilkova	45 min lecture	
15:	00-15		Mikhail Portnoi	Antonio Di Bartolomeo			30 min invited talk	
	15-30				Alexey Basharin	Polina Kuzhir	15 min talk	
	30-45		Andy Wild				ANTICARBI	
	45-00		Lena Golubewa	Ömer Ilday	Anar Ospanova	Marino Lavorgna	Graphene 3D project	
16:00-16:30				Coffee Break				
16:	30-45		Kuniaki Konishi	Peter Kazansky	Eros Mariani	Patrizia Lamberti		
	45-00							
17:	00-15		Feodor Ogrin			Ricardo Andrade		
	15-30				Patrizia Lamberti	Evgeni Ivanov		
	30-45		Andreas Norrman	Junji Yumoto		Hamza Rehman		
	45-00				Natalia Alexeeva	Natia Jalagonia		
18:00-19:30		Dinner	Welcome Dinner	Dinner	Dinner	NPO2022 reception & Höytiäinen cruise		
19:30-21:00				Poster Session	Graphene 3D Poster Session			

Workshop Co-Chairs

Prof. Alexander Obraztsov

Prof. Yuri Svirko

Head of the Program Committee

Prof. Polina Kuzhir

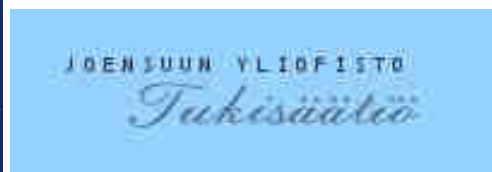
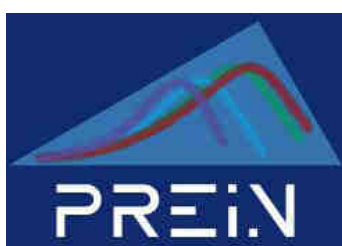
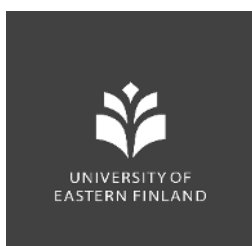
Organizing Committee

Mrs. Hannele Karppinen

Mr. Timofei Eremin

Prof. Yuri Svirko

NPO2022 Sponsor Organisations



ISBN: 978-952-61-4586-0

Welcome to NPO2022

We are pleased to welcome you to the 8th International Workshop on Nanocarbon Photonics and Optoelectronics (NPO2022) that continues a series of meetings organized by the University of Eastern Finland. Since 2008, NPO Workshops have been bringing together research leaders from both academia and industry to discuss the latest achievements in this rapidly developing area of modern physics and nanotechnology, with a strong focus on new carbon nanomaterials. We hope that you will enjoy both the scientific and the social program of NPO2022.

The NPO2022 Workshop publication will appear in a special issue of *physica status solidi (b)* – basic solid state physics. Guest Editors of the special issue are Alexander Obraztsov and Yuri Svirko. Workshop participants will be invited to contribute.

Despite the COVID-19 pandemic and ongoing travel restrictions NPO2022 has attracted sixty researchers and students from around the globe. We are very grateful to all participants for taking part in the Workshop. We also thank our sponsors for their financial backing, which has allowed us to support our lecturers and students.

We hope that the NPO2022 will expand on the success of previous Workshops, while the magnificent scenery will allow all participants to enjoy the beauty of the Finnish Lakeland.

Alexander Obraztsov
Yuri Svirko
NPO2022 Co-Chairs

Contents

Monday, August 1	1
9:15-10:00 Layered quantum materials: characterization and applications Andrea Ferrari, <i>Cambridge Graphene Centre, University of Cambridge, Cambridge, UK</i> . . .	3
10:00-10:30 Terahertz emission from photoexcited carbon nanostructures R. R. Hartmann ¹ and M. E. Portnoi ² , ¹ <i>Physics Department, De La Salle University, Manila, Philippines;</i> ² <i>Physics and Astronomy, University of Exeter, Exeter, United Kingdom</i>	4
11:00-11:45 Nanoengineering and electrochemical probing of carbon nanostructures in TEM Dmitri V. Golberg, <i>School of Chemistry and Physics and Centre for Material Science, Queensland University of Technology (QUT), Brisbane, Australia</i>	5
11:45-12:15 Disordered hyperuniform configurations from artificial atoms to exotic 2D materials Ü. Selem Nizam ^{1,2} , Sercan Hüsnügil ³ , Muhammed H. Güneş ³ , Danial Vahabli ⁴ , Michaël Barbier ¹ , Ghaith Makey ^{1,3} , Yusuf Özer ³ , Serim Ilday ¹ , ¹ <i>UNAM-National Nanotechnology Research Center & Institute of Materials Science and Nanotechnology, Bilkent University, Ankara, Turkey;</i> ² <i>Department of Physics, Boğaziçi University, Istanbul, Turkey;</i> ³ <i>Department of Physics, Bilkent University, Ankara, Turkey;</i> ⁴ <i>Department of Physics, Middle East Technical University, Ankara, Turkey</i>	6
14:45-15:30 Momentum alignment of photoexcited carriers in lowdimensional Dirac materials R. R. Hartmann ¹ , V. A. Saroka ^{2,3} and M. E. Portnoi ² , ¹ <i>Physics Department, De La Salle University, Manila, Philippines;</i> ² <i>Physics and Astronomy, University of Exeter, Exeter, United Kingdom;</i> ³ <i>Institute for Nuclear Problems, Belarusian State University, Minsk, Belarus</i> . . .	7
15:30-15:45 Optics of two-dimensional materials hosting tilted Dirac cones A. Wild, E. Mariani and M. E. Portnoi, <i>Physics and Astronomy, University of Exeter, Exeter, United Kingdom</i>	8
15:45-16:00 All-optical pH sensing with hybrid sp²-sp³ carbon nanostructures Lena Golubewa ¹ , Yaroslau Padrez ¹ , Renata Karpicz ¹ , Tatsiana Kulahava ¹ , Olga Levinson ² , Polina Kuzhir ³ , ¹ <i>Department of Molecular Compound Physics, Center for Physical Sciences and Technology, Lithuania;</i> ² <i>Ray Techniques Ltd., Israel;</i> ³ <i>Department of Physics and Mathematics, Institute of Photonics, University of Eastern Finland, Finland</i>	9
16:30-17:00 Generating THz Pulses with Longitudinal Electromagnetic Field Kuniaki Konishi, <i>Institute for Photon Science and Technology, The University of Tokyo</i> . . .	10
17:00-17:30 Extreme non-linearity in ferrites: from microwave to THz Feodor Y. Ogrin, <i>MaxLLG Ltd. Exeter, United Kingdom</i>	11
17:30-18:00 Complementarity in vectorial quantum light interference Andreas Norrman, <i>Institute of Photonics, University of Eastern Finland, Joensuu, Finland</i> .	12
Tuesday, August 2	13
9:00-09:45 Advances of ultrashort-pulse fiber lasers using nanocarbon-based saturable absorbers Shinji Yamashita, <i>Research Center for Advanced Science and Technology, The University of Tokyo, Tokyo, Japan</i>	15
9:45-10:15 Enhancement of Optical Nonlinearities in 2D Materials Zhipei Sun, <i>Department of Electronics and Nanoengineering, Aalto University, Finland & QTF Centre of Excellence, Department of Applied Physics, Aalto University, Finland</i>	16

10:15-10:30	Influence of the surface roughness of graphene-based biosensing platforms for the living cells functional state monitoring Hamza Rehman ¹ , Lena Golubewa ² , ¹ <i>Institute of Photonics, University of Eastern Finland, Joensuu, Finland</i> ; ² <i>Center for Physical Sciences and Technology, Vilnius, Lithuania</i>	17
11:00-11:45	SWCNT Transparent Conducting Films: Towards the Theoretical Limit Albert G. Nasibulin ^{1,2} , ¹ <i>Skolkovo Institute of Science and Technology, Moscow, Russia</i> ; ² <i>Aalto University, Department of Materials Science and Engineering, Aalto, Finland</i>	18
11:45-12:15	Transport properties of TMDC materials Géza I. Márk, Péter Vancsó, Péter Nemes-Incze, <i>Institute for Technical Physics and Materials Science, Centre for Energy Research, Budapest, Hungary</i>	19
14:45-15:30	2D materials in transistors, memories, and phototransistors Antonio Di Bartolomeo ^{1,2} , Enver Faella ^{1,2} , Filippo Giubileo ² , Arun Kumar ¹ , Aniello Pelella ^{1,2} , ¹ <i>Physics Department “E.R. Caianiello”, University of Salerno, Fisciano, Salerno, Italy</i> ; ² <i>CNR-SPIN, Fisciano, Salerno, Italy</i>	20
15:30-16:00	Self-organized patterning and functionalization of surfaces through Nonlinear Laser Lithography Y. Özgün ¹ , Abdullah bin Aamir ² , Sezin Galioğlu ³ , Serim Ilday ³ , F. Ömer Ilday ^{1,2,3} , ¹ <i>Department of Electrical Engineering, Bilkent University, Ankara, Turkey</i> ; ² <i>Department of Physics, Bilkent University, Ankara, Turkey</i> ; ³ <i>UNAM-National Nanotechnology Research Center & Institute of Materials Science and Nanotechnology, Bilkent University, Ankara, Turkey</i> ;	21
16:30-17:15	The science and art of ultrafast laser writing P.G. Kazansky, <i>Optoelectronics Research Centre, University of Southampton, UK</i>	22
17:15-18:00	Broadband THz anti-reflection moth-eye structures formed by femtosecond laser processing Junji Yumoto, <i>Institute for Photon Science and Technology & Department of Physics School of Science, The University of Tokyo, Tokyo, Japan</i>	23

Poster session I

25

P1	Multi-layered 3D imaging with CNTs broadband photo-sensors Y. Kinoshita ¹ , K. Li ^{2,3} , Y. Kawano ¹⁻⁴ , ¹ <i>Faculty of Science and Engineering, Chuo University, Tokyo, Japan</i> ; ² <i>Department of Electrical and Electronic Engineering, Tokyo Institute of Technology, Tokyo, Japan</i> ; ³ <i>Laboratory for Future Interdisciplinary Research of Science and Technology, Tokyo Institute of Technology, Tokyo, Japan</i> ; ⁴ <i>National Institute of Informatics, Tokyo, Japan</i>	27
P2	An all-printable CNT film-type photo-thermoelectric imager Daiki Sakai ¹ , Satsuki Yasui ^{2,3} , Kou Li ^{2,3} , Yukio Kawano ¹⁻⁴ , ¹ <i>Department of Science and Engineering, Chuo University, Tokyo, Japan</i> ; ² <i>Laboratory for Future Interdisciplinary Research of Science and Technology, Tokyo Institute of Technology, Tokyo, Japan</i> ; ³ <i>Department of Electrical and Electronic Engineering, Tokyo Institute of Technology, Tokyo, Japan</i> ; ⁴ <i>National Institute of Informatics, Tokyo, Japan</i>	28
P3	Fluorescence dynamics in heterostructured trans-stilbene Renata Karpicz ¹ , Gabrielė Kareivaitė ¹ , Mindaugas Mačernis ² , Darius Abramavičius ² , Leonas Valkūnas ^{1,2} , ¹ <i>Center for Physical Sciences and Technology, Vilnius, Lithuania</i> ; ² <i>Institute of Chemical Physics, Faculty of Physics, Vilnius University, Vilnius, Lithuania</i>	29
P4	Bottom-up approach for synthesis of structured diamond films M. Quarshie ¹ , S. Malykhin ¹ , P. Kuzhir ¹ , ¹ <i>Department of Physics and Mathematics, University of Eastern Finland, Joensuu, Finland</i>	30
P5	Spectroscopic characterization of nanodiamonds with sp²-sp³ graphene-like shell Yaraslau Padrez ¹ , Lena Golubewa ¹ , Tatsiana Kulahava ¹ , Boris Zousman ² , Olga Levinson ² , Renata Karpicz ¹ and Polina Kuzhir ³ , ¹ <i>State research institute Center for Physical Sciences and Technology, Vilnius, Lithuania</i> ; ² <i>Ray Techniques Ltd., Israel</i> ; ³ <i>University of Eastern Finland, Joensuu, Finland</i>	31

P6	Random graphene metasurfaces as a perfect broadband THz absorber Isaac Appiah Otoo ¹ , Andrey Novitsky ² , Alesia Paddubskaya ² , Markku Pekkarinen ¹ , Yuri Svirko ¹ , Polina Kuzhir ¹ , ¹ <i>Institute of Photonics, University of Eastern Finland, Joensuu, Finland</i> ; ² <i>Independent researcher</i>	32
P7	Terahertz imaging of optically modulated graphene layers Rusnė Ivaškevičiūtė-Povilauskienė ¹ , A. Paddubskaya ² , D. Seliuta ¹ , D. Jokubauskis ¹ , L. Minkevičius ¹ , A. Urbanowicz ¹ , I. Matulaitienė ¹ , L. Mikoliūnaitė ¹ , P. Kuzhir ³ , Natalia Alexeeva ¹ and G. Valušis ¹ , ¹ <i>Center for Physical Sciences and Technology, Vilnius, Lithuania</i> ; ² <i>Institute for Nuclear Problems of Belarusian State University, Minsk, Belarus</i> ; ³ <i>University of Eastern Finland, Joensuu, Finland</i>	33
P8	Single-walled carbon nanotubes defected by ion beams Valentina A. Eremina ¹ , Petr A. Obraztsov ¹ , Yuri P. Svirko ¹ , Elena D. Obraztsova ^{1,2} , ¹ <i>University of Eastern Finland, Joensuu, Finland</i> ; ² <i>General Physics Institute RAS, Moscow, Russia</i>	34
Wednesday, August 3		35
09:00-09:45	Terahertz beam engineering in imaging: from designs to applications Linas Minkevičius, Domas Jokubauskis, Rusnė Ivaškevičiūtė-Povilauskienė, Irmantas Kašalynas, Natalia Alexeeva, Andzej Urbanowicz, and Gintaras Valušis, <i>Optoelectronics Department, Center for Physical Sciences and Technology, Vilnius, Lithuania</i>	37
09:45-10:15	Hybrid perovskites based photoconductive THz pulse emitters and detectors Petr A. Obraztsov ^{1,2} , Pavel A. Chizhov ² , Dmitry S. Gets ³ , Vladimir V. Bukin ² , Olga I. Semenova ⁴ , Sergey V. Makarov ³ , ¹ <i>Institute of Photonics, University of Eastern Finland, Joensuu, Finland</i> ; ² <i>Prokhorov General Physics Institute of RAS, Moscow, Russia</i> ; ³ <i>Department of Physics and Engineering, ITMO University, St. Petersburg, Russia</i> ; ⁴ <i>Rzhanov Institute of Semiconductor Physics, Novosibirsk, Russia</i>	38
10:15-10:30	Protonation of oxygen doped single-walled carbon nanotubes Timofei V. Eremin ¹ , Petr A. Obraztsov ¹ , Elena D. Obraztsova ^{1,2} , ¹ <i>University of Eastern Finland, Joensuu, Finland</i> ; ² <i>General Physics Institute RAS, Moscow, Russia</i>	39
11:00-11:30	Detection of terahertz radiation with graphene-based plasmonic interferometers G. Fedorov, D. Bandurin I. Gayduchenko, Y. Matyushkin, M. Moskotin, S. Ganichev, D. Svin'tsov, G. Goltsman, <i>Moscow Institute of Physics and Technology (State University), Dolgoprudny, Russia</i> ; <i>Massachusetts Institute of Technology, Cambridge, USA</i> ; <i>Physics Department, Moscow State University of Education (MSPU), Moscow, Russian Federation</i> ; <i>Terahertz Centre, University of Regensburg, Regensburg, Germany</i>	40
11:30-12:00	Ultra-wideband graphene-based absorbers for THz integrated waveguide systems Nikolaos Xenidis ^a , James Champion ^{a,c} , Serguei Smirnov ^a , Aleksandra Przewłoka ^{b,d} , Aleksandra Krajewska ^b , Piotr A. Drozd ^b , Albert Nasibulin ^{d,e} , Joachim Oberhammer ^a , Dmitri Lioubtchenko ^{a,b} , ^a <i>KTH Royal Institute of Technology, Stockholm, Sweden</i> ; ^b <i>CENTERA Laboratories, Institute of High Pressure Physics PAS, Warsaw, Poland</i> ; ^c <i>TeraSi AB, Stockholm, Sweden</i> ; ^d <i>Institute of Optoelectronics, Military University of Technology, Warsaw, Poland</i> ; ^e <i>Department of Chemistry and Materials Science, Aalto University, Finland</i> ; ^f <i>Skolkovo Institute of Science and Technology, Russia</i>	41
12:00-12:15	A mechanically stretchable and optically broadband imager sheet Kou Li ^{1,2} , Yukio Kawano ^{1,4} , ¹ <i>Laboratory for Future Interdisciplinary Research of Science and Technology, Tokyo Institute of Technology, Tokyo, Japan</i> ; ² <i>Department of Electrical and Electronic Engineering, School of Engineering, Tokyo Institute of Technology, Tokyo, Japan</i> ; ³ <i>Department of Electrical, Electronic, and Communication Engineering, Faculty of Science and Engineering, Chuo University, Tokyo, Japan</i> ; ⁴ <i>National Institute of Informatics, Tokyo, Japan</i>	42
14:45-15:15	THz graphene-based metasurfaces for wave manipulation Anna C. Tasolamprou ¹ , Maria Kafesaki ^{1,2} , ¹ <i>Institute of Electronic Structure and Laser, Foundation for Research and Technology Hellas, Heraklion, Crete, Greece</i> ; ² <i>Department of Materials Science and Technology, University of Crete, Heraklio, Greece</i>	43
15:15-15:45	Metamaterials beyond common multipoles Alexey Basharin, <i>Institute of Photonics, University of Eastern Finland, Joensuu, Finland</i>	44

15:45-16:00	Transmission properties of self-complementary metamaterials via Babinet principle Anar Ospanova, <i>Institute of Photonics, University of Eastern Finland, Joensuu, Finland</i> . . .	45
16:30-17:15	Dirac light Eros Mariani, C.-R. Mann, W.L. Barnes, S.A.R. Horsley, T. Sturges and G. Weick, <i>Department of Physics and Astronomy, University of Exeter, Exeter, UK</i>	46
17:15-17:45	Sensitivity analysis on the performance of THz nanocarbon-based passive devices P. Lamberti, M. La Mura, V. Tucci, <i>Dept. of Information and Electrical Eng. and Applied Math., University of Salerno, Fisciano (SA), Italy</i>	47
17:45-18:00	CVD graphene transfer: alcohol/water solvent for improved removal of PMMA with polarity modified under DUV exposure Natalia Alexeeva ¹ , Justinas Jorudasa ¹ , Daniil Pashneva ¹ , Ilja Ignatjev ² , Gediminas Niaura ² , Irmantas Kašalynasa ¹ , ¹ <i>Department of Optoelectronics, Center for Physical Sciences and Technology, Vilnius, Lithuania</i> ; ² <i>Department of Organic Chemistry, Center for Physical Sciences and Technology, Vilnius, Lithuania</i>	48
Thursday, August 4		49
09:00-09:45	Diamond based quantum sensing and imaging Fedor Jelezko, <i>Institute of Quantum optics, Ulm University, Germany</i>	51
09:45-10:00	CVD synthesis of diamond needles with controlled charge state of NV centers S. A. Malykhin ¹ , M. D. Lazareva ² , R. R. Ismagilov ² , A. N. Obraztsov ^{1,2} , ¹ <i>Department of Physics and Mathematics, University of Eastern Finland, Joensuu, Finland</i> ; ² <i>Department of Physics, Lomonosov Moscow State University, Moscow, Russia</i>	52
10:00-10:15	All-optical pH sensing with hybrid sp²-sp³ carbon nanostructures Lena Golubewa ¹ , Yaraslau Padrez ¹ , Renata Karpicz ¹ , Tatsiana Kulahava ¹ , Olga Levinson ² , Polina Kuzhir ³ , ¹ <i>Department of Molecular Compound Physics, Center for Physical Sciences and Technology, Lithuania</i> ; ² <i>Ray Techniques Ltd., Israel</i> ; ³ <i>Department of Physics and Mathematics, Institute of Photonics, University of Eastern Finland, Finland</i>	53
10:15-10:30	Temperature-dependent fluorescence of SiV and NV color centers in micron-sized single crystal diamond needles Yaraslau Padrez ¹ , Lena Golubewa ¹ , Sergei Malykhin ³ , Tatsiana Kulahava ² , Renata Karpicz ¹ , Alexander Obraztsov ³ , Yuri Svirko ³ and Polina Kuzhir ³ , ¹ <i>State research institute Center for Physical Sciences and Technology, Vilnius, Lithuania</i> ; ² <i>Institute for nuclear problems of Belarusian state university, Minsk</i> ; ³ <i>University of Eastern Finland, Joensuu, Finland</i>	54
11:00-11:30	Using nanomaterials and machine learning for advanced sensing applications Antonio Maffucci, <i>Dept. of Electrical and Information Engineering, Univ. of Cassino and Southern Lazio, Cassino, Italy</i>	55
11:30-12:15	Scientific publishing within the new “Open Science” world: how to write for high-impact factor journals Gaia Tomasello, <i>Associate Editor, Materials Science and Physics Department at Wiley-VCH</i>	56

Graphene 3D project Symposium

57

14:45-15:15	Biopolymer-graphene nanocomposites: properties, applications and safety issues R. Kotsilkova ¹ , E. Ivanov ^{1,2} , T. Batakliov ^{1,2} , V. Georgiev ^{1,2} , D. Menseidov ¹ , S. Kotsilkov ¹ , ¹ <i>Institute of Mechanics, Bulgarian Academy of Sciences, Sofia, Bulgaria</i> ; ² <i>NanoTechLab Ltd., Sofia, Bulgaria</i>	59
15:15-15:45	3D printing for terahertz absorbers Polina Kuzhir, <i>Institute of Photonics, Department of Physics and Mathematics, University of Eastern Finland</i>	60
15:45-16:00	Innovative nanocomposites for 3D printing: the effect of carbonaceous fillers segregated morphology on structural and functional properties M. Lavorgna ^{a,e} , C. Santillo ^a , A.P. Godoy ^b , A. Ronca ^{a,e} , G. Rollo ^{a,e} , R.J. Espanhol Andrade ^b , R.K. Donato ^c , G. Fei ^d , G.G. Buonocore ^a , H. Xia ^{d,a} , ^a <i>Institute for Polymers, Composites</i>	

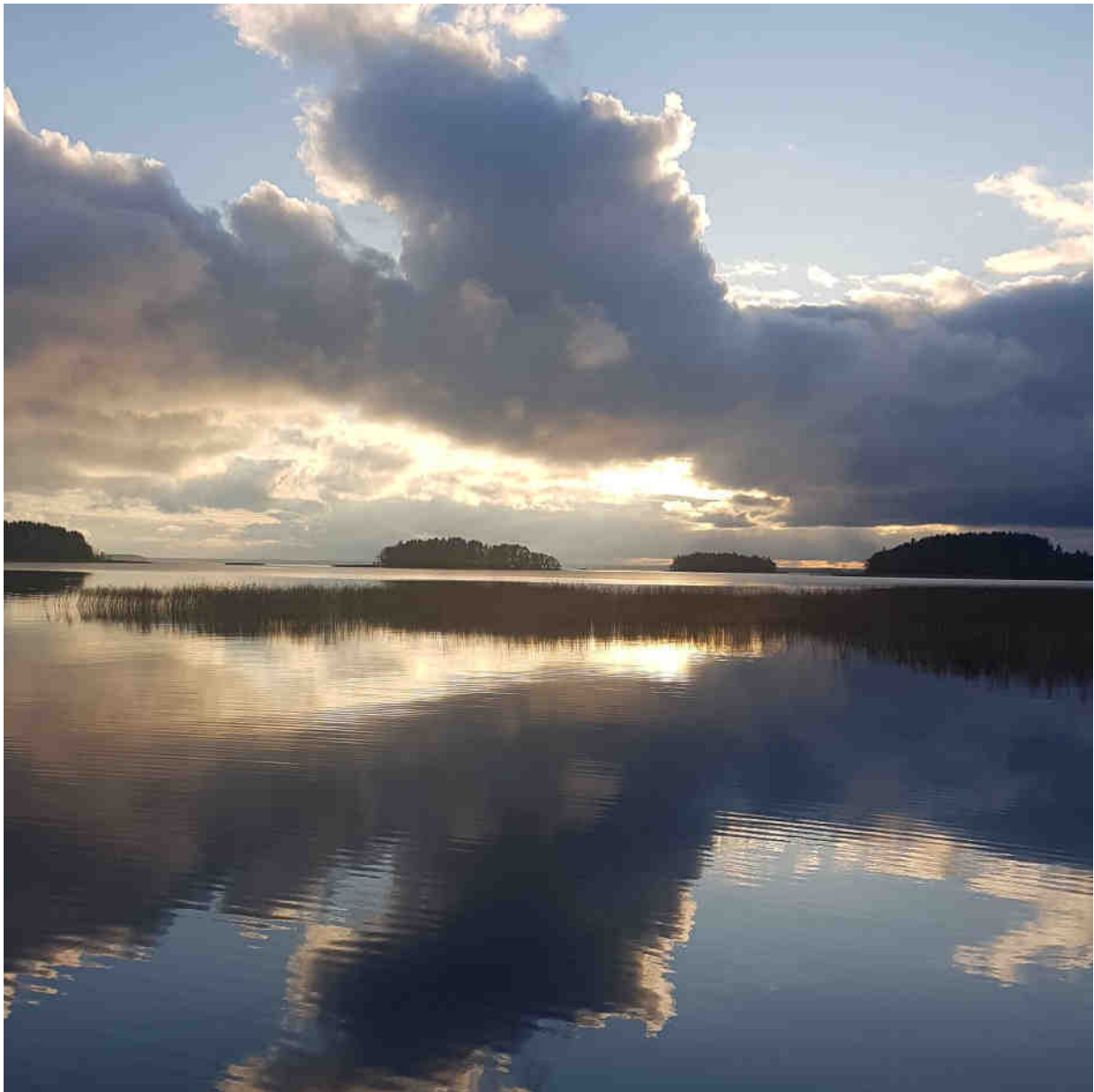
	<i>and Biomaterials-CNR, Italy; ^bMackGrappe, Mackenzie University, São Paulo, SP, Brazil; ^cCentre for Advanced 2D Materials, National University of Singapore, Singapore; ^dPolymer research Institute, Sichuan University, Chengdu, China; ^eInstitute for Polymers, Composites and Biomaterials-CNR, Lecco, Italy)</i>	61
16:30-17:00	Robust design of multifunctional nanocomposites suitable for additive manufacturing of electrical devices P. Lamberti ^{1,2} , M. La Mura ¹ , V. Tucci ^{1,2} , ¹ Dept. of Information and Electrical Eng. and Applied Math., University of Salerno, Fisciano (SA), Italy; ² NANO_MATES (Research Centre for Nanomaterials and Nanotechnology at the University of Salerno), University of Salerno	62
17:00-17:15	Influence of annealing induced phase separation on the shape memory effect of graphene based thermoplastic polyurethane nanocomposites Fernanda Cabrera Flores Valim ^{a,d} ; Gustavo Peixoto Oliveira ^a ; Gibran da Cunha Vasconcelos ^b ; Leice Gonçalves Amurin ^c ; Lucilene Betega de Paiva ^d ; Chiara Santillo ^e , Marino Lavorgna ^e , Ricardo Jorge Espanhol Andrade ^a , ^a Mackgrappe - Mackenzie Institute for Research in Graphene and Nanotechnologies, Mackenzie Presbyterian Institute, São Paulo, Brazil; ^b Institute for Technological Research (IPT) – Lightweight Structures Laboratory (LEL), São Paulo, Brazil; ^c Center of Technology in Nanomaterials (CTNano) at Federal University of Minas Gerais (UFMG), Belo Horizonte, Minas Gerais, Brazil; ^d Institute for Technological Research (IPT) – Laboratory of Chemical Processes and Particle Technology, Group for Bio-nanomanufacturing (BIONANO), São Paulo, Brazil; ^e Institute of Polymers, Composites and Biomaterials (IPCB-CNR), Portici (NA), Italy	63
17:15-17:30	Influence of the type and combination of carbon nanofillers on the nanomechanical properties of PLA-based nanocomposites Evgeni Ivanov ^{1,2} , Todor Batakliiev ^{1,2} , Rumiana Kotsilkova ¹ , ¹ Open Laboratory on Experimental Micro and Nano Mechanics (OLEM), Institute of Mechanics, Bulgarian Academy of Sciences, Sofia ² Research and Development of Nanomaterials and Nanotechnologies (NanoTech Lab Ltd.), Sofia, Bulgaria	64
17:30-17:45	Fragmented graphene on dielectric substrate for THz applications Hamza Rehman ¹ , Lena Golubewa ² , Alexey Basharin ¹ , Andzej Urbanovic ² , Erkki Lahderanta ³ , Ekaterina Soboleva ³ , Ieva Matulaitiene ² , Marija Jankunec ⁴ , Yuri Svirko ¹ , Polina Kuzhir ¹ , ¹ Institute of Photonics, University of Eastern Finland, Joensuu, Finland; ² Center for Physical Sciences and Technology, Vilnius, Lithuania; ³ Lappeenranta-Lahti University of Technology LUT, Lappeenranta, Finland; ⁴ Institute of Biochemistry, Life Sciences Center, Vilnius University, Vilnius, Lithuania	65
17:45-18:00	Electromagnetic wave absorber RGO/PDMS polymer nanocomposite Natia Jalagonia ^{1,2} , Tinatin Kuchukhidze ¹ , Nino Darakhvelidze ¹ , Ekaterine Sanaia ¹ , Guram Bokuchava ¹ , Badri Khvitia ¹ , ¹ Ilia Vekua Sukhumi Institute of Physics and Technologies, Tbilisi, Georgia; ² Institute of Macromolecular Chemistry and Polymeric Materials, Ivane Javakhishvili Tbilisi State; University, Tbilisi, Georgia	66

Graphene 3D project Symposium Poster Session

		67
P9	Graphene electro-optic modulators on silicon nitride waveguides I. Reduto ¹ , M. Roussey ¹ , P. Mustonen ² , Z. Sun ² , H. Lipsanen ² , and S. Honkanen ¹ , ¹ Institute of Photonics, University of Eastern Finland, Joensuu, Finland; ² Department of Electronics and Nanoengineering, Aalto University, Aalto, Finland	69
P10	Electrical properties of composites of poly (lactic) acid and polyvinylidene difluoride with carbon fillers Dzhihan Menseidov, Institute of Mechanics at the Bulgarian Academy of Sciences, Sofia, Bulgaria	70
P11	Back to the future with nanocarbon composite polymers Paolo Ciambelli ^{1,2} , Giuseppe De Filippis ¹ , Antonio Di Grazia ¹ , ¹ Narrando, Fisciano, Italia; ² University of Salerno, Fisciano, Italia	71

P12	Effect of carbon nanofillers on the permeability, conductive and nanomechanical properties of PLA-based composites films C. Santillo ¹ , G.G. Buonocore ¹ , R. Di Maio ¹ , M. Lavorgna ¹ , E. Ivanov ^{2,3} , T. Batakaliyev ² , R. Kotsilkova ² , ¹ National Research Council of Italy, Institute for Polymers, Composites and Biomaterials, Portici, Naples, Italy; ² Open Laboratory on Experimental Micro and Nano Mechanics (OLEM), Institute of Mechanics, Bulgarian Academy of Sciences, Sofia, Bulgaria; ³ Research and Development of Nanomaterials and Nanotechnologies (NanoTech Lab Ltd.), Sofia, Bulgaria)	72
P13	Multifunctional porous conductive TPU/carbon-based system 3D printed for piezoresistive sensors G. Rollo ^{1,2} , R. Di Maio ¹ , A. T. Silvestri ^{1,3} , A. Ronca ^{1,2} , H. Xia ^{4,1} , M. Lavorgna ^{1,2} , ¹ National Research Council of Italy, Institute for Polymers, Composites and Biomaterials, Portici, Naples, Italy; ² National Research Council of Italy, Institute for Polymers, Composites and Biomaterials, Lecco, Italy; ³ University of Naples Federico II., Naples, Italy; ⁴ State Key Laboratory of Polymer Materials Engineering, Polymer Research Institute, Sichuan University, Chengdu, China;	73
P14	Production of reduced graphene oxide for potential industrial graphene nanocomposite manufacture Natia Jalagonia ^{1,2} , Tinatin Kuchukhidze ¹ , Nino Darakhvelidze ¹ , Ekaterine Sanaia ¹ , Guram Bokuchava ¹ , Badri Khvitia ¹ , Leila Kalatozishvili ^{1,2} , ¹ Ilia Vekua Sukhumi Institute of Physics and Technologies, Tbilisi, Georgia; ² Institute of Macromolecular Chemistry and Polymeric Materials, Ivane Javakhishvili Tbilisi State University, Georgia	74
P15	Synthesis of highly amorphous polyvinyl/alcohol reduced graphene oxide nanocomposite with promising electrical percolation threshold R. Adami ¹ , P. Lamberti ^{2,3} , M. Casa ⁴ , N. D'Avanzo ² , M. Sarno ^{1,3} , D. Bychanok ⁶ , P. Kuzhir ⁷ , C. Yu ⁸ , H.Xia ⁸ , P. Ciambelli ⁴ , ¹ Department of Physics, University of Salerno; ² Department of Information and Electrical Engineering and Applied Mathematics, University of Salerno; ³ Centre NANO_MATES, University of Salerno; ⁴ Narrando srl, Fisciano (SA), Italy; ⁶ Research Institute for Nuclear Problems Belarusian State University (Belarus); ⁷ Dept. of Physics and Mathematics, University of Eastern Finland (Finland); ⁸ State Key Lab of Polymer Material Engineering, Sichuan University, Chengdu, Sichuan, P.R. China	75
P16	Graphene enhanced free-standing silicon anapole-type metasurface I. Appiah Otoo ¹ , A. Basharin ¹ , P. Karvinen ¹ , D. Pashnev ² , I. Kasalynas ² , H. Rehman ¹ , Y. Svirko ¹ , and P. Kuzhir ¹ , ¹ Institute of Photonics, University of Eastern Finland, Joensuu, Finland; ² Terahertz photonics laboratory, Center for Physical Sciences and Technology (FTMC), Vilnius, Lithuania	76
Author index		77

Monday, August 1



Layered Quantum Materials: Characterization and Applications

Andrea C. Ferrari

*Cambridge Graphene Centre, University of Cambridge, Cambridge CB3 0FA,
UK acf26@cam.ac.uk*

Layered Materials (LMs) have potential for quantum technologies, as scalable sources of single photon emitters (SPEs) [1,2]. LM heterostructures can be built with tuneable properties depending on the constituent materials and their relative crystallographic orientation [3,4]. Quantum emitters in LMs hold potential in terms of scalability, miniaturization, integration. Generation of quantum emission from the recombination of indirect excitons in heterostructures made of different LMs is a path with enormous potential. I will discuss how LM combinations can be used to generate SPEs and confinement of interlayer excitons [5].

- [1] C. Palacios-Berraquero et al., Nat. Commun. 8, 15093 (2017)
- [2] C. Palacios-Berraquero, et al., Nat. Commun. 7, 12978 (2016)
- [3] P. Rivera et al., Nat. Nanotech. 13,1004 (2018)
- [4] M. Barbone et al. Nat. Commun 9, 3721 (2018)
- [5] A. R. P. Montblanch et al. Commun Phys. 4, 119 (2021)

Terahertz emission from photoexcited carbon nanostructures

R. R. Hartmann¹ and M. E. Portnoi²

¹*Physics Department, De La Salle University, 2401 Taft Avenue, 0922 Manila, Philippines*

²*Physics and Astronomy, University of Exeter, Stocker Road, Exeter EX4 4QL, United Kingdom
m.e.portnoi@exeter.ac.uk*

One of the recent trends in bridging the terahertz (THz) gap in electromagnetic spectrum is to use carbon-based nanostructures [1]. Following our earlier work on narrow-gap carbon nanotubes and graphene nanoribbons [2], as well as graphene bipolar waveguides [3] and double quantum wells [4], we consider terahertz (THz) transitions in two other types of nanocarbons – carbynes and cyclocarbons.

The technology of synthesizing carbynes (also known as linear acetylenic or polyyne carbons) has evolved rapidly over the last few years [5], with stable long chains deposited on substrates now being a reality. A prominent feature of long polyyne chains (chains with two alternating non-equal bonds) is the presence of topologically protected mid-gap edge states. For a finite-length chain the two edge states form an even and odd combination with the energy gap proportional to the edge-state overlap due to tunneling. These split states of different parity support strong dipole transitions. We have shown [6] that for long enough (over 18 atoms) carbyne chains, the energy separation between the HOMO and LUMO molecular orbitals formed by the edge states corresponds to the THz frequency range. There are several other allowed optical transitions in this system which can be used to maintain inversion of population required for THz lasing.

Another recent achievement in nanocarbon technology is a demonstration of controlled synthesis of cyclocarbons, in particular cyclo[18]carbon allotrope [7]. The properties of cyclocarbons in an external electric field differ drastically depending on the parity of the number of dimers in a polyyne ring. This is a direct consequence of breaking the inversion symmetry in a ring consisting of an odd number of dimers, including the famous C₁₈. Our estimates [8] show that adding just one extra carbon dimer to C₁₆ is equivalent to placing this molecule in an external magnetic field of 10^4 T. For an odd-dimer cyclocarbon, as a result of the inversion symmetry absence, an experimentally attainable electric field should open a tunable gap between otherwise degenerate states leading to two states with allowed dipole transitions between them in the THz range. A population inversion can be achieved again using optical pumping.

Acknowledgement

This work was supported by the EU H2020-MSCA-RISE projects TERASSE (H2020-823878) and DiSeTCom (H2020-823728) and by the NATO Science for Peace and Security project NATO.SPS.MYP.G5860.

References

- [1] R. R. Hartmann, J. Kono and M. E. Portnoi, *Nanotechnology*, **25**, 322001 (2014).
- [2] R. R. Hartmann, V. A. Saroka and M. E. Portnoi, *J. Appl. Phys.*, **125**, 124303 (2019).
- [3] R. R. Hartmann and M. E. Portnoi, *Phys. Rev. B*, **102**, 155421 (2020).
- [4] R. R. Hartmann and M. E. Portnoi, *Phys. Rev. B*, **102**, 052229 (2020).
- [5] S. Kutrovskaya, A. Osipov, S. Baryshev, A. Zasedatelev, V. Samyshkin, S. Demirchyan, O. Pulci, D. Grassano, L. Gontrani, R. R. Hartmann, M. E. Portnoi, A. Kucherik, P. G. Lagoudakis and A. V. Kavokin, *Nano Lett.*, **20**, 6502 (2020).
- [6] R. R. Hartmann, S. Kutrovskaya, A. Kucherik, A. V. Kavokin and M. E. Portnoi, *Physical Review Research*, **3**, 033202 (2021).
- [7] K. Kaiser, L. M. Scriven, F. Schulz, P. Gaweł, L. Gross and H. L. Anderson, *Science*, **365**, 1299 (2019).
- [8] R. A. Ng, M. E. Portnoi and R. R. Hartmann, *Phys. Rev. B*, **106**, L041403 (2022).

Nanoengineering and electrochemical probing of carbon nanostructures in TEM

Dmitri V. Golberg

*School of Chemistry and Physics and Centre for Material Science, Queensland University of Technology (QUT), 2 George str., Brisbane, 4000, Australia
dmitry.golberg@qut.edu.au*

1. Introduction

Uncovering mechanical, electrical and optical properties of a carbon nanomaterial, in particular on the individual nanostructure level, is of key importance once its smart integration into modern nanotechnologies is concerned. However, in many cases, these properties have been measured by means of the instruments without direct access to the material atomic structure, its crystallography, and existing defects. Therefore, the acquired results can hardly be linked to a particular morphology, structure, and defect networks. A wide scatter of data has commonly been observed between various samples and research groups. This has typically confused engineers and technologists and led to many uncertainties with respect to carbon nanomaterials' emerging applications.

2. Summary of results

I will demonstrate how diverse state-of-the-art *in situ* transmission electron microscopy (TEM) techniques can be effectively employed for a detailed property and function analysis of carbon nanomaterials, *e.g.*, individual nanotubes and graphene-like nanosheets [1-3]. Young's moduli, fracture strength and toughness, plasticity and electrical conductance may now be precisely determined inside TEM, while employing piezo-driven probes, sensors and nanomanipulators inserted into the microscope column (Fig. 1).

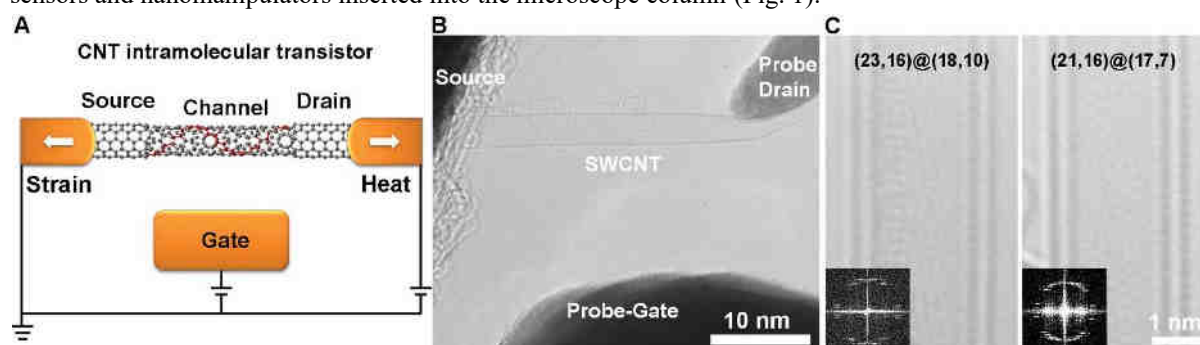


Fig. 1. Fabrication of a CNT intramolecular transistor. (A) Schematics of a CNT transistor with local chirality transformed by mechanical strain and Joule heating. (B) TEM image of a single-wall CNT transistor with a fixed source electrode, a probe as drain electrode, and another probe as gate. (C) Lattice-resolved TEM images and FFT patterns of a double-wall nanotube before and after chirality transition [3].

3. Acknowledgement.

In situ TEM Project at QUT is supported through an Australian Research Council (ARC) Laureate Fellowship FL160100089 (2017-2022). The author is grateful to many colleagues at QUT, *i.e.*, Drs. Joseph Fernando, Konstantin Firestein and Chao Zhang, and the National Institute for Materials Science (NIMS), Tsukuba, Japan, *i.e.*, Drs. Daiming Tang, Ovidiu Cretu, Mingsheng Wang, Xianlong Wei and Naoyuki Kawamoto, for their key experimental contributions to multiple *in situ* TEM projects over the years.

4. References

- [1] Golberg D. *et al. Adv. Mater.* **24**, 177 (2012).
- [2] Zhao L., Luo G., Cheng Y., Li X., Zhou S., Luo C., Wang J., Liao H.-G., Golberg D., Wang M.S. *Nano Lett.* **20**, 2279 (2020).
- [3] Tang D.M., Erohin S., Demin V., Kvashnin D.G., Demin V.A., Cretu O., Jiang S., Zhang L., Hou P.-X., Chen G., Futaba D.N., Zheng Y., Xiang R., Zhou X., Hsia F.-C., Kawamoto N., Mitome M., Nemoto Y., Uesugi F., Takeguchi M., Maruyama S., Cheng H.M., Bando Y., Liu C., Sorokin P.B., Golberg D. *Science* **374**, 1616 (2021).

Disordered hyperuniform configurations from artificial atoms to exotic 2D materials

Ü. Seleme Nizam^{1,2}, Sercan Hüsnügil³, Muhammed H. Güneş³, Danial Vahabli⁴,
 Michaël Barbier¹, Ghaith Makey^{1,3}, Yusuf Özer³, Serim Ilday^{1,*}

¹ UNAM-National Nanotechnology Research Center & Institute of Materials Science and Nanotechnology, Bilkent University, Ankara, 06800, Turkey

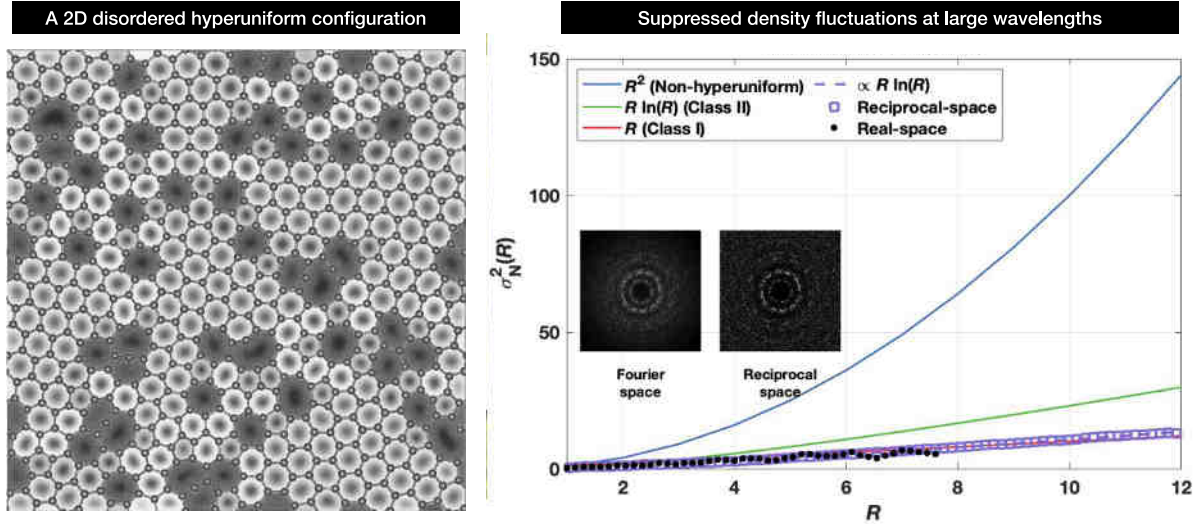
² Department of Physics, Boğaziçi University, Istanbul, 34342, Turkey

³ Department of Physics, Bilkent University, Ankara, 06800, Turkey

⁴ Department of Physics, Middle East Technical University, Ankara, 06800, Turkey

*Corresponding author e-mail (serim@bilkent.edu.tr)

Disordered hyperuniform configurations [1,2] of a material are statistically isotropic but able to suppress density fluctuations at large length scales (long wavelengths), similar to periodic crystals, but with no Bragg peaks. These exotic configurations exhibit interesting properties, explored for various device applications, showing significantly and consistently better performance than their crystalline counterparts [3–8]. Unfortunately, these configurations have been fabricated mainly using additive manufacturing or chemical etching techniques. We recently provided evidence that it is possible to self-assemble disordered hyperuniform configurations with the flexibility of visiting various hyperuniform configurations [9]. Here, I will speculate on the exciting prospects of using our universal dissipative self-assembly methodology to create 2D disordered configurations atom-by-atom from an extensive material library.



Acknowledgement.

We acknowledge funding from the European Research Council (ERC) under the European Union's Horizon 2020 research and innovation programme (Grant agreement No. 853387), TÜBİTAK-EC Marie Skłodowska-Curie Actions Co-fund program (Grant agreement No. 120C074), TÜBİTAK (Grant agreement No. 115F110 and No. 20AG001).

References

- [1] S. Torquato and F. H. Stillinger, *Local density fluctuations, hyperuniformity, and order metrics*, Physical Review E **68**, 041113 (2003).
- [2] S. Torquato *Hyperuniform states of matter*, Physics Reports **745**, 1–95 (2018).
- [3] M. Florescu, S. Torquato and P. J. Steinhardt, *Designer disordered materials with large, complete photonic band gaps*, Proceedings of the National Academy of Sciences, **106**, 20658 (2009).
- [4] W. Man, *et. al.* *Isotropic band gaps and freeform waveguides observed in hyperuniform disordered photonic solids*, Proceedings of the National Academy of Sciences **110**, 15886 (2013).
- [5] H. Zhang, *et. al.* *Experimental demonstration of Luneburg lens based on hyperuniform disordered media*, Applied Physics Letters **114**, 053507 (2019).
- [6] S. Gorsky, *et. al.* *Engineered hyperuniformity for directional light extraction*, APL Photonics **4**, 110801 (2019).
- [7] R. Lin, *et. al.* *On-Chip Hyperuniform Lasers for Controllable Transitions in Disordered Systems*, Laser and Photonics Reviews **14**, 1800296 (2020).
- [8] D. Di Battista, *et. al.* *Hyperuniformity in amorphous speckle patterns*, Optics Express **26**, 15595 (2018).
- [9] Ü. S. Nizam, *et. al.* *Dynamic evolution of hyperuniformity in a driven dissipative colloidal system*, Journal of Physics: Condensed Matter **33**, 304002 (2021).

Momentum alignment of photoexcited carriers in low-dimensional Dirac materials

R. R. Hartmann¹, V. A. Saroka^{2,3} and M. E. Portnoi²

¹Physics Department, De La Salle University, 2401 Taft Avenue, 0922 Manila, Philippines

²Physics and Astronomy, University of Exeter, Stocker Road, Exeter EX4 4QL, United Kingdom

³Institute for Nuclear Problems, Belarusian State University, 220030 Minsk, Belarus

m.e.portnoi@exeter.ac.uk

Devices made from conventional semiconducting materials manipulate electron flow based on their charge or spin (spintronics), the latter offers the promise to revolutionize the way we do computing. In graphene and graphene-like materials, there is an alternative electron property which can be harnessed for device applications: the so-called valley degree of freedom, which could be utilized in an analogous manner to spin in spintronics and has been suggested as a basis for carrying information in graphene-based devices. The ability to control the valley degree of freedom practically is still an outstanding problem. We have proposed a new method of control, using linearly polarized light, to open the door to optovalleytronics.

One of graphene's most widely known optical properties is its universal absorption, defined through the fine-structure constant, which holds true across a broad range of frequencies from the sub-infrared into the visible. A lesser-known feature is that linearly polarized light creates a strongly anisotropic distribution of photoexcited carriers with their momenta predominantly aligned normally to the polarization plane [1]. We show how this momentum alignment effect together with graphene's spectrum anisotropy (trigonal warping) at high energies can be utilized for the spatial separation of carriers belonging to different valleys in graphene and gapped graphene-like materials. The optical control of valley polarization in gapped 2D Dirac materials such as phosphorene and single-layer transition metal dichalcogenides can also be achieved via a well-known effect of using circularly polarized light. In gapped materials, the optical selection rules associated with linearly polarized light of near-band-gap energies are valley-independent, in stark contrast to the valley-dependent optical selection rules associated with circularly polarized light. This valley dependence of the circularly-polarized transitions can be utilized to measure the degree of valley polarization induced by linearly polarized light of high (well above the band gap) energies, by analyzing the degree of circular polarization of the band-edge luminescence at different sides of the light spot.

The celebrated Rashba effect, caused by substrate-induced system asymmetry, leads to a strong anisotropy in the low-energy part of the spectrum (near the Dirac cone apex in graphene). This results in optical valley separation by a linearly-polarized excitation at much lower frequencies compared to the high-energy trigonal warping regime discussed above. Accounting for the Rashba term shows that it is possible to control valley and spin spatial distributions using linearly-polarized photoexcitation of both low and high frequencies.

The momentum alignment phenomenon also explains the effect of the giant enhancement of the band gap edge interband optical transition rate in narrow-gap carbon nanotubes and graphene nanoribbons which occurs in the terahertz frequency range [2], thus opening a route for creating novel terahertz radiation emitters.

Acknowledgement

This work was supported by the EU H2020 RISE projects TERASSE (Project No. 823878) and DiSeTCom (Project No. 823728).

References

- [1] R. R. Hartmann and M. E. Portnoi, *Optoelectronic Properties of Carbon-based Nanostructures: Steering electrons in graphene by electromagnetic fields* (LAP LAMBERT Academic Publishing, Saarbrücken, 2011).
- [2] R. R. Hartmann, V. A. Saroka, and M. E. Portnoi, *J. Appl. Phys.* **125**, 124303 (2019).

Optics of two-dimensional materials hosting tilted Dirac cones

A. Wild, E. Mariani and M. E. Portnoi

*Physics and Astronomy, University of Exeter, Stocker Road, Exeter, EX4 4QL, United Kingdom
a.wild@exeter.ac.uk*

We analyse the interband optical absorption of linearly polarised light by 2D Dirac semimetals hosting tilted Dirac cones in the band structure [1]. Super-critically tilted (type-II) Dirac cones are characterised by an absorption that is highly dependent on incident photon polarization and tuneable by changing the Fermi level with a back-gate voltage. Unlike their sub-critically tilted (type-I) counterparts, type-II Dirac cones have open Fermi surfaces meaning that there exist large regions of the Brillouin zone where both bands sit either above or below the Fermi level causing many states that would otherwise contribute to absorption to be Pauli blocked. We analyse Dirac cones featuring tilt as well as anisotropy in the Fermi velocity, yielding a wide range of qualitatively unique absorption spectra. Guided by our in-depth discussion we develop an optical recipe to fully characterise the tilt and Fermi velocity anisotropy of any 2D tilted Dirac cone solely from its absorption spectra. We also show that tilted Dirac cones allow spatial separation of carriers belonging to two different valleys under illumination by linearly polarized light, leading to novel optovalleytronic applications. Our results are used to analyse polarisation-dependent light absorption of 8-Pmmn borophene [2,3].

Acknowledgement

This work was supported by the EU H2020-MSCA-RISE projects TERASSE (Project No. 823878) and DiSeTCom (Project No. 823728) and by the NATO Science for Peace and Security project NATO.SPS.MYP.G5860.

References

- [1] A. Wild, E. Mariani, and M. E. Portnoi, arXiv:2112.00542 (2021)
- [2] X.-F. Zhou, X. Dong, A. R. Oganov, Q. Zhu, Y. Tian, and H.-T. Wang, Phys. Rev. Lett. 112, 085502 (2014)
- [3] A. D. Zabolotskiy and Y. E. Lozovik. Phys. Rev. B 94, 165403 (2016)

Structure analysis of carbon nanomaterials using black silicon-based SERS substrate

Lena Golubewa^{1,2}, Yaraslau Padrez¹, Hamza Rehman², Renata Karpicz¹, Tatsiana Kulahava¹, Olga Levinson³, Polina Kuzhir²

¹Department of Molecular Compound Physics, Center for Physical Sciences and Technology, Lithuania

²Department of Physics and Mathematics, Institute of Photonics, University of Eastern Finland, Finland

³Ray Techniques Ltd., Israel

lena.golubewa@ftmc.lt

1. Introduction

Surface Enhanced Raman Spectroscopy (SERS), as compared with Raman spectroscopy, where compound analysis is strongly depended on the substance quantity (it should be high), has significant advantage as it allows receiving the ‘fingerprints’ of trace amounts of analytes and analysing single monolayers, strongly diluted solutions with concentrations for up to 10^{-12} - 10^{-9} M), etc. The efficiency and sensitivity of this method is determined by a substrate used. Black silicon (bSi) refers to silicon surfaces with a layer of “needle” or “pyramidal”-like microstructures on top which suppress reflection and enhance the scattering and absorption of light. Sputtered with gold, high curvature cone-like structures can serve as active sites for electromagnetic field enhancement. In the present study we implied bSi sputtered with gold (bSi/Au) for fluorescence graphene quantum dots (GQDs) structure analysis and their modification under the action of various oxidants in biological systems, and for characterization of fluorescent nanodiamonds (NDs) obtained by laser synthesis.

2. Result and discussion

Raman spectrum of GQD suspension and SERS spectra of untreated GQDs and GQDs exposed to hydrogen peroxide, NaClO or oxygen plasma are presented in Fig.1. Structural features and presence of specific functional groups are not resolved in Raman spectra, while SERS spectrum shows that GQDs are strongly passivated with oxygen-containing groups, with high inclusion of epoxy-groups. GQDs exposed to NaClO lose their fluorescence but are not affected by H_2O_2 . SERS spectra demonstrate the degradation of GQD structures under the action of NaClO and C-O-C bands vanishing allows assuming that the degradation mechanism of GQDs is through the targeting epoxy-groups in them. It was also demonstrated that NDs obtained by laser synthesis have similar passivation with oxygen-containing groups, however, the difference in the fraction of epoxy-groups (NDs contain less) likely explains the insensitivity of NDs to the NaClO exposure.

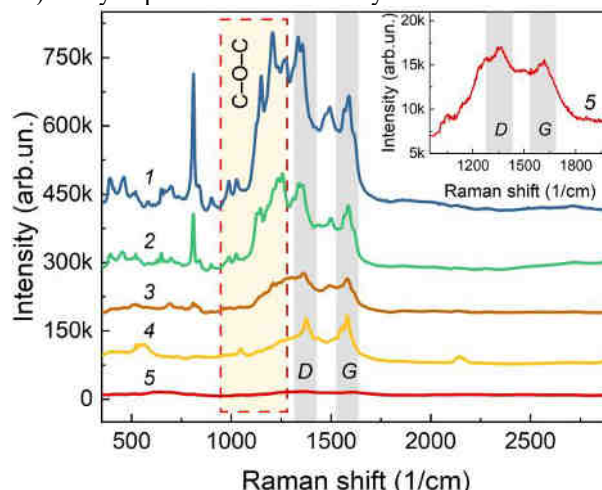


Fig. 1. SERS and Raman spectra of GQDs: 1 – GQDs on bSi/Au, 2 – GQDs on bSi/Au exposed to 10 mM H_2O_2 (30 min), 3 – GQDs on bSi/Au exposed to 10 mM NaClO (30 min), 4 – GQDs (treated with oxygen plasma) on bSi/Au, 5 – GQDs in water.

3. Conclusions

Gold-coated bSi-based SERS substrate is a powerful tool for carbon nanomaterials analysis, which allowed revealing specific features of GQDs and NDs and structural changes underlying the mechanism of biodegradation of GQDs by NaClO.

4. Acknowledgements

This work was supported by H2020 RISE DiSeTCom (No 823728) and H2020 RISE Graphene 3D (No 734164)

Generating THz Pulses with Longitudinal Electromagnetic Field

Kuniaki Konishi

Institute for Photon Science and Technology, The University of Tokyo
 kkonishi@ipst.s.u-tokyo.ac.jp

Ultrafast control of materials by terahertz (THz) waves has attracted great interest in the area fundamental physics and in technological applications. Response of THz to two dimensional materials, and the ability to suggest unique response when strong THz fields are applied vertically to their plane, makes it the candidate of choice for future high frequency electronics. Studies of such responses at ultrafast timescales expand our understanding of these materials, and allow for ultrafast control over their properties. For the application of vertical electromagnetic fields, cylindrical vector (CV) beams, which have a polarization state with axial symmetry in the beam cross section, are suitable because of the production of longitudinal electric or magnetic field components in the vicinity of the focal point (Fig. 1(a)) [1].

For the generation of the CV beam in the optical region, a segmented waveplate is commonly used, and as such not suitable to convert THz pulse with broadband spectral components to the CV beam. Therefore, a method to directly generate a broadband THz vector beam has been developed using a GaP (111) crystal with threefold symmetry for terahertz generation. Results from this study demonstrated that it is possible to directly generate a broadband THz CV beam by exciting the segmented GaP (111) crystal with linearly polarized femtosecond pulses [2] or by exciting a normal GaP (111) crystal with polarization-controlled femtosecond pulses [3]. It revealed that THz longitudinal electric field was generated by focusing them, and that these broadband THz CV beams can be easily converted to THz vortex beam [4].

These methods limit the intensity of the THz longitudinal electric field due to the generation efficiency of the nonlinear crystals. In recent years, higher-intensity THz light sources such as THz free electron lasers have also been developed [5]. If a CV beam can be generated from any linearly polarized light regardless of the type of light source, higher intensity of longitudinal electric THz field can be realized. Thus, this study demonstrates a new method for converting linear polarized THz Gaussian beams into Hermite–Gaussian 01 (HG₀₁) beams, and by generating strong longitudinal electric fields by focusing them. A specially designed silicon prism is used for the polarization-conversion (Fig. 1(b)), which has a total internal reflection plane, half of which is coated by gold. Since gold has a larger refractive index than silicon, half of the incident beam is phase shifted when reflected. When the THz beams were incident at a specific angle, the relative phase shift between the two halves was equal to π , resulting in relative polarization reversal. Using this technique, we successfully converted the THz pulse generated from a lithium niobate crystal into a HG₀₁ mode and generated a 36 kV/cm THz longitudinal electric field by focusing them [6].

In this talk, I will introduce these our study for THz longitudinal electromagnetic field generation so far and discusses the future developments.

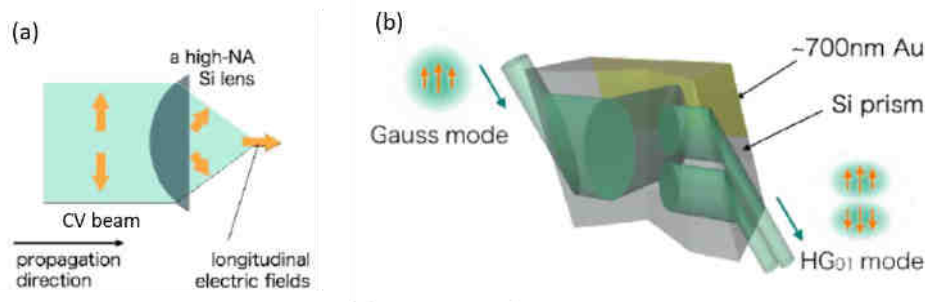


Fig. 1. (a) scheme of longitudinal electric fields from CV beam (b) Schematic of the silicon polarization-conversion prism

References

- [1] Q. Zhan, Cylindrical vector beams: from mathematical concepts to applications, *Adv. Opt. Photon.* **1**, 1 (2009).
- [2] R. Imai, N. Kanda, T. Higuchi, Z. Zheng, K. Konishi and M. Kuwata-Gonokami, Terahertz vector beam generation using segmented nonlinear optical crystals with three-fold rotational symmetry, *Opt. Express* **20**, 21896 (2012).
- [3] Z. Zheng, N. Kanda, K. Konishi and M. Kuwata-Gonokami, Efficient coupling of propagating broadband terahertz radial beams to metal wires, *Opt. Express* **21**, 10642 (2013).
- [4] R. Imai, N. Kanda, T. Higuchi, K. Konishi and M. Kuwata-Gonokami, Generation of broadband terahertz vortex beams, *Opt. Lett.* **39**, 3714 (2014).
- [5] K. Kawase, R. Kato, A. Irizawa, M. Fujimoto, S. Kashiwagi, S. Yamamoto, F. Kamitsukasa, H. Osumi, M. Yaguchi, A. Tokuchi, S. Suemine and G. Isoyama, The high-power operation of a terahertz free-electron laser based on a normal conducting RF linac using beam conditioning, *Nucl. Instrum. Meth. Phys. Res. A* **726**, 96 (2013).
- [6] M. Matoba, N. Nemoto, N. Kanda, K. Konishi, J. Yumoto and M. Kuwata-Gonokami, Generation of Intense Terahertz Pulses with Longitudinal Electric fields, *CLEO/QELS 2018*, JW2A.80, USA (May 2018)

Extreme non-linearity in ferrites: from microwave to THz.

Feodor Y. Ogrin

*MaxLLG Ltd. Exeter, United Kingdom
f.y.ogrin@maxllg.com*

Electromagnetic (EM) shock waves are normally associated with nuclear explosions, and as such a rare phenomenon. Analogous to a sonic boom, it is an interference effect, resulting in a surge of EM power, propagating with a speed of light. Since early 60s there was an interest to harness the effect to make it more technologically practical. One possible way to do that is within the configuration of a magnetically loaded transmission line (e.g. coaxial line). While the coaxial design has been proven to be viable for generating high power microwaves [1], its practicality in consumer technology is less so obvious due to high voltages (typically 10-100th kV) needed in order to obtain the effect. Theoretically, this problem can be resolved by scaling down the dimensions of the transmission line. Reducing down to microscopic dimensions, it is possible to obtain the effect at voltages as low as 1-10 Volts. At this level the effect can be usefully utilised in a range of electronic devices, and particularly the high frequency communications, which are of great demand in the development of modern IC technologies. Modelling extremely non-linear EM dynamics is however a challenging problem, that can not be done by the available conventional solvers. Here we approach the problem by using a unique modelling technique allowing to solve Maxwell equations in parallel to Landau-Lifshits-Gilbert's (LLG) [2]. The unique nature of our 3D FDTD-LLG code, is in the fact that LLG equation is solved exactly, accounting for the given geometry with the presence of any type of conducting or non-conducting materials [3]. This means that all non-linear effects can be calculated precisely without any linearization or imposed constraints.

In this contribution I will demonstrate the main characteristics and parameters of the shock wave propagation in microstrip transmission line. In particular, I will show the dispersion characteristics of the wave, its dependence on the geometric and material parameters of the device and those of the source of actuation. As well as the typical effects, such as applied field dependence and anisotropy, I will demonstrate some unique features, such as tuneability with the electric field pulse, allowing to manipulate the response in a broad GHz to THz frequency range. I will also demonstrate the possibility of guiding the waves in microstrips with non-linear geometric designs, and discuss the potential for application in communication technologies.

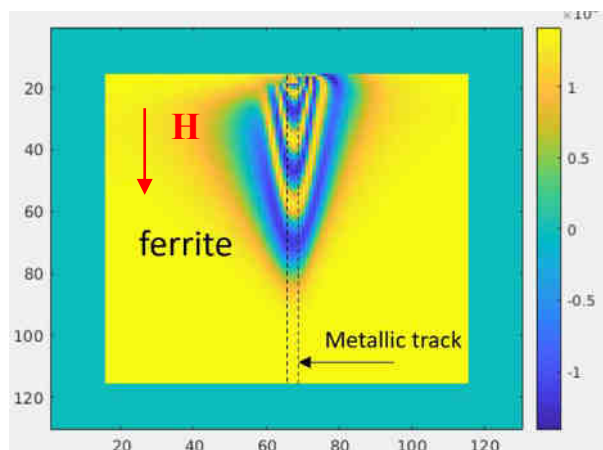


Figure 1. Electromagnetic shock-wave propagation in a thin-film microstrip transmission line. The wave is actuated with a short electric pulse between the microstrip (shown with dashed lines) and the base metalised plane. Ferrite thin film (10micron) extended over the base line. Shock wave propagates below the strip, but deviates also into the whole slab. Intensity map: out-of-plane magnetisation. Initial orientation of the magnetisation is parallel to the applied field (red arrow).

References

- [1] Ulmasculov et al. (2017), J. Phys.: Conf. Ser. 830 012027.
- [2] M. M. Aziz, Progress In Electromagnetics Research B 15, (2009) 1–29.
- [3] <https://www.maxllg.com/>

Complementarity in vectorial quantum light interference

Andreas Norrman

*Institute of Photonics, University of Eastern Finland, P.O. Box 111, FI-80101 Joensuu, Finland
andreas.norrman@uef.fi*

1. Introduction

The principle of complementarity, stating that quantum systems share mutually exclusive properties, is a central concept in physics. The arguably most recognized appearance of such complementarity is wave–particle duality, which limits the coexistence of wave and particle properties of a quantum object. In two-way interferometry, such as the celebrated double-slit experiment, the dual wave–particle quantum character can be quantified as [1]

$$D_0^2 + V_0^2 \leq 1. \quad (1)$$

Here D_0 is the path predictability, representing the particle aspect or “which-path information” (WPI) of the object, and V_0 is the interferometric intensity fringe visibility, describing the wave aspect of the object. Photons, however, may exhibit interference not only in terms of intensity fringes but also (or merely) in terms of polarization-state fringes [2], a distinctive quality of vectorial light fields that has no correspondence in scalar-light interferometry. The manifestation and quantification of quantum complementarity under such interferometric polarization-state modulation is therefore of fundamental interest. In this work, we explore polarization modulation in double-slit interference and establish three general complementarity relations for quantized vector-light fields, revealing new foundational features of the dual wave–particle nature of photons [3,4].

2. Results and discussion

It can be shown that any vectorial quantum light in two-slit interference obeys the complementarity relations [3]

$$D_0^2 + V_S^2 \leq 1, \quad D_S^2 + V_0^2 \leq 1. \quad (2)$$

Here the Stokes visibility V_S is the vector-light generalization of the usual intensity fringe visibility V_0 encountered in the scalar-light context, that also characterizes the visibility of polarization-state fringes in the detection plane. The Stokes distinguishability D_S in turn describes the polarization-state difference of the light field at the two slits, thus providing another central measure to quantify the WPI in the system in addition to the path predictability D_0 . At the single-photon level, the complementarity relations in Eq. (2) reflect two very different, fundamental aspects of wave–particle duality of the photon [3] having no correspondence within the scalar-light framework of Eq. (1). Especially, in the vector-light scenario the path predictability D_0 does not couple to the intensity visibility V_0 but instead to the Stokes visibility V_S which accounts also for the polarization-state modulation. This feature highlights an essential quality concerning wave–particle duality of vectorial quantum light fields.

Let us consider further a quantum plane-wave field that contains two orthogonal polarization modes and whose degree of polarization is P [2]. The two modes are separated and directed towards the slits where arbitrary local unitary operations can be performed, which allows one to control the intensity and/or polarization modulation in the detection plane where the modes are eventually superposed. In this case we discover that [4]

$$P^2 = D_0^2 + V_S^2, \quad (3)$$

forming a fundamental link among the path predictability at the slits, the Stokes visibility in the observation plane, and the degree of polarization of the initial (undivided) light field. It implies that a change of D_0 or V_S alters its complementary partner so that the sum of their squares strictly equals P^2 . We can thereby interpret P as specifying the “complementarity strength” between D_0 and V_S . Equation (3) also indicates that $D_0, V_S \leq P$, dictating that the degree of polarization sets the upper bound both for the path predictability and for the Stokes visibility.

Hence our work, together with its current extension to more complex topologies involving geometric phases, quantum polarization uncertainties, as well as materials displaying nonlinear interactions, provides deeper insights into foundational quantum photonics.

3. Acknowledgement

We thank Jenny and Antti Wihuri Foundation, Emil Aaltonen Foundation, Swedish Cultural Foundation in Finland, Jane and Aatos Erkko Foundation, and Academy of Finland (268480, 268705, 310511) for financial support.

4. References

- [1] B.-G. Englert, *Physical Review Letters*, **77**, 2154 (1996).
- [2] A. T. Friberg and T. Setälä, *Journal of the Optical Society of America A*, **33**, 2431 (2016).
- [3] A. Norrman, K. Blomstedt, T. Setälä, and A. T. Friberg, *Physical Review Letters*, **119**, 040401 (2017).
- [4] A. Norrman, A. T. Friberg, and G. Leuchs, *Optica*, **7**, 93 (2020).

Tuesday, August 2



Advances of ultrashort-pulse fiber lasers using nanocarbon-based saturable absorbers

Shinji Yamashita

*Research Center for Advanced Science and Technology, The University of Tokyo, 4-6-1, Komaba, Meguro-ku, Tokyo, 153-8904, Japan
syama@ee.t.u-tokyo.ac.jp*

Optical pulsed lasers offer a broad-range of applications in various fields, such as optical communications, optical signal processing, nonlinear microscopy, optical metrology, laser surgery, etc. Passively mode-locked fiber lasers are amongst the best pulsed sources available today due to their simplicity and their ability to generate transform-limited ultrashort optical pulses in the picosecond and sub-picosecond regimes. Such lasers offer superb pulse quality and there is no need for costly modulators as required in actively mode-locked lasers. Instead, passively mode-locked fiber lasers employ a saturable absorber (SA) as a mode-locker, a device that possesses an intensity-dependent response to favor optical pulse formation over continuous-wave lasing. Although saturable absorption itself is a common phenomenon happening in any absorbing materials, it is not easy to find a fast SA responding at timescales of 1ps or faster suitable for ultrashort-pulse generation. Conventionally, semiconductor-based SA (semiconductor saturable absorber mirror (SESAM)) or fiber Kerr-based SA (nonlinear polarization rotation (NPR) or nonlinear loop mirror (NOLM)) has been used. The third SA is the CNT-based SA, which was proposed in 2003. CNT-based SAs have been demonstrated to have significant advantages over the former SAs for passively mode-locked fiber lasers. It was also discovered that graphene and other 2D materials have similar fast saturable absorption and are applicable to passively mode-locked fiber lasers.

In this talk, we will review our recent advances on ultrashort-pulse fiber lasers using nanocarbon-based SA and their applications. The talk will mainly focus on

- (1) Fabrication of nanocarbon-based SA device
- (2) SWCNT@BNNT-based SA having high optical damage threshold
- (3) Dual-comb fiber lasers using CNT-based SA

References

- [1] S. Yamashita, “A tutorial on nonlinear photonic applications of carbon nanotube and graphene (Invited Tutorial),” *Journal of Lightwave Technology*, vol.30, no.4, pp.427-447, Feb. 2012.
- [2] S. Yamashita, Y. Saito, and J. H. Choi (ed.), *Carbon nanotubes and graphene for photonic applications*, Woodhead Publishing, 2013.
- [3] A. Martinez, B. Xu and S. Yamashita, “Nanotube based nonlinear fiber devices for fiber lasers (Invited),” *Journal of Selected Topics in Quantum Electronics*, vol.20, no.5, pp.89-98, Sept. 2014.
- [4] S. Yamashita, A. Martinez, and B. Xu, “Short pulse fiber lasers mode-locked by carbon nanotube and graphene (Invited),” *Optical Fiber Technology*, vol.20, no.6, pp.702-713, Dec. 2014.
- [5] S. Yamashita, “Nonlinear optics in carbon nanotube, graphene, and related 2D materials (Tutorial),” *APL Photonics*, Special Issue on Nonlinear Optical 2D Materials, vol.4, 034301, Dec. 2018, doi:10.1063/1.5051796.
- [6] Z. Zhang et al., “SWCNT@BNNT with 1D Van Der Waals heterostructure with a high optical damage threshold for laser mode-locking,” *Journal of Lightwave Technology*, vol. 39, no. 18, pp. 5875-5883, Sept.15, 2021, doi:10.1109/JLT.2021.3092522.
- [7] K. Uyama, T. Shirahata, L. Jin, S. Y. Set, and S. Yamashita, “All-PM dual-comb fiber ring laser using CNT-SA,” *Conference on Lasers and Electro-Optics (CLEO2020)*, paper SW4R.2, May 2020.
- [8] K. Uyama, T. Shirahata, S. Y. Set, and S. Yamashita, “Orthogonally-polarized bi-directional dual-comb fiber laser,” *Conference on Lasers and Electro-Optics (CLEO2022)*, paper SW4R.2, May 2022.

Enhancement of Optical Nonlinearities in 2D Materials

Zhipei Sun

*Department of Electronics and Nanoengineering, Aalto University, Tietotie 3, FI-02150, Finland
QTF Centre of Excellence, Department of Applied Physics, Aalto University, FI-00076 Aalto, Finland
Zhipei.sun@aalto.fi*

Nonlinear optics plays an essential role in various photonic and optoelectronic applications, such as wavelength conversion and information processing. Recently, the extraordinarily large nonlinear optical properties of 2D materials have attracted significant attention. However, the conversion efficiency of 2D materials is typically limited by the atomically thin light-matter interaction length. Here, I will discuss the strategies to enhance optical nonlinearities of two-dimensional layered materials (e.g., graphene, transition metal dichalcogenides) for various integrated photonic and optoelectronic applications, such as high-purity quantum emitters, wavelength converters, and ultrafast lasers. I will also present our recent results of employing hybrid structures, such as mixed-dimensional heterostructures, plasmonic structures, and silicon/fibre waveguides integrated).

References

- [1] A. Autere et al., Adv. Mater. 30, 1705963 (2018).
- [2] L. Du et al., Nat. Rev. Phys., 3, 193-206 (2021).
- [3] Y. Dai et al., ACS Nano, 14, 8442 (2020).
- [4] L. Du et al., Nat. Commun., 12, 4822 (2021).
- [5] Y. Dai et al., Nano Lett., 21, 6321 (2021).
- [6] Y. Wang et al., ACS Photon., 8, 2713 (2021).
- [7] Y. Wang, et al., ACS Photon. 8, 2320 (2021)
- [8] Y. Wang, et al., Adv. Mater., 2107104 (2021).
- [9] V. Pelgrin, et al., Opt. Lett., 47, 734 (2022).

Influence of the surface roughness of graphene-based biosensing platforms for the living cells functional state monitoring

Hamza Rehman¹, Lena Golubewa²

¹ Institute of Photonics, University of Eastern Finland, Yliopistokatu 2, FI-80100 Joensuu, Finland,

² Center for Physical Sciences and Technology, Sauletekio Ave. 3, LT-10257 Vilnius, Lithuania
hamza.rehman@uef.fi

Biosensors are devices that measures the extent of biological activity and translates it into electrical signals. A lot of interest is being put into the research and development of biosensor for the functional state monitoring of the living cells [1]. Great focus has been placed on studies related to the material's interaction with the living cells, and the development of various suitable bio-platforms. The efficacy of these platforms is strongly connected to material's 1) physical properties (elasticity, stiffness, roughness etc.), 2) morphology, thickness, macro, micro and nano topography), and 3) biochemical properties (surface charge, hydrophobicity/hydrophilicity, etc. [2].

In this work we have compared various substrates deposited with graphene and its derivative, nanometrically thin Pyrolytic carbon (PyC), for the cultivation of living cells. Experiments were done with C6 glioma cells, and we discovered that PyC coating is a promising technique for controlling the cell proliferation and directional intercellular contact (Fig.1). The ease with which the nano topography and the physical/chemical properties of the PyC films can be controlled makes it a suitable interface in the development of biosensors and 3D bio scaffolds (Fig.2).

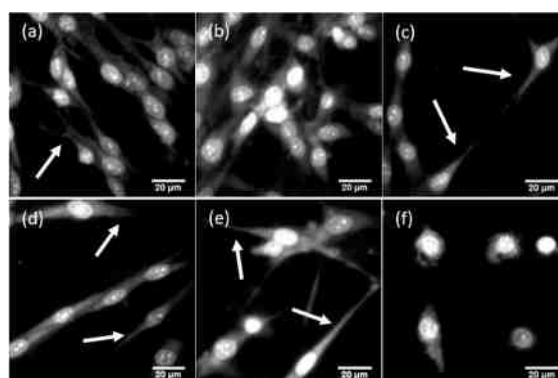


Fig. 1. Glioma cells were grown on (a) plastic (as a control); (b) bSi; (c) PyC (20 nm) on bSi; (d) PyC (20 nm) on SiO₂; (e) PyC (40 nm) on SiO₂; (f) graphene nano-walls

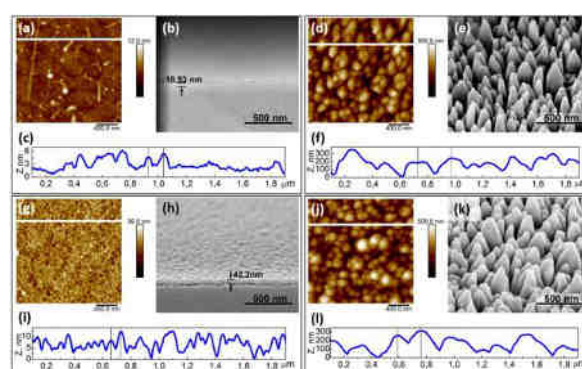


Fig. 2. Typical two-dimensional AFM and SEM surface images of PyC of 20 nm (a,b) and 40 nm thickness (g,h) on SiO₂, bSi (d,e), PyC of 20 nm on bSi (j,k), respectively. The cross-sectional profiles are marked with a white line on the AFM images (a,d,g,j).

Acknowledgement

This work was financially supported by H2020 RISE DiSeTCom Project 823728.

References

- [1] Haizhou Huang, Shi Su, Nan Wu, Hao Wan, Shu Wan, Hengchang Bi, Litao Sun, *Frontiers in Chemistry*, 2019
- [2] Lena Golubewa, Hamza Rehman, Tatsiana Kulahava, Renata Karpicz, Marian Baah, *MDPI sensors*, 2020, 20(18)

SWCNT Transparent Conducting Films: Towards the Theoretical Limit

Albert G. Nasibulin^{1,2}

¹ Skolkovo Institute of Science and Technology, Nobel str. 3, Moscow, 143026, Russia

² Aalto University, Department of Materials Science and Engineering, 00076, Aalto, Finland
a.nasibulin@skoltech.ru

Electrically conducting thin-film materials possessing high transmittance are critical elements for many optoelectronic devices. Nowadays, the advancement of the transparent conductor applications requires the replacement of indium tin oxide (ITO), which at the moment is the key material in electronics. Single-walled carbon nanotube (SWCNT) films were proposed to be a cheap alternative for the transparent conductive film (TCF) production due to their unique mechanical properties, such as flexibility and stretchability. Here, we analyze the latest advancement in the optoelectronic performance of TCFs based on SWCNTs. We describe the roadmap for further research and development of TCFs by means of "rational design", which breaks the deadlock for the obtaining of TCFs close to the theoretically limited performance.

First, we propose to use machine learning techniques such as artificial neural networks [1] and support vector regression [2] to process the experimental data and to predict the performance of the aerosol CVD synthesis of SWCNTs and to enhance the SWCNT thin-film performance for transparent and conducting applications. The predictive model trained on the experimental data allowed to achieve the synthesis conditions toward the advanced optoelectronic performance of multiparameter processes such as nanotube growth. Using gold chloride as the most effective dopant for the SWCNTs, we improve their optoelectrical characteristics by optimizing the doping conditions [3]. Doping of the improved carbon nanotube films with H₂AuCl₄ results in the equivalent sheet resistance of 39 Ω/□.

For the first time we demonstrate that electrochemical doping of SWCNTs can be successfully applied in transparent electronics. This method provided fine and reversible tuning of the optoelectrical properties of the material over a wide range of sheet resistances and transmittances. A wide electrochemical window imidazolium-based (BMIM-PF₆) ionic liquid allowed us to achieve the Fermi level shift up to 1.4 eV and an equivalent sheet resistance (sheet resistance of the film with the 90% transmittance at 550 nm) value of 53 Ω/sq for the SWCNT films. The results open new avenues for electrochemical control and fine-tuning of the electronic structure of carbon nanomaterials for rigid and flexible highly conductive and transparent device applications. We report that the electrochemical doping can tailor nonlinear optical absorption of SWCNT films and demonstrate its application to control pulsed fiber laser generation [4]. With a pump-probe technique, we show that under an applied voltage below 2 V the photobleaching of the material can be gradually reduced and even turned to photoinduced absorption. We show that the pulse generation regime can be reversibly switched between femtosecond mode-locking and microsecond Q-switching using different gate voltages. This approach paves the road toward carbon nanotube optical devices with tunable nonlinearity.

Here, we develop a novel transparent p-type flexible electrode based on SWCNTs combined with poly(3,4-ethylenedioxythiophene) polystyrene sulfonate (PEDOT:PSS), molybdenum oxide and SWCNT fibers [5]. We achieved a record equivalent sheet resistance of 17 Ω/sq with a transmittance of 90% at 550 nm and a high degree of flexibility. We demonstrate that our solar cells based on the proposed electrode and hydrogenated amorphous silicon (a-Si:H) yield an outstanding short-circuit current density of $J_{sc} = 15.03$ mA/cm² and a record power conversion efficiency of PCE = 8.8% for SWCNTs/a-Si:H hybrid solar cells.

The author thanks Eldar Khabushev, Daniil A. Ilatovskii, Pramod M. Rajanna, Dr. Alexey P. Tsapenko, Dr. Daria S. Kopylova, Dr. Evgenia P. Gilshteyn, Dr. Fedor S. Fedorov, Dr. Dmitry V. Krasnikov, Dr. Yuri Gladush, Prof. Glukhova, Prof. Sergey Shandakov and Prof. Tanja Kallio for their valuable contributions to the work presented. This work was supported by the Russian Science Foundation (project number 22-13-00436) and the Council on grants of the President of the Russian Federation (grant number HIII-1330.2022.1.3).

[1] V. Ya. Iakovlev, D. V. Krasnikov, E. M. Khabushev, J. V. Kolodiaznaia, A. G. Nasibulin Carbon **153**, 100 (2019).

[2] E. M. Khabushev, D. V. Krasnikov, O. Zaremba, A. P. Tsapenko, A. E. Goldt, A. G. Nasibulin, J. Phys. Chem. Lett. **10**, 6962 (2019).

[3] A. P. Tsapenko, S. Romanov, D. Satco, D. Krasnikov, P. Rajanna, M. Danilson, O. Volobujeva, A. Anisimov, A. Goldt, A. G. Nasibulin, J. Phys. Chem. Lett. **10**, 3961 (2019).

[4] Y. Gladush, A. A. Mkrtchyan, D. S. Kopylova, A. Ivanenko, B. Nyushkov, S. Kobtsev, A. Kokhanovskiy, A. Khagai, M. Melkumov, M. Burdanova, M. Staniforth, J. Lloyd-Hughes, A. G. Nasibulin, Nano Letters **19**, 5836 (2019).

[5] P. M. Rajanna, H. Meddeb, O. Sergeev, A. P. Tsapenko, S. Bereznev, M. Vehse, O. Volobujeva, M. Danilson, P. D. Lund, A. G. Nasibulin, Nano Energy **67**, 104183 (2020).

Transport properties of TMDC materials

Géza I. Márk, Péter Vancsó, Péter Nemes-Incze

*Institute for Technical Physics and Materials Science, Centre for Energy Research, 1121 Budapest, Hungary
mark.geza@ek-cer.hu*

1. Introduction

One of the possible material families of the post-Silicon era is the family of the two-dimensional (2D) materials. Whereas graphene was the first member of this group, transition-metal dichalcogenides (TMDCs) provide a large variety of properties. Single-layer molybdenum disulfide (MoS_2), is one of the most intensively studied materials from the TMDC family. Compared to the bulk and few layer MoS_2 , the monolayer form is a direct band gap semiconductor that makes it a good candidate for transistor, photodetector, and optoelectronic device applications. Real 2D materials, however, are newer perfect and the structural defects, such as vacancies and grain boundaries can substantially alter the properties of the material.

2. Methods

We investigated the graphene- and MoS_2 structural defects by scanning probe methods and calculated their effect on the transport properties by wave packet dynamics (WPD). Experimentally, the real-space modulation of the LDOS is accessible by Fourier transformation of the topography or tunnelling conductance maps, measured by scanning tunnelling microscopy (STM) [1]. In our WPD formulation [2] the electronic structure of the perfect crystal is described by the kinetic energy operator and the local defects are modelled by the potential energy operator [3], hence the two input quantities of the WPD calculation are the band structure of the perfect 2D crystal which is known from DFT calculations and the localized potential describing the defects.

3. Results

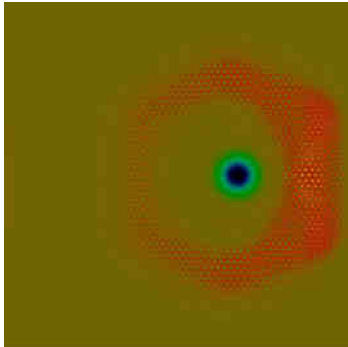


Figure 1 shows the scattering of an electronic wave packet on a localized defect of the graphene surface. This is accomplished by calculating the difference of the time dependent wave functions of a perfect lattice and a lattice containing the localized defect. Though the local potential describing the defect is isotropic, the scattering shows an anisotropic [4] (hexagonal) pattern, because of the anisotropic nature of the graphene dispersion relation. Such anisotropic quasiparticle interferences are clearly seen in scanning probe microscopy experiments [1,3].

Fig. 1. Probability density of the difference wave function, $|\varphi_{with\ pot} - \varphi_{without\ pot}|^2$

4. Acknowledgement

This work was supported by the European H2020 GrapheneCore3 project no. 881603, Graphene Flagship.

5. References

- [1] P. Vancsó, G. Z. Magda, J. Pető, J. Y. Noh, Y. S. Kim, C. Hwang, and L. Tapasztó, *Sci. Rep.*, **6**, 29726 (2016).
- [2] G. I. Márk, G. R. Fejér, P. Vancsó, P. Lambin, and L. P. Biró, *Phys. Status Solidi B*, **254**, 1700179 (2017).
- [3] P. Vancsó, A. Mayer, P. Nemes-Incze, and G. I. Márk, *Appl. Sci.*, **11**, 4730 (2021).
- [4] G. I. Márk, P. Vancsó, C. Hwang, P. Lambin, and L. P. Biró, *Phys. Rev. B*, **85**, 125443 (2012).

2D materials in transistors, memories, and phototransistors

Antonio Di Bartolomeo,^{1,2*} Enver Faella,^{1,2} Filippo Giubileo,² Arun Kumar,¹ Aniello Pelella^{1,2}

¹ Physics Department "E.R. Caianiello", University of Salerno, 84084 Fisciano, Salerno, Italy

² CNR-SPIN, 84084 Fisciano, Salerno, Italy

Corresponding author e-mail: adibartolomeo@unisa.it

Two-dimensional materials hold great promises for electronics and optoelectronics applications. Their atomic thickness enables highly scaled field-effect transistors with reduced short-channel effects and relatively high carrier mobility. The intrinsic electrical transport properties of 2D materials are commonly investigated using back-gated field-effect transistors, due to the low density of process-induced defects and the easy fabrication.

In this presentation, the electrical and optical properties of several 2D materials are discussed. The focus is on the wide family of transition-metal dichalcogenides (TMDs), such as MoS₂, PtSe₂, PdSe₂, WSe₂, ReSe₂, [1-3] and on black phosphorus (BP).[4] Electrical transport, modulation of the conductivity by a back-gate, effect of electron irradiation, the role of surface adsorbates and the photoresponse are investigated in nanosheets obtained by either mechanical exfoliation or chemical vapor deposition on SiO₂/Si substrates.

The formation of low-resistance contacts and the control of process-induced defects or interface states are issues to consider in the electrical characterization of 2D materials. It is shown that the contact resistance can be tuned by electron irradiation that reduces the Schottky barrier and improves the 2D material/metal contacts.[5-7] It is demonstrated that adsorbates can change the polarity of the charge-carriers and enhance the hysteresis in the transfer characteristics of TMD-based field-effect transistors.[8] It is shown that slow excitation from intrinsic or extrinsic trap states enables slow optical response and persistent photoconductivity.[2] It is highlighted how positive and negative photoconductivity can coexist in the same device, the dominance of one type over the other being controlled by the adsorbed oxygen.

The strong dependence of the channel conductance on the environmental gas, air pressure, light and electrical stress make 2D materials-based devices suitable for memory, gas and light sensing applications.

Finally, the tunable conductivity and the sharp-edge geometry facilitate the extraction of electrons (field emission) from 2D materials upon application of an electric field.[9-10] It is shown that several 2D materials are effective field emitters and that their emission current can be modulated by a back-gate.

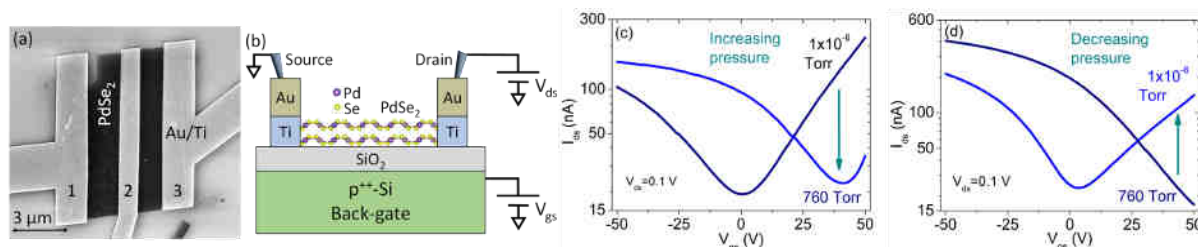


Fig. 1. (a) SEM top view and (b) schematic cross section and measurement setup of a back-gate PdSe₂ field-effect transistor. Effects of air pressure on the transfer characteristics of the PdSe₂ transistor (c) for increasing and (d) decreasing pressure.

References

- [1] E. Faella, K. Intonti, L. Viscardi, F. Giubileo, A. Kumar, H. T. Lam, K. Anastasiou, M. F. Craciun, S. Russo and A. Di Bartolomeo, *Electric Transport in Few-Layer ReSe₂ Transistors Modulated by Air Pressure and Light* *Nanomaterials* **12** (2022) 1886 (feature paper)
- [2] A. Grillo, E. Faella, A. Pelella, F. Giubileo, L. Ansari, F. Gity, P.K. Hurley, N. McEvoy, and A. Di Bartolomeo *Coexistence of negative and positive photoconductivity in few-layer PtSe₂ field-effect transistors* *Advanced Functional Materials* **31** (2021) 2105722
- [3] A. Pelella, A. Grillo, F. Urban, F. Giubileo, M. Passacantando, E. Pollmann, S. Slezione, M. Schleberger, and A. Di Bartolomeo *Gate-controlled field emission current from MoS₂ nanosheets* *Advanced Electronic Materials* **7** (2021) 2000838.
- [4] A. Grillo, A. Pelella, E. Faella, F. Giubileo, S. Slezione, O. Kharsah, M. Schleberger, A. Di Bartolomeo *Memory effects in black phosphorus field effect transistors* *2D Materials* **9** (2022) 015028
- [5] A. Di Bartolomeo, F. Urban, A. Pelella, A. Grillo, M. Passacantando, X. Liu, F. Giubileo *Electron irradiation on multilayer PdSe₂ field effect transistors* *Nanotechnology* **31** (2020) 375204
- [6] A. Pelella, O. Kharsah, A. Grillo, F. Urban, M. Passacantando, F. Giubileo, L. Iemmo, S. Slezione, E. Pollmann, L. Madau, M. Schleberger, and A. Di Bartolomeo *Electron irradiation of metal contacts in monolayer MoS₂ Field-Effect Transistors* *ACS Applied Materials and Interfaces* **2020**, **12** (36) 40532–40540
- [7] A. Grillo and A. Di Bartolomeo *A current-voltage model for double Schottky barrier devices* *Advanced Electronic Materials*, **7** (2021) 2000979.
- [8] A. Di Bartolomeo, A. Pelella, A. Grillo, F. Urban, F. Giubileo *Air pressure, gas exposure and electron beam irradiation of 2D transition-metal dichalcogenides* *Applied Sciences* **2020**, **10**, 5840
- [9] A. Di Bartolomeo, A. Grillo, F. Giubileo, L. Camilli, J. Sun, D. Capista, M. Passacantando *Field emission from two-dimensional GeAs* *Journal of Physics D: Applied Physics* **54** (2021) 105302
- [10] A. Di Bartolomeo, A. Pelella, F. Urban, A. Grillo, L. Iemmo, M. Passacantando, X. Liu, F. Giubileo *Field emission in ultrathin PdSe₂ back-gated transistors* *Advanced Electronic Materials* **6** (2020) 2000094

Self-organized patterning and functionalization of surfaces through Nonlinear Laser Lithography

Y. Özgün¹, Abdullah bin Aamir², Sezin Galioglu³, Serim Ilday³, F. Ömer Ilday^{1,2,3*}

¹ Department of Electrical Engineering, Bilkent University, Ankara, 06800, Turkey

² Department of Physics, Bilkent University, Ankara, 06800, Turkey

³ UNAM-National Nanotechnology Research Center & Institute of Materials Science and Nanotechnology, Bilkent University, Ankara, 06800, Turkey

*Corresponding author e-mail (ilday@bilkent.edu.tr)

Laser-induced pattern formation is nearly as old as the laser — the first report dates to 1965. Yet, after several decades, it suffered from poor uniformity and controllability. In 2013, we introduced *nonlinear laser lithography* (NLL), which reached unprecedented levels of uniformity (better than 0.1 nm), long-range order, perfect repeatability, and the possibility to create diverse patterns [1]. We designed the nonlinear dynamics of NLL in analogy to modelocking. Mode-locking creates preferential gain for modes that lock up in phase, leading to a coherent structure in time. We created its analogue by invoking nonlinearities in the form of positive feedback: In NLL, each laser pulse modifies the material surface, and the modified surface changes how the next pulse is scattered, creating a feedback loop (Fig. 1a). A coherent structure grows in space out of initial surface roughness. This growth is regulated by a negative feedback process, as in modelocking. The result is a periodic structure with sub-wavelength periodicity — typically ~ 700 nm when using $1\ \mu\text{m}$ light (Fig. 1b).

NLL can be used to control not only the tribological properties [2] and wettability [3] but also to form nanostructures to orient liquid crystals [4] and even to pattern 2D materials such as graphene [5]. NLL is universally applicable to any material for which a thermally activated chemical reaction occurs, which we have demonstrated over a dozen different materials, including on flexible, bendable glass substrates. More recently, we achieved advanced control over the dynamics to enact a *programmable* sequence of symmetry breakings to create patterns of nearly unbounded complexity (Fig. 1c). An immediate application is the creation of structured color, achieved straightforwardly by diffraction from the nanostructures.

NLL is a fast, maskless, ambient-air fabrication technique. Encouraged by the preliminary indications of compatibility with graphene applications, we might begin to contemplate exploiting the material-dependent feedback mechanism of NLL together with the electro-optic and nonlinear properties of 2D materials. Such an approach may lead to functional and even dynamic adaptive 2D-material coatings on flexible surfaces.

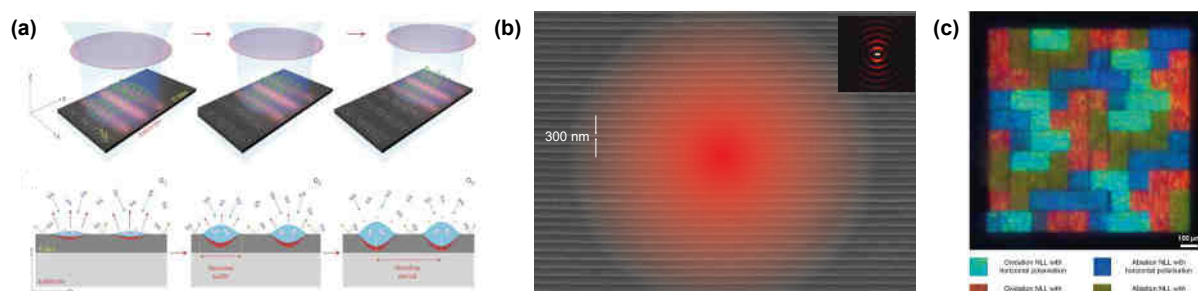


Fig. 1. (a) Top row: schematic of the NLL process is based on the surface being modified, which, in turn, changes how that surface scatters laser light as a laser beam is scanned over the surface. Bottom row: Schematic showing a cross-sectional view of the surface, depicting the deceleration of the growth process due to negative feedback. (b) A typical NLL pattern that was achieved with a $1\text{-}\mu\text{m}$ laser beam. (c) A programmable sequence of symmetry breakings allows the creation of complex patterns.

Acknowledgement.

We acknowledge funding from the European Research Council (ERC) Projects ‘NLL’ and ‘Supersonic’ (Grant agreement Nos. 617521 and 966846) and TÜBİTAK Project (Grant agreement No. 120F147).

References

- [1] B. Öktem, I. Pavlov, S. Ilday, H. Kalaycioglu, A. Rybak, S. Yavas, M. Erdogan and F. Ö. Ilday, *Nonlinear laser lithography for indefinitely large-area nanostructuring with femtosecond pulses*, Nature Photon. 7, 897–901 (2013).
- [2] L. Orazi, Ia. Gnilitzkiy, I. Pavlov, A.P. Serro, S. Ilday, F. Ö. Ilday, *Nonlinear laser lithography to control surface properties of stainless steel*, CIRP Annals – Manufacturing Technology 64, 193–196 (2015).
- [3] S. Ilday, I. Pavlov, O. Tokel, P. Deminskyi, I. Gnilitzkiy, L. Orazi, and F. Ö. Ilday, *Surface engineering via Nonlinear Laser Lithography for efficient shaping, splitting, transport and collection of water at the microscale*, MRS Spring Meeting, Phoenix, AZ, April 2017.
- [4] I. Pavlov, A. Rybak, A. Dobrovolskiy, V. Kadan, I. Blonskiy, F. Ö. Ilday, Z. Kazantseva, I. Gvozdevskyy, *The alignment of nematic liquid crystal by the Ti layer processed by nonlinear laser lithography*, Liq. Cryst., DOI: 10.1080/02678292.2018.1429027 (2018).
- [5] E. Kovalska, I. Pavlov, P. Deminskyi, A. Baldycheva, F. Ö. Ilday, and C. Kocabas, *NLL-assisted multilayer graphene patterning*, ACS Omega 3, 1546–1554 (2018).

The science and art of ultrafast laser writing

P. G. Kazansky

Optoelectronics Research Centre, University of Southampton, SO17 1BJ, UK
pgk@orc.soton.ac.uk

Femtosecond laser writing in transparent materials has attracted considerable interest due to new science and a wide range of applications from laser surgery, 3D integrated optics and optofluidics to optical data storage [1]. Two decades ago it was discovered that under certain irradiation conditions subwavelength periodic structures with record small features of 20 nm, can self-organize in the volume of fused quartz [2-4]. On the macroscopic scale the self-assembled nanostructure behaves as a uniaxial crystal with negative birefringence. The control of the polarization azimuth allows direct writing of flat optics elements with spatially variant anisotropy, which exploits the geometrical or Pancharatnam-Berry phase and in particular S-waveplates for polarization shaping (Fig. 1a) [5]. The applications of S-waveplates ranges from material processing and optical trapping to extreme UV generation [6].

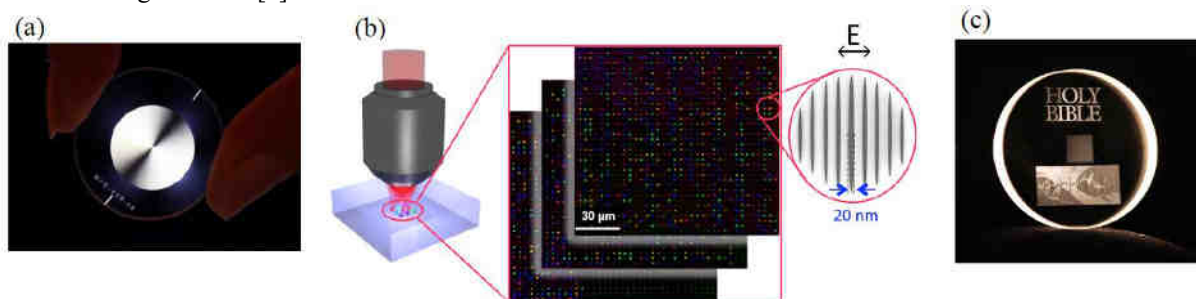


Fig. 1. (a) Femtosecond laser written S-waveplate in cross-polarized light. (b) 5 D optical storage. Each voxel contains a self-assembled nanograting oriented perpendicular to the light polarization. (c) Eternal copy of King James Bible imprinted in silica glass.

More recently ultralow-loss birefringent optical elements including UV retarders and geometrical phase lenses and prisms have been demonstrated exploiting new type of anisotropic nanoporous modification in glass, referred to as Type X [7].

A remarkable phenomenon was also discovered, referred to as quill or calligraphic laser writing, which reveals strong dependence of the material modification, in particular the self-assembled nanostructures, on the writing direction relative to the pulse front tilt [8]. Moreover, coupling of polarization with the angular dispersion, has been demonstrated as a new degree of freedom in ultrafast laser material processing [9].

It was also explored for the optical data storage in the bulk of silica glass, in addition to three spatial coordinates, using two independent parameters of induced form birefringence, the slow axis orientation (4th dimension) and the strength of retardance (5th dimension) (Fig. 1b). The slow axis orientation and retardance can be independently controlled by the polarization and intensity of the femtosecond laser beam. The data optically encoded into five dimensions can be successfully retrieved by quantitative birefringence measurements. The storage allows hundreds of terabytes per disc data capacity and thermal stability up to 1000° and is vital step towards an internal archive (Fig. 1c) [10]. Project Silica is exploiting 5D optical storage in glass for the first-ever storage technology designed and built from the media up, for the cloud [11].

- [1] R. R. Gattas and E. Mazur, "Femtosecond laser micromachining in transparent materials," *Nature Photonics* **2**, 219 (2008).
- [2] P. G. Kazansky, H. Inouye, T. Mitsuyu, K. Miura, J. Qiu, K. Hirao and F. Starrost, "Anomalous anisotropic light scattering in Ge-doped silica glass," *Phys. Rev. Lett.*, **82**, 2199 (1999).
- [3] J. D. Mills et al., "Embedded anisotropic microreflectors by femtosecond-laser nanomachining," *Appl. Phys. Lett.* **81**, 196 (2002)
- [4] Y. Shimotsuma et al., "Self-organized nanogratings in glass irradiated by ultrashort light pulses," *Phys. Rev. Lett.* **91**, 247705 (2003).
- [5] M. Beresna, M. Gecevicius and P. G. Kazansky, "Ultrafast laser direct writing and nanostructuring in transparent materials," *Advances in Optics and Photonics* **6**, 293 (2014).
- [6] C. Hernández-García, et al., "Extreme ultraviolet vector beams driven by infrared lasers," *Optica*, **5**, 520 (2017).
- [7] Y. Lei, M. Sakakura, L. Wang, Y. Yu, R. Drevinskis and P. G. Kazansky, "Low-loss geometrical phase elements by ultrafast laser writing in silica glass," *CLEO, OSA Technical Digest (Optical Society of America, 2019)*, paper ATu4I.4.
- [8] P. G. Kazansky et al., "Quill" writing with ultrashort light pulses in transparent materials," *Appl. Phys. Lett.* **90**, 151120 (2007).
- [9] A. Patel, V. T. Tikhonchuk, J. Zhang and P. G. Kazansky, "Non-paraxial polarization spatio-temporal coupling in ultrafast laser material processing," *Laser & Photonics Reviews* **11** (3) (2017).
- [10] J. Zhang et al., "Seemingly unlimited lifetime data storage in nanostructured glass," *Phys. Rev. Lett.* **112**, 033901 (2014); <https://www.archmission.org/>
- [11] <https://www.microsoft.com/en-us/research/project/project-silica/>

Broadband THz anti-reflection moth-eye structures formed by femtosecond laser processing

Junji Yumoto

*Institute for Photon Science and Technology & Department of Physics School of Science, The University of Tokyo, 7-3-1 Hongo, Bunkyo-ku, Tokyo 113-0033, Japan
yumoto@ipst.s.u-tokyo.ac.jp*

The terahertz (THz) frequency range has become increasingly important for the study of the physics of materials, including superconducting materials and topological insulators. One of the features of THz waves is high field compared with IR and visible light, and this feature is used for the study of nonlinear carrier dynamics and electron acceleration. THz wave detectors with high sensitivity have also been developed and used for the observation of the cosmic microwave background. In addition to physics applications, THz technologies are expected to contribute to security related instrumentation and wireless communications applications. The extraordinary properties of THz waves are expected to open up approaches to new devices and technologies. However, electromagnetic waves in this frequency region resonate with vibration modes of molecules and bandgaps in materials. This resonance causes large absorption and therefore a limited number of materials with less absorption are available for the THz region. Even for materials with less absorption, Fresnel reflection is a serious problem. For example, high-resistivity silicon is one of the most important optical materials for making optical components due to its high transparency to the far-infrared to microwave frequencies, including the THz region. However, since its refractive index in the THz range is about 3.4, 30% of the radiation is lost at every air-silicon interface. As a result, about half of the incident power will be lost for every passive THz silicon component regardless of absorption.

Broadband anti-reflection (AR) functionality has been realized by a moth-eye structure consisting of arrayed tapered protrusions of the substrate material with sub-wavelength dimensions [1]. I will describe the basic principle, the design constraints, fabrication technique and the experimental results which we have achieved with moth-eye structures on high-resistivity silicon as shown in Fig. 1 [2]. The moth-eye structure on sapphire substrates will be also described [3].

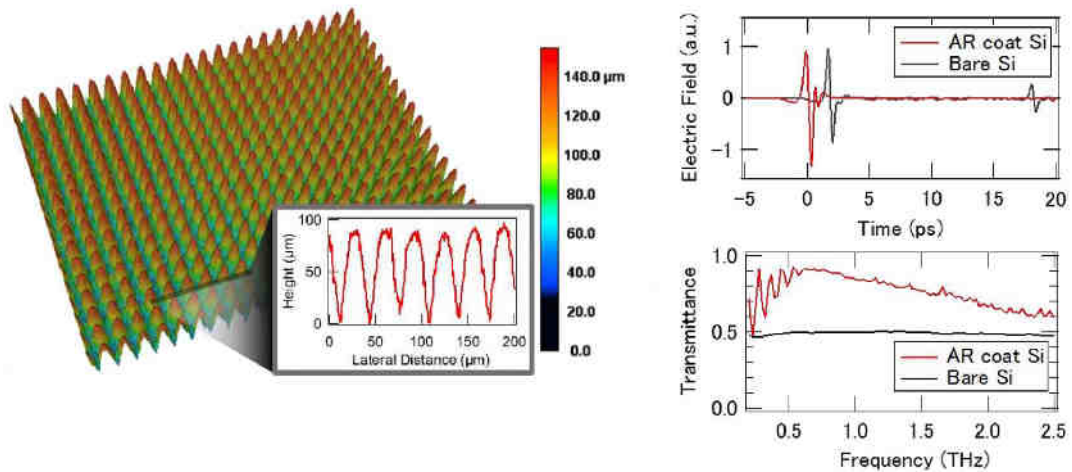


Fig. 1. (a) 3D height profile of a moth-eye-processed silicon substrate, (b) THz-TDS transmission signal and (c) the improved transmission (red) of TDS signal.

[1] S. Wilson and M. Hutley, *Opt. Acta* **29**(7), 993(1982).

[2] H. Sakurai, et al., *OSA CONTINUUM* **2**, 2764 (2019)

[3] R. Takaku, et al., *IRMMW-THz 2019*, Th-Po4-93, Paris (2019)

Poster session I



Multi-layered 3D imaging with CNTs broadband photo-sensors

Y. Kinoshita¹, K. Li^{2,3}, Y. Kawano¹⁻⁴

¹Faculty of Science and Engineering, Chuo University, 1-13-27 Kasuga, Bunkyo-ku, Tokyo 112-8551, Japan

²Department of Electrical and Electronic Engineering, Tokyo Institute of Technology, 2-12-1 Ookayama, Meguro-ku, Tokyo 152-8550, Japan

³Laboratory for Future Interdisciplinary Research of Science and Technology, Tokyo Institute of Technology, 2-12-1 Ookayama, Meguro-ku, Tokyo 152-8550, Japan

⁴National Institute of Informatics, 2-1-2 Hitotsubashi, Chiyoda-ku, Tokyo 101-8430, Japan.
a18.r8js@g.chuo-u.ac.jp

1. Introduction

Non-destructive testing technology is indispensable in the industry. In addition, demand for high-precision internal inspections of 3D-structured objects is increasing, and inspection techniques using electromagnetic waves attracts significant attention. Although conventional non-destructive inspection utilizes X-ray, their hazardous configurations associated with invasiveness need to be addressed. On the other hand, photo-sensing in broadband ranging from infrared (IR) to millimeter-waves (MMW), which non-invasively exhibits high transmittance, potentially solves the above problem. In these bands, CNT films are well known for their highly efficient absorption^[1]. Herein, this study utilizes CNTs photo-thermal broadband sensors for IR–MMW imaging of three-dimensional objects. As a result, the combination of the multi-wavelengths imaging and typical silhouette-based 3D reconstruction techniques^[2] enables non-destructive inspection of multi-layered objects.

2. Result

Fig.1a shows the multi-layered object used in this work. The target object consists of a metallic bar in the center, an inner plastic container around the bar, and an opaque wall at the outside. In addition, glass and silicon boards locate between the plastic container and the opaque wall (Figs. 1b–c presents each sectional view). Directions (1) and (2) in the figure are perpendicular to the glass and silicon faces. The use of near-IR (NIR) irradiation and the CNTs photo-sensor enables non-destructive transmissive imaging of the object. Figs.1d–e shows the obtained images from two different viewing directions. The plastic container is visible in the image obtained from the direction (1), as the NIR irradiation exhibits transparency to the outer wall and the glass. On the other hand, the image obtained from direction (2) does not visualize the plastic container, as the silicon is invisible to the NIR irradiation.

The use of images with different appearances such as the above enables simple 3D reconstruction of the target. Furthermore, the CNTs sensor functions in broadband imaging. Multi-layer 3D reconstruction of the object, employing multiple images obtained by sensing with visible light, IR, terahertz waves, and MMW will be reported at the workshop.

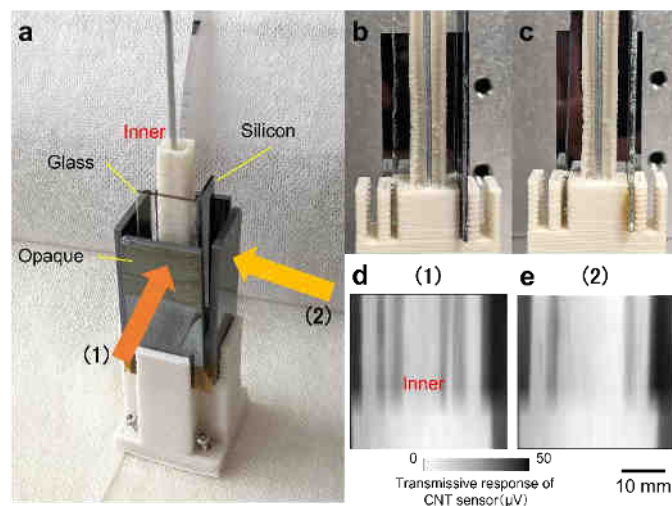


Fig.1. **a**, Photograph of the multilayered object to be examined. **b**, Cross sectional view from direction (1) in **(a)**. **c**, Cross sectional view from direction (2) in **(a)**. Near-infrared imaging with CNTs sensor non-destructively obtains **d**, image from direction (1) in **(a)**, and **e**, image from direction (2) in **(a)**.

3. References

[1] K. Li, et al. Nature Communications, 12, 3009 (2021).

[2] A. Y. Mulyim, U. Yilmaz and V. Atalay, IEEE Transactions on Systems, Man, and Cybernetics, Part B, vol. 33, no. 4, 582-591 (2003)

An all-printable CNT film-type photo-thermoelectric imager

Daiki Sakai¹, Satsuki Yasui^{2,3}, Kou Li^{2,3}, Yukio Kawano¹⁻⁴

¹Department of Science and Engineering, Chuo University, 1-13-27 Kasuga, Bunkyo-ku, Tokyo 112-8551, Japan

²Laboratory for Future Interdisciplinary Research of Science and Technology, Tokyo Institute of Technology, 2-12-1 Ookayama, Meguro-ku, Tokyo 152-8550, Japan

³Department of Electrical and Electronic Engineering, Tokyo Institute of Technology, 2-12-1 Ookayama, Meguro-ku, Tokyo 152-8550, Japan

⁴National Institute of Informatics, 2-1-2 Hitotsubashi, Chiyoda-ku, Tokyo 101-8430, Japan

E-mail: a17.rx5w@g.chuo-u.ac.jp

1. Introduction

CNTs-related materials have excellent physical and chemical properties and, can be adaptable for various applications including solar cells and capacitors. Furthermore, CNT films are flexible and exhibit broadband photo-absorption properties, making them suitable for stereoscopic imaging by employing CNT films as photo-thermoelectric imagers^[1]. On the other hand, from the viewpoint of imaging usage, fine-integration is essential to facilitate high-resolution visualization or video capturing applications.

The conventional method employs the suction filtration process for fabricating the CNT film-type broadband flexible imagers^[2]. The device consists of CNT film channels and electrodes, and also requires the chemical carrier doping on the channel. However, manual alignment of each device material component, which is associated with the suction filtration, has been a bottleneck for realizing the fine-integration of the CNT film imager. To this end, this work reports on the all-printable device fabrication by inkjet dispensers, enabling mechanical alignment of each device material component.

2. Results and discussion

Fig. 1a shows the materials used in printing the CNT film-type photo-thermoelectric imager. The channel printing process employs an aqueous solution at 0.5 wt% concentration of the semiconducting-metallic-mixed SWCNTs. In addition, the dispenser performs the chemical carrier doping with an aqueous solution at 0.7 mol/L concentration of 15 Crown 5 Ether and KOH, and the electrode formation with a conductive mixture paste of silver nanoparticles and acrylic resin. As shown in Fig. 1b, the device consists of the printed channel and electrodes on a polyimide substrate. The channel width, length, and pitch are 300 μm , 10 mm, and 2 mm, respectively. Each half region of the originally P-type CNT film channel at the GND side is chemically doped into N-type, and the PN junction corresponds to the photodetection interface.

The presented approach advantageously enables mechanical alignment of respective device materials, and potentially facilitates fine integration of the CNT film-based flexible broadband imagers.

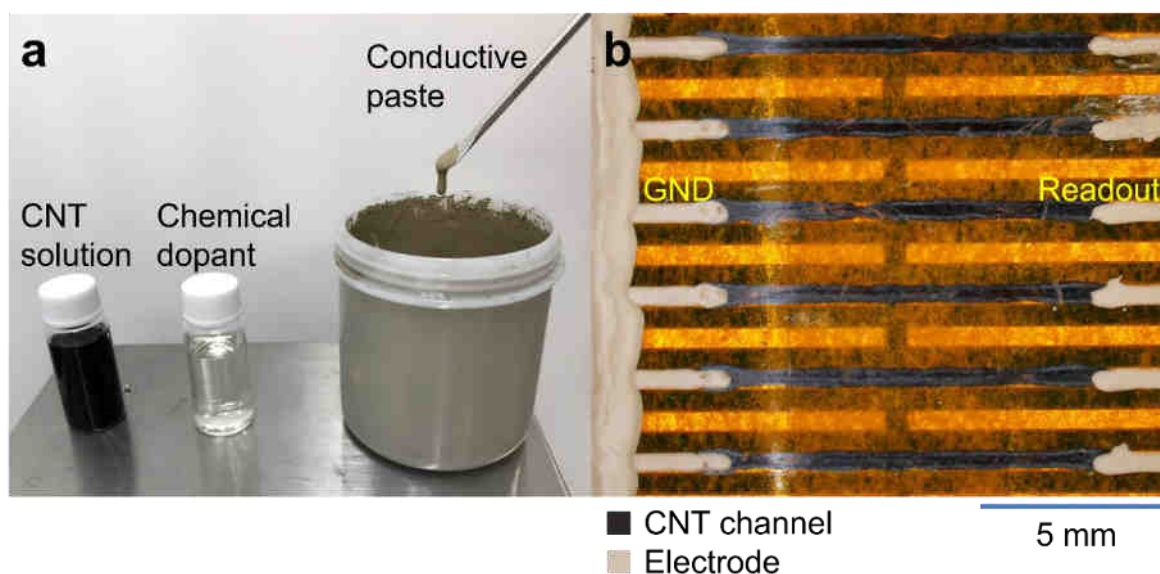


Fig. 1. **a**, Photograph of device component materials for CNT film-type photo-thermoelectric imager. **b**, Photograph of the printed CNT film photodetector.

3. References

[1] K. Li, et al., Nat. Commun., **12**, 3009 (2021).

[2] D. Suzuki, K. Li, K. Ishibashi, Y. Kawano, Adv. Funct. Mater., **31**,14, 2008931 (2021).

Fluorescence Dynamics in Heterostructured *trans*-Stilbene

Renata Karpicz¹, Gabrielė Kareivaitė¹, Mindaugas Mačernis², Darius Abramavičius², Leonas Valkūnas^{1,2}

¹Center for Physical Sciences and Technology, Saulėtekio al. 3, Vilnius, Lithuania

²Institute of Chemical Physics, Faculty of Physics, Vilnius University, Saulėtekio al. 3, Vilnius, Lithuania
Renata.karpicz@ftmc.lt

1. Introduction

A variety of organic molecules, especially diarylethylenes, due to their sensing abilities, is considered promising components of highly sensitive instruments for various applications. A range of this type of molecules demonstrates specific photochemical properties, such as, for instance, *trans-cis* isomerization or variability of the fluorescence lifetime depending on environmental conditions. Stilbene is a classic example of such a type of molecules [1]. For example, stilbene monocrystals have been used in scintillating devices, demonstrating the ability to distinguish between effects caused by different illuminations [2].

2. Result and Discussion

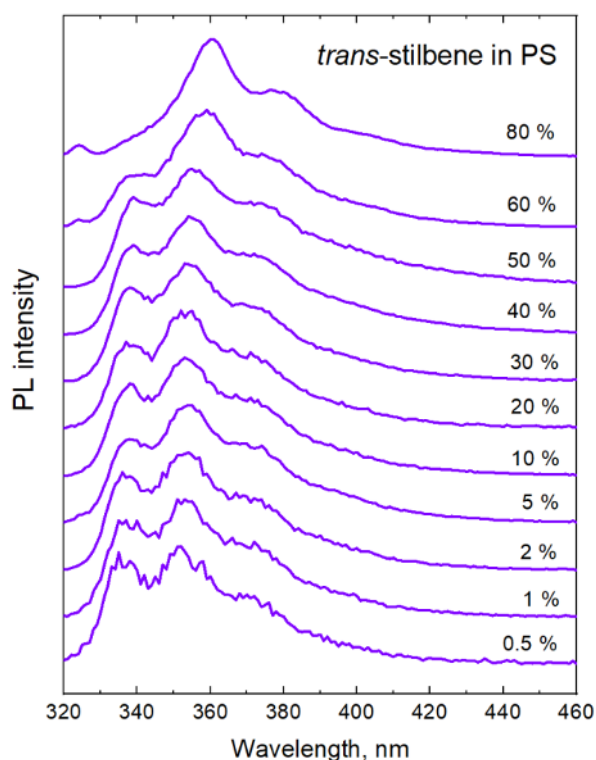


Fig. 1. Photoluminescence spectra of the films with different concentrations of *trans*-stilbene in PS matrix.

In this presentation, studies of the excitation dynamics in polystyrene (PS) films of stilbene are considered in a wide concentration of *trans*-stilbene range, from 0.5% up to 80% wt. The fluorescence spectra and their kinetics are analyzed together with the time-resolved fluorescence measurements performed for the stilbene solutions in chloroform and stilbene in PS matrix. Although there is no isomerization of *trans*-stilbene in PS matrix, by varying concentration, only the aggregates may cause the changes of spectroscopic properties. The increase of *trans*-stilbene concentration resulted in redshift broadening of fluorescence spectral bands (Fig.1). At low concentrations, spectral bands are narrow due to the excitation of separated molecules. The increase in concentration results in the creation of dimers and leads to shorter relaxation times. Contrary to the results obtained in solution and PS matrix, where the excitation dynamics is controlled by molecular twisting process, the fast exciton diffusion yields thermalized exciton distribution and a small number of fluorescence centers responsible for fluorescence line shape and timescale and their temperature dependencies of the bulk solids. The conclusions are also supported by purposeful fluorescence studies at different concentrations of stilbene molecules.

3. Conclusions

Comparing the time-resolved fluorescence of stilbene in solution, PS matrix, and bulk solids, we found that fluorescence decay in solution and PS matrix is controlled by molecular rotation at low stilbene concentrations and nanocluster formation with subsequent aggregation processes at higher stilbene concentrations. The relevant theoretical description explaining these experimental observations based on quantum chemical calculations is analyzed for the stilbene aggregates.

4. Acknowledgement

This work has received funding from European Regional Development Fund under grant agreement No 01.2.2-LMT-K-718-03-0048 with the Research Council of Lithuania (LMTLT).

5. References

- [1] D. H. Waldeck, Chem. Rev., 1991, 91, 415-436
- [2] S. K. Lee, Prog. Nuclear Sci. Techn., 2011, 292-295

Bottom-Up approach for synthesis of structured diamond films

M. Quarshie¹, S. Malykhin¹, P. Kuzhir¹

¹*Department of Physics and Mathematics, University of Eastern Finland, Yliopistokatu 7, FI-80101 Joensuu, Finland*

Corresponding author: Mariam Quarshie, mquarshi@uef.fi

The discovery of how to make synthetic diamonds, as well as their associated 0D, 1D, 2D, and 3D defects, and unique optical, electrical, thermal, chemical, and mechanical properties, has piqued curiosity. Many applications today call for structured diamond arrays, but diamond's hardness and chemical resistance make it challenging to etch and design in top-down approach. Using viewpoints from physics and material science, this research intends to introduce an approach that leverages bottom-up diamond film manufacturing by plasma-enhanced chemical vapor deposition (PECVD) with controlled nucleation sites.

The study used controlled seeding through the masking of seeded Si substrate to prevent diamond growth in the areas covered by mask. Prepared substrates with masks were then used to synthesize diamond films by PECVD technique. Masks made of Au, Cu, SiO₂, TiO₂, and Cr were applied using combination of electron beam lithography and physical vapor deposition methods. PECVD processes were performed at substrate temperature of 720–960 °C and pressure of 98 mbar. Deposited diamond films contained nano-crystalline diamonds, single-crystal diamond needles, and polycrystalline diamond films with diamond phases composing cubic <100>, octahedral <111>, cubo-octahedral (consisting of both <100> and <111> oriented crystals), and twinned faceted faces. The composition and surface morphology of the crystals were studied using scanning electron microscopy and Raman spectroscopy.

The quality of the five diamond suppressing masks deposited by physical vapor deposition was evaluated using scanning electron microscopy, and SiO₂, TiO₂, and Cr masks performed admirably. Synthesized diamond films were optically examined with Raman and photoluminescence spectroscopies at room temperature and revealed NV color centers with narrow zero phonon lines centered at roughly 575 nm (neutral NV centers). The proposed approach is perspective for quantum technological applications due to the successful structuring of diamond films.

This work was supported by H2020 RISE Graphene 3D (734164) project and Academy of Finland (decision 340733). The work is part of the Academy of Finland Flagship Programme, Photonics Research and Innovation (PREIN), decision 320166.

Spectroscopic characterization of nanodiamonds with sp²-sp³ graphene-like shell

Yaraslau Padrez¹, Lena Golubewa¹, Tatsiana Kulahava¹, Boris Zousman², Olga Levinson²,
Renata Karpicz¹ and Polina Kuzhir³

¹State research institute Center for Physical Sciences and Technology, Sauletekio Av. 3, Vilnius, LT-10257, Lithuania

²Ray Techniques Ltd., Israel

³University of Eastern Finland, Yliopistokatu 7, Joensuu, 80101, Finland
yaraslau.padrez@fmf.lt

1. Introduction

Fluorescent nanodiamonds (FNDs) are promising objects for various applications spreading from biomedical ones, where FNDs are used as fluorescent labels for bioimaging and systems for drug delivery [1], to optical sensing of chemical reactions and controlling of environmental parameters such as temperature, pH, etc. FNDs exhibit a low level of toxicity and are biocompatible. However, spectroscopic properties of FNDs strongly depend on synthesis procedure. Precise determination of the origin and mechanisms of photoluminescence (PL) will allow more effectively using the specific features of FNDs in particular application areas.

2. Result and Discussion

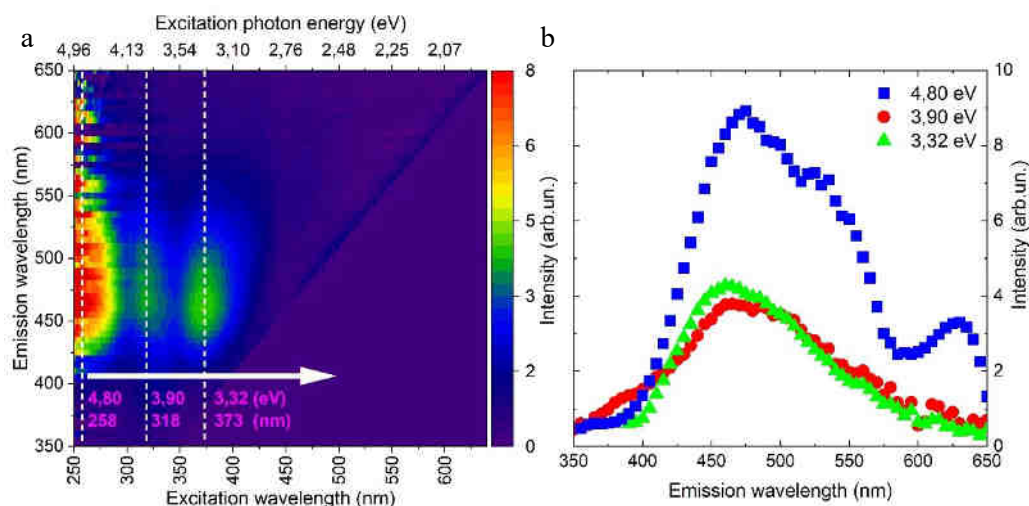


Fig. 1: a) PLE mapping and b) PL spectra for 258, 318 and 373 nm excitation wavelengths of 0.01% FND water solution

In the present work, high-purity and high-homogeneity solutions of FNDs (RayND-M, Ray Techniques Ltd) produced by laser synthesis were investigated. They have core-shell structure as they have diamond inner core (sp³ carbon atoms) and chemically active hybrid graphene-like outer shell (sp² carbon atoms) with hanging bonds ended with functional groups.

On the photoluminescence excitation (PLE) mapping (Fig.1a) of 0.01% FND water solution, three areas of pronounced emission are present. For these areas, excitation photon energies tentatively correspond to 4.80, 3.90 and 3.32 eV (Fig.1b). The first one (at 258 nm) is associated with $\pi \rightarrow \pi^*$ transition of the C=C bond. The other two, less pronounced, around 318 and 373 nm, are more likely associated with the presence of oxygen functional groups (C=O/COOH) on hybrid graphene-like structures on the FND surface or related to lattice defects and impurities like in natural and synthetic diamonds [2]. These groups in line with heterogeneity of graphene-like sheets in the shell determine excitation dependent PL of FNDs.

3. Conclusions

Investigated FNDs are unique multifunctional nanoobjects, which have specific PLE properties and can be applied for e.g., multiwavelength imaging, pH-sensing through COOH groups presented on the FNDs surface.

4. Acknowledgement

This work was supported by Horizon 2020 RISE DiSeTCom (Project No 823728) and Academy of Finland (Flagship Programme PREIN, decision 320166).

5. References

- [1] S. Prabha, D. Durgalakshmi, S. Rajendran, and E. Lichtfouse, *Environ Chem Lett*, **19**, 2, 1667–1691 (2021)
- [2] A. E. Aleksenskii, A. Ya. Vul', S. V. Konyakhin, K. V. Reich, L. V. Sharonova, and E. D. Eidel'man, *Phys. Solid State*, **54**, 3, 578–585 (2012).

Random graphene metasurfaces as a perfect broadband THz absorber

Isaac Appiah Otoo¹, Andrey Novitsky², Alesia Paddubskaya², Markku Pekkarinen¹, Yuri Svirko¹, Polina Kuzhir¹

¹Institute of Photonics, Department of Physics and Mathematics, University of Eastern Finland, Joensuu, Finland

²Independent researcher
iisaac.appiah.otoo@uef.fi

We present theoretical model and experimental investigation of THz metasurface made of an array of hemispheres made of defected multilayer graphene covered with a thin (100-200 nm) PMMA layer. The fabrication flow of the structure is sketched in Fig. 1 and involves ink-jet 3D printing, Ni sputtering and electroplating followed by chemical vapor deposition (CVD) of graphene on the top of Ni support, which shape reproduces that of the polymer 3D printed template.

The fabricated structure (Fig.2), i.e. a bubble wrap polymer nanomembrane covered with multilayered graphene, demonstrates extreme broadband and almost perfect absorption at THz frequencies and shows robustness against macroscopic random structural defects of the two-dimensional periodic lattice.

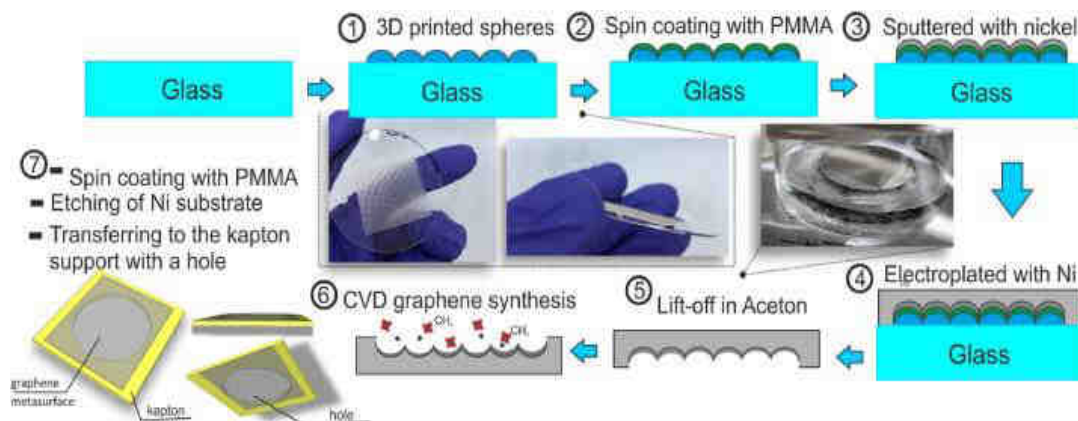


Fig. 1. Fabrication flow of free-standing graphene metasurface.

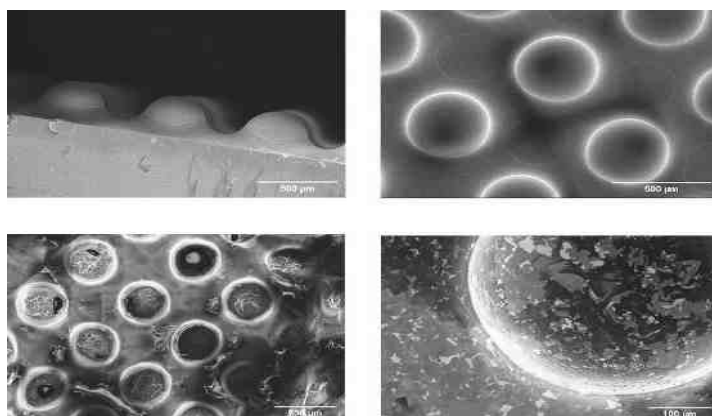


Fig. 2. (a), (b) SEM images of 3D printed polymer nanomembrane hemispheres on a silica substrate (polymer template). (c) SEM images of the graphene-based metasurface ("bubble wrap" polymer nanomembrane covered with graphene) and (d) hemisphere unit cell.

Moreover, these defects may result in the enhancement of the absorptance ability of the free-standing THz metasurface. The conductivity of graphene metasurface can be tuned by changing it's the Fermi energy level by applying external stimuli including electrostatic doping. Full control of the graphene metasurface can be achieved if the voltage is independently applied to individual unit cells.

We propose a method that enables a closed-form description of a so-called random metasurface comprising unit cells randomly distributed on the planer substrate and having different properties.

[1] A. Paddubskaya, N. Valynets, S. Maksimenko, M. Kumar, M. Baah, M. Pekkarinen, Y. Svirko, G. Valusis, P. Kuzhir, THz photonics with graphene enhanced polymer hemispheres array, *Nanomaterials* 2021, 11(10), 2494

[2] A. Novitsky, A. Paddubskaya, I. A. Otoo, M. Pekkarinen, Y. Svirko, P. Kuzhir, Random Graphene Metasurfaces: Diffraction Theory and Giant Broadband Absorptivity, *Phys. Rev Applied*, 17, 044041 (2022)

Terahertz imaging of optically modulated graphene layers

Rusnė Ivaškevičiūtė-Povilauskienė¹, A. Paddubskaya², D. Seliuta¹, D. Jokubauskis¹, L. Minkevičius¹,
A. Urbanowicz¹, I. Matulaitienė¹, L. Mikoliūnaitė¹, P. Kuzhir³, Natalia Alexeeva¹ and G. Valušis¹

¹ Center for Physical Sciences and Technology, Saulėtekio av. 3, Vilnius, 10257, Lithuania

² Institute for Nuclear Problems of Belarusian State University, Bobruiskaya Str. 11, Minsk 220006, Belarus

³ University of Eastern Finland, Yliopistokatu 7, Joensuu 80101, Finland

rusne.ivaskeviciute@ftmc.lt

Terahertz (THz) imaging systems are currently one of the most attractive tools in many types of applications [1]. Real implementation require that all systems elements, both active and passive, would be compact and convenient in use.

Exceptional properties of graphene [2] make it attractive for a large variety of THz applications, including, for instance, production of diffractive optical elements, filters or modulators. However, this approach stimulates a strong need to develop characterization techniques – preferably contactless – to control properties and quality of this material.

In this work, it was demonstrated that optical modulation [3] together with simultaneous terahertz (THz) imaging application enables characterization of samples based on single and double layer graphene transferred on a high resistivity silicon (Si) substrate.

It was demonstrated that an optical excitation applied simultaneously with THz imaging allows to increase a contrast by an order of magnitude illustrating that the technique can be found as convenient contactless tool for characterization of graphene deposited on high-resistivity silicon substrates. Furthermore, it was shown that the single- and double-layer graphene can be discriminated and characterized via variation of THz image contrast using a discrete frequency in a continuous wave mode. Modulation depth of 45 % has been reached, the contrast variation from 0.16 up to 0.23 is exposed under laser illumination for the single and double layer graphene, respectively (see Fig.1).

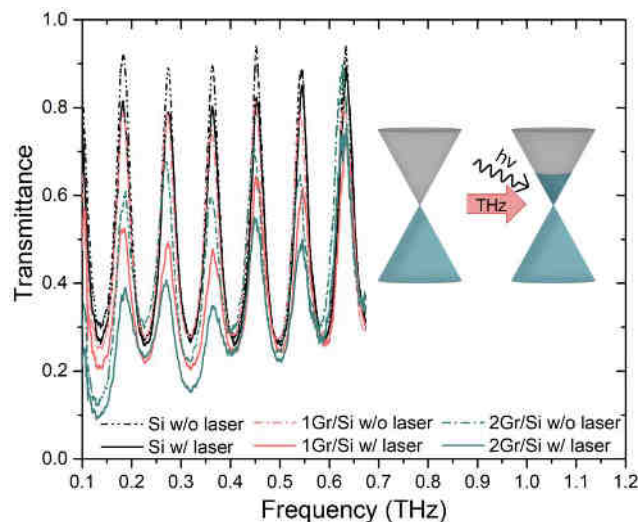


Fig.1. Transmittance spectrum of bare Si, single and double graphene layers. Inset depicts graphene's Dirac cones before and after photoexcitation.

Possibilities to apply the technique for investigation of graphene-based THz diffractive elements will be illustrated in addition.

References

- [1] G. Valušis, A. Lisauskas, H. Yuan, W. Knap and H. G. Roskos, *Sensors*, **21**, 4092 (2021).
- [2] R. Binder, *Optical Properties of Graphene*, (University of Arizona, USA, 2016).
- [3] M. Fu, X. Wang, S. Wang, Z. Xie, S. Feng, W. Sun, J. Ye, P. Han and Y. Zhang, *Optical Materials*, **66**, 381-385 (2017).

Single-walled carbon nanotubes defected by ion beams

Valentina A. Eremina, Petr A. Obratsov, Yuri P. Svirko, Elena D. Obratsova

University of Eastern Finland, Joensuu, Finland
valentina.eremina@uef.fi

Defective single-walled carbon nanotubes (SWCNTs) is a promising material for various applications such as nanowire processing [1], beams control [2], cross-linking [3], optoelectronics [4], and others. There are several ways to create defects in SWCNTs. One of them is the use of ion beams [5,6]. Accepting the stability of SWCNTs over the energetic ion beams and investigating the irradiation with different fluences it is possible to controllably create the required amount of defects in SWCNTs. Raman spectroscopy is a powerful tool for the estimation of the amount and type of defects in SWCNTs [7].

In the work, we used single-walled carbon nanotubes produced by OCSiAl company with an average diameter equal to 1.8 nm. We prepared thin films on the Si or glass substrates and irradiated them with Ar and He ions with energies of 80 and 50 keV respectively. We varied fluences from 10^{12} to $2 \cdot 10^{16}$ ions/cm² in order to achieve the smooth change of the defects density up to the amorphous stage. We conclude the defectiveness of SWCNTs by Raman spectra.

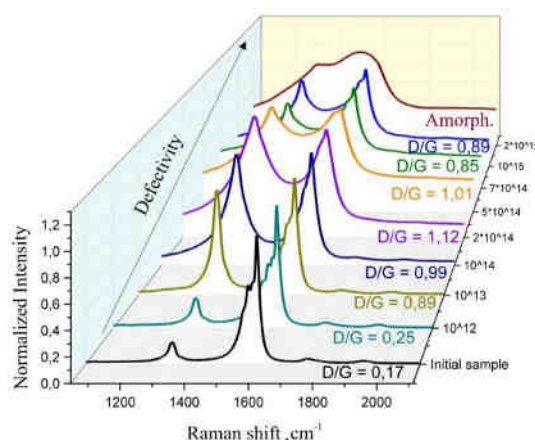


Fig. 1. Raman spectra of defected single-walled carbon nanotubes by Ar⁺ ions

In some applications, it is important to further modify the properties of SWCNTs by various dopants [8]. We used a gas-phase technique to obtain the doping of SWCNTs with iodine [9-10]. We found by Raman spectra and by the UV-vis-NIR absorbance spectroscopy that the effectiveness of doping can be increased for ion irradiated SWCNTs with low fluences. We also found that the conductivity of the films with any level of defectiveness was dramatically reduced after the iodine doping.

Acknowledgments:

The research was funded by the Academy of Finland project 340831.

- [1] Yun, W. S., Kim, J., Park, K. H., Ha, J. S., Ko, Y. J., Park, K., ... & Forró, L. (2000). Fabrication of metal nanowire using carbon nanotube as a mask. *Journal of Vacuum Science & Technology A: Vacuum, Surfaces, and Films*, 18(4), 1329-1332.
- [2] D'Acunto, G., Ripanti, F., Postorino, P., Betti, M. G., Scardamaglia, M., Bittencourt, C., & Mariani, C. (2018). Channelling and induced defects at ion-bombarded aligned multiwall carbon nanotubes. *Carbon*, 139, 768-775.
- [3] Krashennnikov, A. V., Nordlund, K., Keinonen, J., & Banhart, F. (2002). Ion-irradiation-induced welding of carbon nanotubes. *Physical Review B*, 66(24), 245403.
- [4] Sevik, C., Sevincli, H., Cuniberti, G., & Cagin, T. (2011). Phonon engineering in carbon nanotubes by controlling defect concentration. *Nano Letters*, 11(11), 4971-4977.
- [5] Zhang, Y., Chen, L., Xu, Z., Li, Y., Shan, M., Liu, L., ... & Wang, C. (2012). Effects of ion irradiation on carbon nanotubes: a review. *International Journal of Materials and Product Technology*, 45(1-4), 1-30.
- [6] Shemukhin, A. A., Stepanov, A. V., Nazarov, A. V., & Balakshin, Y. V. (2019). Simulation of defects formation in nanotubes under ion irradiation. *Nuclear Instruments and Methods in Physics Research Section B: Beam Interactions with Materials and Atoms*, 460, 230-233.
- [7] Dresselhaus, M. S., Jorio, A., Souza Filho, A. G., & Saito, R. (2010). Defect characterization in graphene and carbon nanotubes using Raman spectroscopy. *Philosophical Transactions of the Royal Society A: Mathematical, Physical and Engineering Sciences*, 368(1932), 5355-5377.
- [8] Terrones, M., & Rao, A. M. (2007). Doped carbon nanotubes: synthesis, characterization and applications. In *Carbon nanotubes* (pp. 531-566). Springer, Berlin, Heidelberg.
- [9] Tonkikh, A. A., Obratsova, E. D., Obratsova, E. A., Belkin, A. V., & Pozharov, A. S. (2012). Optical spectroscopy of iodine-doped single-wall carbon nanotubes of different diameter. *physica status solidi (b)*, 249(12), 2454-2459.
- [10] Tonkikh, A. A., Tsebro, V. I., Obratsova, E. A., Suenaga, K., Kataura, H., Nasibulin, A. G., ... & Obratsova, E. D. (2015). Metallization of single-wall carbon nanotube thin films induced by gas phase iodination. *Carbon*, 94, 768-774.

Wednesday, August 3



Terahertz beam engineering in imaging: from designs to applications

**Linās Minkevičius, Domas Jokubauskis, Rusnė Ivaškevičiūtė-Povilauskienė, Irmantas Kašalynas,
Natalia Alexeeva, Andzej Urbanowicz, and Gintaras Valušis**

*Optoelectronics Department, Center for Physical Sciences and Technology, Sauletekio ave. 3, LT-10257, Vilnius, Lithuania
Corresponding author e-mail: gintaras.valusis@ftmc.lt*

Laser beam engineering is one of the main techniques widely used in microfabrication and laser ablation, therefore, its management possibilities play essential role aiming to optimize a large variety of laser-material processing applications [1].

Room temperature terahertz (THz) imaging is a powerful tool for non-destructive inspection covering different kind of materials, security checks, or medical scanning [2]. However, practical implementation of compact THz imaging and spectroscopy systems in real outside laboratory environment still meets significant obstacles because of low powers of THz emitters, reliability of sensitive THz detectors and effective solutions in design and technology of planar optical components. In particular, it gains a significant importance if the aim is alignment-free THz imaging systems. Therefore, design solutions in passive optical THz components in reducing their dimensions remains one of the main topics in THz photonics. As a rule, investigated objects are bulky, hence, bearing in mind the fact that image quality is strikingly sensitive to the sample position in respect to diffractive optical elements, obtained images can be blurred resulting in complication to resolve the recorded data.

In this lecture, we present silicon-based THz beam profile engineering via planar optics solutions providing both compact focusing as well as extended focus geometry in THz imaging and enabling thus precise inspection of thick objects with weak sensitivity of the object position.

We have revealed recently that thin silicon based multilevel phase Fresnel lenses are suitable solution for optical components for the entire THz range [3]. It was exposed that at least 4 and up to 8 phase quantization levels are required for efficient diffractive element compromising the performance and fabrication complexity of phase structures. We extended the silicon optics approach to so-called Fibonacci or bifocal THz imaging and Bessel THz imaging employing diffractive zone plates fabricated by laser ablation technology [3,4]. Zone plates simulated by 3D finite-difference-time-domain method displayed bifocal focusing operation. Features of the performance were studied both theoretically and experimentally via spatial profiles, distances between the foci and the focal depth at frequencies of 0.3 THz and 0.6 THz. Terahertz images of various packaged objects at 0.6 THz frequency were simultaneously recorded with the spatial resolution of the wavelength in two different planes of the packaged volume. It is worth noting that Bessel zone plates provide a $2\times\lambda$ resolution at 0.6 THz frequency with weak dependence of the object positioning between the diffractive elements [5].

THz beam engineering properties using flexible materials shaped in zone plates with integrated filters will be considered.

Further steps in development of THz beam profile engineering in imaging and its application for investigation of carbon-based materials will be discussed as well.

The support from the project Dirac Semimetals based Terahertz Components (DISETCOM) in carbon-related research is sincerely acknowledged.

- [1] G. Račiukaitis, E. Stankevičius, P. Gečys, M. Gedvilas, Ch. Bischoff, E. Jäger, U. Umhofer, F. Völklein, *Journal of Laser Micro/Nanoengineering*, **6**, 37 (2011).
- [2] G. Valušis, A. Lisauskas, H. Yuan, W. Knap and H. G. Roskos, *Sensors*, **21**, 4092 (2021)
- [3] L. Minkevičius, S. Indrišiūnas, R. Šniaukas, B. Voisat, V. Janonis, V. Tamošiūnas, I. Kašalynas, G. Račiukaitis and G. Valušis, *Optics Letters*, **42**, 1875 (2017).
- [4] D. Jokubauskis, L. Minkevičius, M. Karaliūnas, S. Indrišiūnas, I. Kašalynas, G. Račiukaitis and G. Valušis, *Optics Letters*, **43**, 2795 (2018).
- [5] L. Minkevičius, D. Jokubauskis, I. Kašalynas, S. Orlov, A. Urbas and G. Valušis, *Optics Express*, **27**, 36358 (2019).

Hybrid perovskites based photoconductive THz pulse emitters and detectors

Petr A. Obraztsov^{1,2}, Pavel A. Chizhov², Dmitry S. Gets³, Vladimir V. Bukin², Olga I. Semenova⁴, Sergey V. Makarov³

1. Institute of Photonics, University of Eastern Finland, 80101 Joensuu, Finland

2. Prokhorov General Physics Institute of RAS, 119991 Moscow, Russia

3. Department of Physics and Engineering, ITMO University, 197101 St. Petersburg, Russia

4. Rzhanov Institute of Semiconductor Physics, 630090 Novosibirsk, Russia

petr.obraztsov@uef.fi

The main properties of halide perovskites useful for solar cells make them also attractive for terahertz (THz) applications. This class of materials, well studied in the optical range, remains much less studied in the THz range. Meanwhile, increasing the efficiency of pulsed terahertz sources and detectors due to more advanced designs or new materials is one of the main directions in the field of terahertz technologies.

Here, we experimentally demonstrate the first attempt to apply solution-processed polycrystalline films of hybrid perovskites for the development of photoconductive terahertz emitters and detectors. By using polycrystalline films and single crystals of widely studied methylammonium-based perovskites MAPbI₃ and MAPbBr₃, we fabricate and characterize large-aperture photoconductive antennas [1]. The combination of ultrafast time-resolved spectroscopy and terahertz emission experiments allows us to determine the still-debated room temperature carrier lifetime and mobility of charge carriers in halide perovskites using an alternative noninvasive method. The ultrafast change of conductivity that occurs in single crystals and polycrystalline films of lead methylammonium halides excited by a femtosecond laser both above and below the bandgap enables efficient emission and detection of THz radiation [2]. Under excitation with 40 fs pulses centered at 400 nm the fabricated perovskite photoconductive detectors in the frequency range of 0.1-2 THz demonstrate detectivity comparable to traditional detectors based on electro-optical sampling in nonlinear crystals [3].

The results demonstrate the viability of solution-processable halide perovskite for the fabrication of photoconductive THz antennas and the further development of scalable and cost-effective sensor manufacturing for THz time-domain spectroscopy, imaging, and other photonic THz devices.

[1] P. Obraztsov, D. Lyashenko et al. *Commun Phys* **1**, 14 (2018)

[2]. P. Obraztsov, V. Bulgakova et al. *Nanomaterials* **11**, 313 (2021)

[3]. P.Obraztsov, P.Chizhov et al. *ACS Photonics* **9**, 1663 (2022).

Protonation of oxygen doped single-walled carbon nanotubes

Timofei V. Eremin, Petr A. Obratsov, Elena D. Obratsova

University of Eastern Finland, Joensuu, Finland
timofei.eremin@uef.fi

Oxygen-doped single-walled carbon nanotubes (O-SWNT) attract huge interest because such nanotubes demonstrate brighter luminescence compared to pristine nanotubes [1] and possess such advances as photon antibunching [2], both due to inducing 0D-like excitonic states in addition to ordinary 1D excitons of pristine nanotubes. However, such aspect as the susceptibility of 0D states to the local environment, is not been sufficiently investigated so far, unlike the case of 1D states in pristine nanotubes.

To unveil this issue, we performed oxygen doping of single-walled carbon nanotubes by adding NaOCl to the SWNT aqueous suspension followed by lingering UV irradiation [3]. Efficient oxygen doping was confirmed by the appearance of a bright photoluminescence peak corresponding to recombination of 0D excitons which is redshifted from the ordinary photoluminescence peak corresponding to recombination of 1D excitons (Fig.1). Subsequently, a protonation of SWNT was performed by adding HCl to the suspension and the dependencies of 1D and OD-states photoluminescence intensity on the concentration of HCl were investigated. It was found that OD states demonstrate sufficiently higher sensitivity to pH compared to 1D states of both oxygen-doped and pristine nanotubes. Differences in sensitivity of 1D and 0D states may reflect differences in the distribution of electronic and hole states, which 0D and 1D excitons consist of.

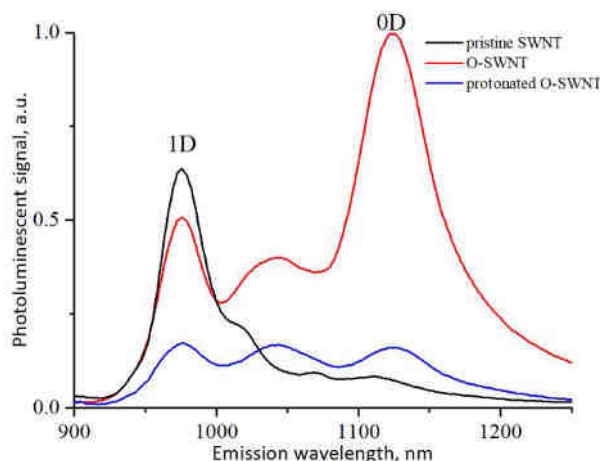


Fig.1. Photoluminescence spectra of pristine SWNTs (black line), oxygen doped SWNT before protonation (red line) and oxygen doped SWNT after protonation (blue line).

This work was supported by Academy of Finland project #340831

[1] Ghosh S. et al. Oxygen doping modifies near-infrared band gaps in fluorescent single-walled carbon nanotubes // *Science*. 2010. Vol. 330, № 6011. P. 1656–1659.

[2] Ma X. et al. Room-temperature single-photon generation from solitary dopants of carbon nanotubes // *Nat. Nanotechnol.* Nature Publishing Group, 2015. Vol. 10, № 8. P. 671–675.

[3]. Lin C.W. et al. Creating fluorescent quantum defects in carbon nanotubes using hypochlorite and light // *Nat. Commun.* Springer US, 2019. Vol. 10, № 1.

Detection of terahertz radiation with graphene-based plasmonic interferometers

G. Fedorov, D. Bandurin I. Gayduchenko, Y. Matyushkin, M. Moskotin, S. Ganichev, D. Svintsov, G. Goltzman

Moscow Institute of Physics and Technology (State University), Dolgoprudny, Russia

Massachusetts Institute of Technology, Cambridge, USA

Physics Department, Moscow State University of Education (MSPU), Moscow, Russian Federation

Terahertz Centre, University of Regensburg, Regensburg, Germany

fedorov.ge@mipt.ru

1. Introduction

Plasmons, collective oscillations of electron systems, can efficiently couple light and electric current, and thus can be used to create sub-wavelength photodetectors, radiation mixers, and on-chip spectrometers. Despite considerable effort, it has proven challenging to implement plasmonic devices operating at terahertz frequencies. The material capable to meet this challenge is graphene as it supports long-lived electrically tunable plasmons. In this talk we discuss plasmon-assisted detection of terahertz radiation by antenna-coupled graphene-based transistors that act as both plasmonic Fabry-Perot cavities and rectifying elements.

2. Resonant detection of terahertz radiation

First we discuss observed resonant enhancement of detector response when the channel using FETs based on high-quality van der Waals heterostructures [1]. In particular, we employ graphene encapsulated between hexagonal boron nitride (hBN) crystals which have been shown to provide the cleanest environment for long-lived graphene plasmons. Antenna-mediated coupling of such FETs to freespace radiation results in the emergence of dc photovoltage that peaks when the channel hosts an odd number of plasmon quarter-wavelengths. Exploiting the gate-tunability of plasmon velocity, we switch our detectors between more than 10 resonant modes, and use this functionality to measure plasmon wavelength and lifetime. Thanks to the far-field radiation coupling, our compact devices offer a convenient tool for studies of plasmons in two-dimensional electron systems under non-ambient conditions (e.g. cryogenic environment and high magnetic fields) where other techniques may be arduous.

3. Helicity sensitive detector based on plasmon interference

Next, we discuss how plasmonic effects could be recognized even when CVD-grown graphene is used. By using a specially designed antenna and controlling ellipticity and helicity of the THz radiation [2] we can tune the phase difference between the plasma waves excited at the source and drain electrodes. With a channel length and radiation frequency from 700GHz to 2.5 THz our data unambiguously show that response of such detectors is determined by the interference of plasmons in the transistor channel. As a result, these devices operate as all-electric detectors of the helicity of circularly polarized terahertz radiation that can be further used in terahertz optoelectronics

3. Acknowledgement.

The work was supported by the Russian Foundation for Basic Research (Project 18-29-20116).

4. References

- [1] D. Bandurin, et al, Nature communications, **9**, 5392 (2018).
- [2] Matyushkin, et al., submitted.

Ultra-wideband graphene-based absorbers for THz integrated waveguide systems

Nikolaos Xenidis^a, James Campion^{a,c}, Serguei Smirnov^a, Aleksandra Przewłoka^{b,d}, Aleksandra Krajewska^b, Piotr A. Drozd^b, Albert Nasibulin^{d,e}, Joachim Oberhammer^a, Dmitri Lioubtchenko^{a,b}

^aKTH Royal Institute of Technology, Malvinas vag, Stockholm, SE-100 44, Sweden

^bCENTERA Laboratories, Institute of High Pressure Physics PAS, ul. Sokolowska, Warsaw, 01-142, Poland

^cTeraSi AB, Kolviksvägen 38, Stockholm, SE-139 33, Sweden

^dInstitute of Optoelectronics, Military University of Technology, ul. gen. Sylwestra Kaliskiego 2, Warsaw, 00-098, Poland

^eDepartment of Chemistry and Materials Science, Aalto University, Finland

^fSkolkovo Institute of Science and Technology, Russia

dml@kth.se

Historically, terahertz science and technology has been restricted to specialized applications such as radio astronomy due to various technological challenges. Hollow rectangular waveguides are the primary transmission line medium in many terahertz systems due to their mechanical stability, low electromagnetic losses, enclosed nature, and compatibility with active circuit elements. Electromagnetic wave devices such as circulators, couplers and power dividers require that one or more of their ports be terminated to eliminate unwanted signals and ensure correct operation. Waveguide terminations are often realized by short-circuited waveguide sections that present low reflection and absorb the incident energy due to the presence of an absorbing material inside the waveguide [1]. We proposed a new kind of ultra-wideband THz absorber which can be directly integrated into a standard metallic waveguide (Fig. 1a-c) [2], allowing it to be used in conventional THz systems.

In order to analyze the electromagnetic properties of the absorbing materials in the frequency range from 67 GHz to 500 GHz, the absorbing material has to be embedded inside a waveguide. At the sub-millimeter frequencies, these dimensions get too small to insert any absorber material; therefore, we use vacuum filtration to directly deposit the absorber material inside a specialized waveguide cassette. This cassette can then be integrated with a waveguide system for material characterization. The integration method developed here is easily scalable to different frequency ranges and waveguide geometries and requires only standard laboratory equipment and techniques, making it viable for high-volume production. In addition, by utilising the same method with precision silicon micromachined components [3], our approach could be used to develop compact, low-cost THz waveguide absorbers of complex geometry.

The attenuation of the embedded samples across a wide band of frequencies is shown in Fig. 1c. The measured insertion loss between 67 GHz to 110 GHz is greater than 20 dB and exceeds 40 dB at frequencies above 400 GHz. The reflection coefficient of the samples measured below 200 GHz is in excess of -10 dB, indicating that much of the incident energy is reflected by the step change in impedance at the material's interface at these frequencies. The short electrical length of the samples at these frequencies ($0.2\lambda_0$ at 88.5 GHz) leads to a relatively low insertion loss, despite the material's high reflectivity. Above 200 GHz, the GAIN samples exhibit a reflection coefficient below -10 dB.

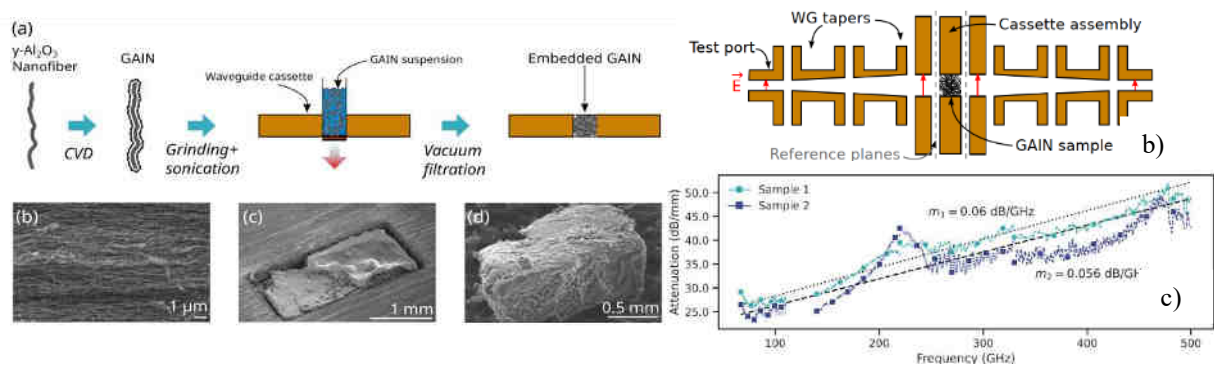


Fig.1. Schematic of a) method of deposition, b) wideband waveguide measurement setup. c) Measured attenuation of the absorbers

References

- [1] I.V. Anoshkin, J. Campion, D.V. Lioubtchenko, J. Oberhammer "Freeze-dried carbon nanotube aerogels for high frequency absorber application" *ACS Applied Materials & Interfaces*, **10** (23), 2018, pp 19806–19811.
- [2] J. Campion, N. Xenidis, S. Smirnov, R. Ivanov, J. Oberhammer, I. Hussainova, D. Lioubtchenko, "Ultra-Wideband Integrated Graphene-Based Absorbers for Terahertz Waveguide Systems" *Advanced Electronic Materials*, 2022, pp. 22001106,
- [3] Campion, J. and Oberhammer, J., "Silicon Micromachined Waveguide Calibration Standards for Terahertz Metrology", *IEEE Transactions on Microwave Theory and Techniques*, **69** (8), 2021, pp.3927-3942.

A mechanically stretchable and optically broadband imager sheet

Kou Li^{1,2}, Yukio Kawano¹⁻⁴

¹Laboratory for Future Interdisciplinary Research of Science and Technology, Tokyo Institute of Technology, 2-12-1 Ookayama, Meguro-ku, Tokyo 152-8552, Japan

²Department of Electrical and Electronic Engineering, School of Engineering, Tokyo Institute of Technology, 2-12-1 Ookayama, Meguro-ku, Tokyo 152-8552, Japan

³Department of Electrical, Electronic, and Communication Engineering, Faculty of Science and Engineering, Chuo University, 1-13-27 Kasuga, Bunkyo-ku, Tokyo 112-8551, Japan

⁴National Institute of Informatics, 2-1-2 Hitotsubashi, Chiyoda-ku, Tokyo 101-8430, Japan
lee.k.al@m.titech.ac.jp

1. Introduction

This work presents the fabrication of a mechanically stretchable and optically broadband imager sheet. As photo-visualization techniques non-destructively capture physical information in large areas, the use of imager devices facilitate variety of applications including industrial testing, agricultural monitoring, and security screening. For the sensing of transformable objects such as soft liquid tubes, plants, and so on, mechanical stretchability is essential for the imager to stably attach to the outer surface of targets. However, studies on developing stretchable imagers are yet to be fully performed, and some existing stretchable photodetectors only function in narrow ultraviolet or visible light bands. To this end, this work integrates carbon nanotube (CNT) films-based flexible and high efficient broad infrared (IR)-terahertz (THz) absorbers and soft device frameworks. The device collectively satisfies transmissive inner imaging of opaque objects and repetitive mechanical deformation, demonstrating non-destructive inspections of arbitral-structure targets^[1].

2. Results

Fig. 1a shows the proposed device. The device consists of flexible CNT film channels and stretchable silver nanoparticles-based stretchable electrodes, and a polyurethane film stretchable substrate. The device functions under photo-thermoelectric (PTE) effect in broadband frequency regions ranging from near-IR to sub-THz, and the PN junction at the center of the channel serves as the photodetection interface^[2]. As shown in Fig. 1b, the use of the device enables photodetection even during the whole device stretching, and the device stretchability in universal directions ranges 70–280 %. The obtained device stretchability is well comparable with that of the existing stretchable narrowband photodetector^[3].

In conclusion, this work presents the device design of the stretchable broadband photodetector, and its multi-functional sensing and imaging applications will be reported at the workshop.

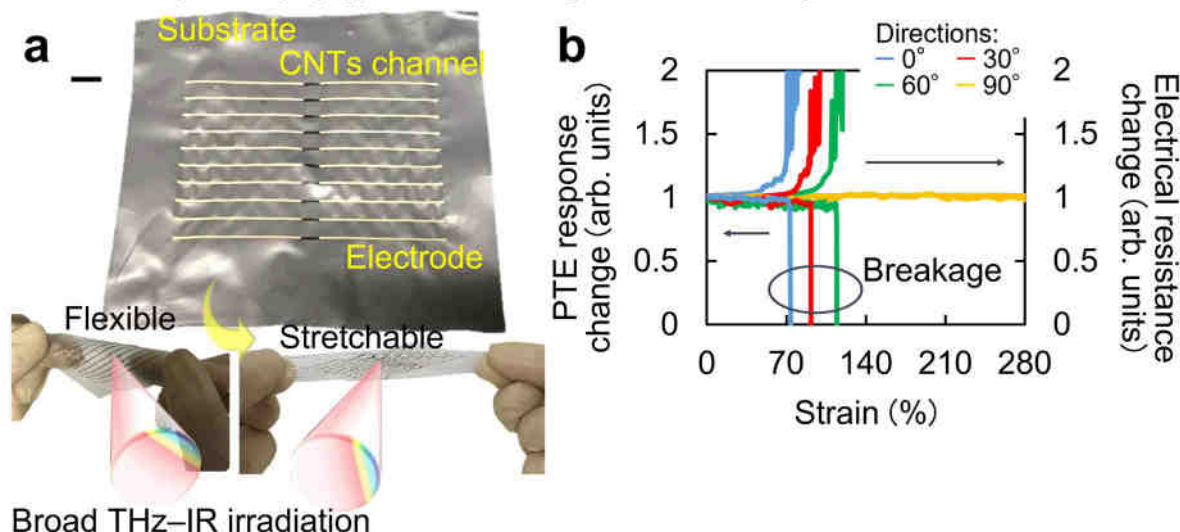


Fig. 1. **a**, Photograph of the proposed PTE imager sheet, being bent and stretched. Scar bar 3 mm. **b**, Mapping of the PTE responses and electrical resistances of the imager sheet against changes in strain of the device. An IR laser was used as a photo source.

3. Acknowledgement

The authors acknowledge Assis. Prof. Teppei Araki and Prof. Tsuyoshi Sekitani (Osaka University, Japan).

4. References

- [1] K. Li, *et al. Sci. Adv.* **8**, eabm4349, 2022.
- [2] K. Li, *et al. Nat. Commun.* **12**, 3009, 2021.
- [3] J. Yoo, *et al. Adv. Mater.* **27**, 1712–1717, 2015.

THz graphene-based metasurfaces for wave manipulation

Anna C. Tasolamprou^{*1}, Maria Kafesaki^{1,2}

1. *Institute of Electronic Structure and Laser, Foundation for Research and Technology Hellas, N. Plastira 100, 71110, Heraklion, Crete, Greece*

2. *Department of Materials Science and Technology, University of Crete, Heraklion, 70013, Greece*
atasolam@iesl.forth.gr

We discuss the unique possibilities stemming from exploiting the exotic properties of artificial metasurfaces designed for operation in the THz regime. Metasurfaces are electromagnetically ultrathin artificial materials with macroscopic properties defined by the architecture of the building blocks, the meta-atoms. Adjusting the meta-atoms enables the control over different aspects the electromagnetic waves and the realization of unusual electromagnetic functions. Within this framework we present groups of metasurface configurations incorporating different constituent materials. We mainly focus on graphene based metasurfaces acting as modulators for the THz regime. Graphene, the acclaimed two-dimensional (2D) material made of carbon atoms arranged in a honeycomb lattice, exhibits unique optical properties particularly in the THz spectrum, where it predominantly exhibits a Drude-like response. We focus on planar metasurfaces structures, starting from the simple metal-insulator-metal scheme to carbon nanotubes of variable number of interlayers and we show that the effective medium analysis unveils a rich palette of electromagnetic features that can be engineered by the adjustment of the geometry [1,2]. Additionally we show that ultrafast modulation response can be assessed with the use of a broadband THz time-domain-spectroscopic system (THz-TDS) in an IR pump-THz probe configuration and also with nonlinear self-action [2,3]. The proper design of the metasurface provides the means for achieving critical coupling and hence increased/perfect tunable absorption. The near-IR stimulus generates hot carriers in the graphene metasurface which effectively reduces its THz conductivity. Similar phenomenon can be induced by self-modulation using intense THz fields. The simple scheme of the absorber can be used as a platform for ultrafast flat optics and metasurfaces. Apart from that, we review additional recent THz metasurface findings with some interesting features. For example it has been shown, that using hybrid metasurfaces with metals combined with graphene one is able to produce switchable and tunable terahertz electromagnetic advanced functions like wavefront shaping.

References

- [1] Ch. Mavidis, A. C. Tasolamprou, E. N. Economou, C. M. Soukoulis, M. Kafesaki, "Effective medium description for coated and multicoated cylinders", under review, 2022.
- [2] Ch. Mavidis, A. C. Tasolamprou, E. N. Economou, C. M. Soukoulis, M. Kafesaki, "Perfect absorption conditions in metasurface-based perfect absorbers: a transfer matrix approach", in preparation, 2022.
- [4] A. D. Koulouklidis, A. C. Tasolamprou, S. Doukas, E. Kyriakou, M. S. Ergoktas, C. Daskalaki, E. N. Economou, C. Kocabas, E. Lidorikis, M. Kafesaki and S. Tzortzakis, "Ultrafast THz nonlinear modulation in an electrically tunable graphene thin film perfect absorber", under review, 2022.
- [4] A. C. Tasolamprou, A. D. Koulouklidis, C. Daskalaki, C. P. Mavidis, G. Kenanakis, G. Deligeorgis, Z. Viskadourakis, P. Kuzhir, S. Tzortzakis, M. Kafesaki, E. N. Economou and C. M. Soukoulis, "Experimental demonstration of ultrafast THz modulation in a graphene-based thin film absorber through negative photoinduced conductivity", *ACS Photonics*, 6 (3), 720-727, 2782-2788, 2019. Cover Page March 2019.

Metamaterials beyond common multipoles

Alexey Basharin

*Institute of Photonics, University of Eastern Finland, Joensuu, Finland
Alexey.basharin@uef.fi*

Multipole decomposition is a promising method for study of radiating or scattering response of electromagnetic sources or particles, even in the case of relatively complicated and compound scatterers like multilayer particles, clusters or asymmetrical systems. Indeed, the radiation fields of point electric or magnetic sources are decomposed only into electric or magnetic dipole moments, while real sources can be described by series of multipoles, including higher multipoles, toroidal moments and moments of mean-square radii. In this talk, we discuss the concept of modified multipoles describing the real sources of electric, magnetic and more complicated toroidal types. We discuss the secondary multipole decomposition for explanation of light interaction with compound particles, asymmetrical particles. We discuss high Q-factor resonances in metamaterials and meta-particles due to interference effects, like anapole mode, Kerker effects and Bound state in the continuum. Our approach will be useful for multipole analysis of complex systems in photonics such as nanoparticle clusters, metamaterials and nanoantennas and hybrid systems based on plasmonic/all-dielectric/carbon structures.

Acknowledgement.

This work was supported by H2020 RISE 734164 Graphene 3D

Transmission properties of self-complementary metamaterials via Babinet principle

Anar Ospanova

*Institute of Photonics, University of Eastern Finland, Joensuu, Finland
anar.ospanova@uef.fi*

Babinet principle is a modern tool for light controlling and widely used in electrodynamics [1]. Here we demonstrate a novel type of Babinet principle based metamaterials exhibiting broadband transmission of absolute amplitude in microwave frequency range. Another feature of the given structure is the simplicity of the unit cell representing a checkerboard-like pattern that simplifies both analysis and fabrication stage.

The well-known Babinet principle here is exploited in the form of two similar metasurfaces (i.e. surfaces whose unit cells are of subwavelength dimension) outstanding from each other at half wavelength distance and providing complementary patterns (see Fig. 1(a)) [2]. The simulated transmission characteristics have demonstrated the absolute transmission at the region of 5-6.5 GHz corresponding to ultra-broadband transmission. Furthermore, experimental measurement in an anechoic chamber of metamaterial sample perfectly matched the theoretical one and confirmed ultra-broadband transmission at 4.5-6.5 GHz frequencies (Fig. 1(b)).

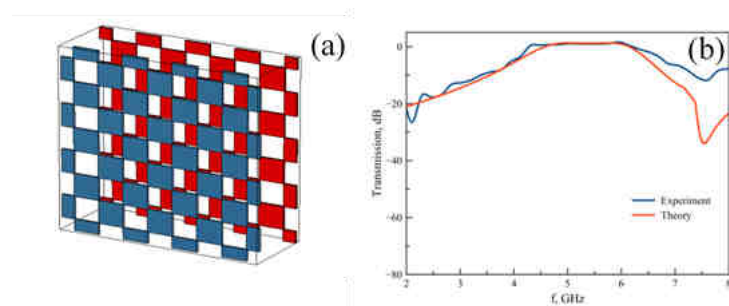


Fig. 1. :Illustration of Babinet metamaterial (a) and its simulated and measured transmission characteristics (b).Poincare sphere

Given results are of great interest of modern technologies, since this ability of light manipulation able to provide number of applications, namely, they could serve as frequency selective surfaces, polarizers, filter design and broadband transparent screens for different spectra ranges.

Acknowledgement.

This work was supported by H2020 RISE 734164 Graphene 3D.

4. References

- [1] M. Babinet, "Memoires d'optique meteorologique," *Acad. Sci., Paris, C. R.* 4, pp. 638–648, 1837
- [2] Yoshiro Urade, Yosuke Nakata, Toshihiro Nakanishi, and Masao Kitano, "Frequency-Independent Response of Self-Complementary Checkerboard Screens," *Physical Review Letters* 114, pp. 237401, 2015

Dirac Light

Eros Mariani, C.-R. Mann, W.L. Barnes, S.A.R. Horsley, T. Sturges and G. Weick

*Department of Physics and Astronomy, University of Exeter, Stocker Rd EX4 4QL Exeter, UK
E.Mariani@exeter.ac.uk*

Abstract

Pseudorelativistic Dirac quasiparticles have emerged in a plethora of artificial graphene systems that mimic the honeycomb symmetry of graphene. However, in these metamaterials it is notoriously difficult to manipulate the properties of Dirac quasiparticles without modifying the lattice structure.

Here we theoretically investigate Dirac polaritons (called "Dirac light") supported by honeycomb metasurfaces embedded in photonic cavities and unveil rich Dirac physics stemming from the competition between short-range Coulomb interactions and long-range photon-mediated interactions. By modifying only the photonic environment via the enclosing cavity we show that we can induce qualitatively different polariton phases and alter the fundamental properties of Dirac light [1-3].

Among several effects we discuss in particular the creation and manipulation of type I and type II Dirac points, the inversion of chirality of Dirac light [1], as well as the tunable fictitious magnetic fields for Dirac light in strained lattices. The latter is accompanied by a tunable Lorentz-like force that can be switched on/off and by a collapse and revival of polariton Landau levels [2].

We stress that the crossover between the different phases of Dirac light can be achieved by varying only the photonic cavity width while preserving the lattice structure—a unique scenario that has no analog in real or artificial graphene systems. Exploiting the photonic environment thus gives rise to unexplored Dirac physics beyond the conventional paradigms of metamaterials science.

Acknowledgements

This work has been supported by the Rank Prize Funds and the Engineering and Physical Sciences Research Council of the United Kingdom through the EPSRC Centre for Doctoral Training in Metamaterials (grant number EP/L015331/1). S.A.R.H. acknowledges financial support from a Royal Society TATA University Research Fellowship (grant number RPG-2016-186). E.M. acknowledges financial support from the Royal Society International Exchanges grant number IEC/R2/192166 and EU H2020-MSCA-RISE 652 project DiSeTCom (Project No. 823728).

References

- [1] Mann C-R, Sturges TJ, Weick G, Barnes WL, Mariani E., *Nature Communications*, **9**, 2194 (2018)
- [2] Mann C-R, Horsley SAR, Mariani E., *Nature Photonics*, **14**, 669 (2020)
- [3] Mann C-R, Mariani E., *Physical Review Research*, **4**, 013078 (2022)

Sensitivity analysis on the Performance of THz nanocarbon-based passive devices

P. Lamberti^{1*}, M. La Mura¹, V. Tucci¹

¹Dept. of Information and Electrical Eng. and Applied Math., University of Salerno, via Giovanni Paolo II 132, Fisciano (SA) - ITALY
*plamberti@unisa.it

1. Summary

A FEM model of THz passive component will be presented and used to assess the effect on the whole device performance of the uncertainties affecting geometrical and physical parameters of the device by means of sensitivity analysis. Moreover, with the aim of support the experimental validation, the overbounding and underbounding of the performance will be derived ranging the actual behaviour of the designed component.

2. Description of the problem and proposed approaches

The performance f of an electromagnetic system is the output that the designer looks for: several efforts have to be applied in order to ensure the satisfaction of the customer constraints. Usually, the designed parameters are considered fixed and well known, i.e. the vector $\underline{x}_0 = (x_{10}, x_{20}, \dots, x_{n0})$ of the n design parameters, and it corresponds to a point in the parameter space $D = [x_{1L}, x_{1U}] \times \dots \times [x_{nL}, x_{nU}]$ with x_{iL} and x_{iU} the min and max values of x_i parameter respectively. Nevertheless, there are actually several sources of uncertainty leading to unavoidable Δ_i variation in the parameters. It means that each component of the design parameter vector becomes “interval value”, given by $x_{i0} \pm \Delta_i$, and the point \underline{x}_0 becomes the hyper-rectangle

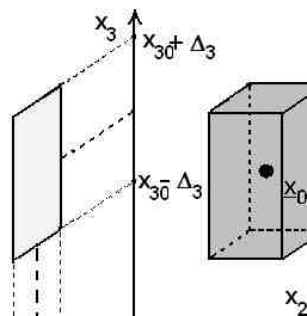


Figure 1 Hyper-rectangle $U(\underline{x}_0)$ representing all the possible values assumed by the vector \underline{x} when each component is affected by a variation Δ_i

$U(\underline{x}_0) = [x_{10} - \Delta_1, x_{10} + \Delta_1] \times \dots \times [x_{n0} - \Delta_n, x_{n0} + \Delta_n]$ (fig. 1 for $n=3$) [1]. As a consequence, also the performance will be an “interval function” that could be mismatched with respect to the desired design. This is especially true when the technology is not well established or the material behaviour and its physics is still under studies such as the case of nanocarbon-based device [2]. In this case, bounding of the performance function and sensitivity analysis can help to identify the more effective parameter and the results of such analysis can be used as a support in the experimental validation [3]. To this aim, A FEM model of THz passive component will be presented [4] and used to assess the effect on the whole device performance of the uncertainties affecting geometrical and physical parameters of the device [5]. In particular, a Monte Carlo procedure, supported by Vertex Analysis, will be applied on a numerically solved model of the device, developed with a commercial software (Comsol Multiphysics). From the simulated data an underestimation of the

overbounding, $f_M(\underline{x}) = \max_{\underline{x}_0 \in D} \left(\max_{\underline{x} \in U(\underline{x}_0)} f(\underline{x}) \right)$ and an overestimation of the underbounding, $f_m(\underline{x}) = \min_{\underline{x}_0 \in D} \left(\min_{\underline{x} \in U(\underline{x}_0)} f(\underline{x}) \right)$

of the performance will be derived from the N Monte Carlo trials, ranging the actual behaviour of the designed component by considering uncorrelated and uniformly distributed uncertain design parameters in the space parameters D . Moreover, simulated scattered data will be used to evaluate the sensitivity of the performance due to the assumed variability in discrete way [6].

3. Acknowledgement.

The work was carried out within the framework of the H2020 project 823728 DiSeTCom and of H2020-SGA-FET- Graphene Flagship- Graphene Core 3, GA881603

4. References

- [1] Egiziano, L., Lamberti, P., Spinelli, G., Tucci, V., Kuzhir, P.P. “Sensitivity analysis of a multilayer shielding device based on graphene” (2017). Int. Conf. ETCMOS 2017 Emerging Technologies: Communications, Microsystems, Optoelectronics, Sensors, Warsaw, Poland - May 28 – 30, 2017.
- [2] La Mura, M., Lamberti, P., Tucci, V. “Numerical evaluation of the effect of geometric tolerances on the high-frequency performance of graphene field-effect transistors” (2021) Nanomaterials, 11 (11), art. no. 3121. doi: 10.3390/nano11113121
- [3] P. Kuzhir, et al. “Main principles of passive devices based on graphene and carbon films in microwave - THz frequency range” JOURNAL OF NANOPHOTONICS. Vol. 11. (2017) 03250401 (19pp), doi: <http://dx.doi.org/10.1117/1.JNP.11.032504>
- [4] Kuzhir, P., et al. “FEM Approach to the Robust Design of a Graphene-Based 3D Structure for THz Devices” (2021) 2021 IEEE 16th Nanotechnology Materials and Devices Conference, NMDC 2021. doi: 10.1109/NMDC50713.2021.9677563
- [5] Lamberti, P., et al. “The Performance of Graphene-Enhanced THz Grating: Impact of the Gold Layer Imperfectness” (2022) Materials, 15 (3), art. no. 786. doi: 10.3390/ma15030786
- [6] Y. Jin, B. Sendhoff: “Trade-off between performance and robustness: an evolutionary multiobjective approach”, Lecture Notes in Computer Science, Springer-Verlag Heidelberg, Vol. 2632, August 2003, pp. 237-251.

CVD graphene transfer: Alcohol/water solvent for improved removal of PMMA with polarity modified under DUV exposure

Natalia Alexeeva^a, Justinas Jorudas^a, Daniil Pashnev^a, Ilja Ignatjev^b, Gediminas Niaura^b, Irmantas Kašalynas^a

^{a)} Department of Optoelectronics, Center for Physical Sciences and Technology, Saulėtekio av. 3, LT-10257 Vilnius, Lithuania.

^{b)} Department of Organic Chemistry, Center for Physical Sciences and Technology, Saulėtekio av. 3, LT-10257 Vilnius, Lithuania.
natalia.alexeeva@ftmc.lt

1. Two-stage removal of PMMA supportive layer for the CVD graphene transfer.

We demonstrate the development of a simple, environmentally-friendly technique to remove the poly(methyl methacrylate) (PMMA) layer from graphene, synthesized by a chemical vapor deposition (CVD), on different substrates.

As the first step, the polarity of the PMMA was modified under the influence of deep-UV irradiation as a result of its photodegradation, namely scissions of main-chain, as well as side chains of the polymer [1]. Since the DUV intensity is lower than that of an e-beam or X-ray radiation, this avoids destructive crosslinking under DUV exposure. Moreover, the main-chain scission products have time to absorb photons and contribute to polymer degradation due to side-chain scission too. As a result, stable products are formed, including ketone-type and aldehyde-type carbonyl compounds, which have a higher polarity than pristine PMMA. The modification of PMMA polarity was confirmed by UV and FTIR spectrometry and the contact angle measurements (see Fig.1).

Consecutive dissolution of a polarity modified polymer in a binary mixture of isopropyl alcohol/water (more commonly alcohol/water), prepared in a certain proportion (see Fig.2), results in rapid and complete removal of PMMA without degradation of graphene properties. The mechanism is that when the number of water and IPA molecules is equal, they begin to form water-alcohol hydrogen bonds, destroying existing intermolecular clusters with hydrogen-bonds (water-water and IPA-IPA), and thus simplifying access to the surface of the soluble substance.

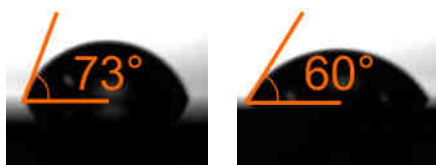


Fig.1 Polarity of PMMA pristine (left) and after deep-UV exposure (right)

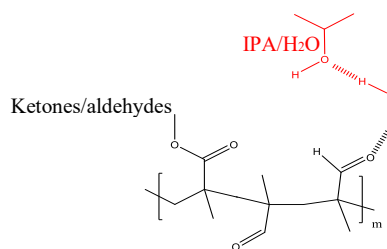


Fig.2 Dissolution of modified PMMA with aqueous isopropyl alcohol

The high quality of graphene after PMMA removal was confirmed by Raman spectrometry. For comparison, PMMA removal from graphene was also performed by the most common methods. The electrical properties of graphene films were investigated using THz time-domain and infrared spectroscopy methods, which, being contactless, are perspective for characterization of CVD graphene in commercial applications [2]. The mobility has reached $6900 \text{ cm}^2/(\text{V}\cdot\text{s})$, which makes the proposed PMMA removal method promising for use in the fabrication of high-performance large-scale graphene-based electronic devices [3].

2. Acknowledgement.

Work was supported from the Research Council of Lithuania (Lietuvos mokslo taryba) through project "Hybrid plasmonic components for THz range (T-HP)" under Grant No. 01.2.2-LMT-K-718-03-0096 (DOTSUT-184).

3. References

- [1] A. Torikai, M. Ohno, K. Fueki, J. Appl. Polym. Sci., 41, 1023–1032 (1990), doi:10.1002/app.1990.070410513.
- [2] J. Jorudas, D. Pashnev, N. Alexeeva, I. Ignatjev, A. Urbanowicz, and I. Kašalynas, in 46th International Conference on Infrared, Millimeter and Terahertz Waves (IRMMW-THz), Aug. 2021, pp. 1–2, doi: 10.1109/IRMMW-THz50926.2021.9567542.
- [3] J. Jorudas, D. Pashnev, I. Kašalynas, I. Ignatjev, G. Niaura, N. Alexeeva, "PMMA polarity modified by DUV exposure to improve its removal for CVD graphene transfer". under submission.

Thursday, August 4



Diamond based quantum computers and simulators

Fedor Jelezko

*Institute of quantum optics, Ulm University
fedor.jelezko@uni-ulm.de*

Synthetic diamond has recently emerged as a candidate material for a range of quantum-based applications including: secure quantum communication, quantum information processing and quantum sensing. In such applications, the synthetic diamond acts as a host for impurities or defects, acting like a solid-state atom trap. The quantum states of these impurities, such as the Nitrogen-Vacancy (NV) and Silicon-Vacancy (SiV) defects, can be individually manipulated and made to interact, and photons of light emitted from these impurities can be used to read out. Notably, synthetic diamond (along with silicon carbide) offers advantages over competitive materials as the quantum properties of NV centres it hosts can be manipulated and probed at room temperature.

In this presentation we will show how single colour centres can be created with a few nanometres accuracy and coherent dipole-dipole coupling was employed to generate their entanglement. We will also present experimental realisation of room temperature quantum simulator based on C^{13} nuclear spins arrays.

CVD synthesis of diamond needles with controlled charge state of NV centers

S. A. Malykhin¹, M. D. Lazareva², R. R. Ismagilov², A. N. Obratsov^{1,2}

¹Department of Physics and Mathematics, University of Eastern Finland, Joensuu, Finland

²Department of Physics, Lomonosov Moscow State University, Moscow, Russia

sermal92@mail.ru

Manipulations with the objects of few nanometers size and characterization of their properties are required during variety of modern research performed in Physics, Chemistry, Biology and even Medicine. Decreasing size of the analysed objects significantly complicates investigations and requires development of particular research approaches and devices. Nanoscale quantum-optical sensors are promising for such small objects analysis. The nitrogen-vacancy (NV) centers in diamond are of great interest for the quantum-optical sensing. It is because of combination of unique properties of diamond itself (biocompatibility, high thermal conductivity, record hardness) and quantum features of NV centers [1]. The NV centers in diamond were demonstrated as high-sensitive nano-thermometer [2], sensors of magnetic and electric fields [3], mechanical stress sensor [4]. To provide nanoscale spatial resolution diamond probes with NV centers their size should be in nanometer scale at least in two dimensions. Moreover, robust methodology for manipulation and assembling of the diamond crystallites are required for production of the nanoscale sensors. Single crystal diamond needle (SCDN) demonstrates one of the most promising shape for nanoscale quantum sensors (see Figure 1a) [5]. Formation of NV centers in SCDN and their optical properties were previously demonstrated in works [6–9].

Here we present the recent research results aimed at controlling of the luminescent charge states of NV centers (Figure 1b) in SCDNs by adjusting parameters of chemical vapor deposition (CVD) process.

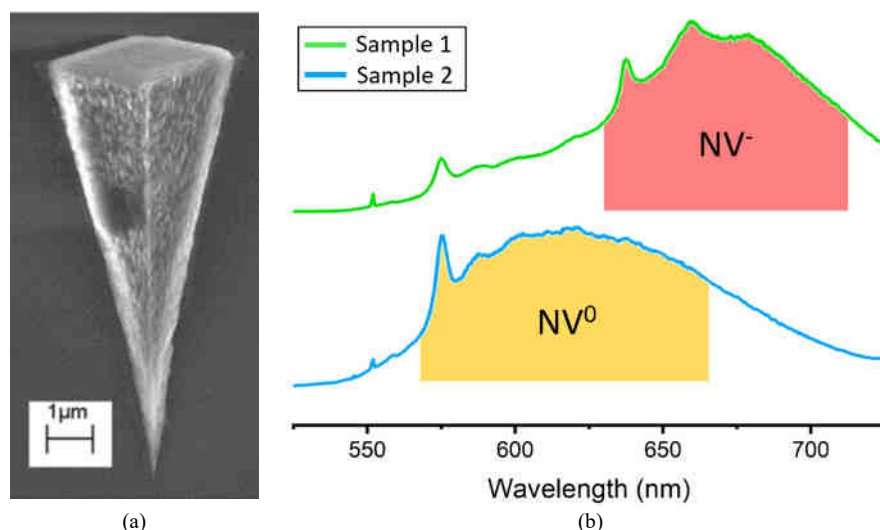


Fig. 1. Electron image of individual SCDN (a) and photoluminescence spectra of two samples obtained at different parameters of CVD process (b). Main spectral areas of NV⁰ and NV⁻ centers luminescence highlighted by yellow and red colors respectively.

This work was supported by Academy of Finland (decision 340733) and H2020 RISE Graphene 3D (734164). The work is part of the Academy of Finland Flagship Programme, Photonics Research and Innovation (PREIN), decision 320166.

- [1] A.M. Zaitsev, *Optical properties diamond Data handbook*, Springer Science & Business Media **2013**.
- [2] G. Kucsko, P.C. Maurer, N.Y. Yao, M. Kubo, H.J. Noh, P.K. Lo, H. Park, M.D. Lukin, *Nature* **2013**, 500, 54.
- [3] S. Hong, M.S. Grinolds, L.M. Pham, D.L. Sage, L. Luan, R.L. Walsworth, A. Yacoby, *MRS Bulletin* **2013**, 38, 155.
- [4] L. Rigutti, L. Venturi, J. Houard, A. Normand, E.P. Silaeva, M. Borz, S.A. Malykhin, A.N. Obratsov, A. Vella, *Nano Letters* **2017**, 17, 7401.
- [5] A.N. Obratsov, P.G. Kopylov, A.L. Chuvinin, N.V. Savenko, *Diamond Related Materials* **2009**, 18, 1289.
- [6] S. Malykhin, Y. Mindarava, R. Ismagilov, A. Orekhov, F. Jelezko, A. Obratsov, *Physica status Solidi (b)* **2019**, 256, 1800721.
- [7] S.A. Malykhin, A.M. Alexeev, E.A. Obratsova, R.R. Ismagilov, V.I. Kleshch, A.N. Obratsov, *Materials Today Proceedings* **2018**, 5, 26146.
- [8] S.A. Malykhin, J. Houard, R.R. Ismagilov, A.S. Orekhov, A. Vella, A.N. Obratsov, *Physica status Solidi (b)* **2017**, 255, 1700189.
- [9] S. Malykhin, Y. Mindarava, R. Ismagilov, F. Jelezko, A. Obratsov, *Diamond Related Materials* **2022**, 125, 109007.

All-optical pH sensing with hybrid sp²-sp³ carbon nanostructures

Lena Golubewa¹, Yaraslau Padrez¹, Renata Karpicz¹, Tatsiana Kulahava¹, Olga Levinson²,
Polina Kuzhir³

¹Department of Molecular Compound Physics, Center for Physical Sciences and Technology, Lithuania

²Ray Techniques Ltd., Israel

³Department of Physics and Mathematics, Institute of Photonics, University of Eastern Finland, Finland
lena.golubewa@ftmc.lt

1. Introduction

Nanodiamonds (NDs) with a hybrid sp²-sp³ shell decorated with oxygen-containing functional groups has attracted much interest as promising materials with high sensing potential for applications in various fields of science and technology. Tunable surface chemistry determines photoluminescent (PL) properties of these nanoparticles which can be adjusted to be sensitive to changes of a desired external parameter. Nano-scale size, chemical stability inherited from the diamond, and biocompatibility allows to extend the use of hybrid sp²-sp³ carbon nanostructures in the field of biomedicine and cell technologies, where accurate, remote, and non-destructive control of such environmental parameters as pH, temperature, and ionic strength, which are of great importance as small shifts in these parameters may lead to dramatic results and cell death.

2. Result and discussion

In the present study, all-optical method of pH control with high-purity and high-homogeneity water solutions of NDs (RayND-M, Ray Techniques Ltd), produced by laser synthesis followed by an undisclosed surface modification process is proposed. Based on UV-vis absorption, FTIR, steady-state, and time-resolved fluorescence spectroscopic analysis of NDs it was revealed that NDs exhibit excitation-dependent fluorescence originating from hydroxyl, carbonyl, and carboxyl groups. The latter ones are sensitive to pH changes through protonation-deprotonation which is reflected in the decrease of PL with excitation at $\lambda_{\text{ex}} = 371$ nm and emission at $\lambda_{\text{em}} = 456$ nm (see Fig.1a) and simultaneous increase of PL when excited with $\lambda_{\text{ex}} = 470$ nm with emission centered at $\lambda_{\text{em}} = 553$ nm (see Fig.1b). Both excitations/emissions were used to obtain calibration curves which allow determining the pH values of water solutions by PL measurements (see Fig.1b). Ratio of normalized PL intensities I_{553} and I_{456} (with excitation at 470 nm and 371 nm, respectively) is well approximated with linear function ($R^2 = 0.97$) (see Fig.1c).

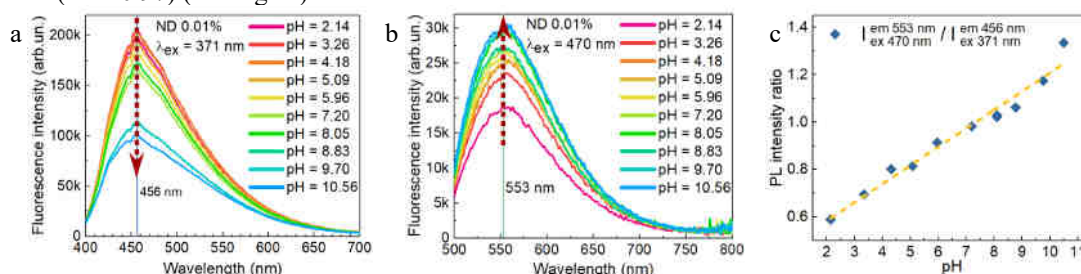


Fig. 1. pH screening with NDs with two-wavelength excitation and two-wavelength emission detection

Intensities ratio allows to avoid errors caused by the laser power fluctuations, ND-concentration dependence of the detected signal, increasing reliability of all-optical approach of $[H^+]$ detection. Based on the obtained calibration, pH value can be calculated using the following formula:

$$pH = 12.8 \cdot \frac{I_{553}^{norm} I_{max}}{I_{456}^{norm} I_{max}} - 5.5,$$

where $I_{553}^{norm} I_{max}$ and $I_{456}^{norm} I_{max}$ are PL intensities when excited with $\lambda_{\text{ex}} = 470$ nm and $\lambda_{\text{ex}} = 371$ nm and normalized on the maximum values of the PL measured for the calibration solutions with pH 10 and pH 2, respectively; '12.8' and '5.5' are empirically obtained coefficients.

3. Conclusions

Diamond-like NDs produced by laser synthesis decorated with carboxylic functional groups are demonstrated to be accurate all-optical sensors of pH values of solutions. pH can be easily recalculated from the PL intensities with two-wavelength excitation/emission approach, avoiding undesirable errors caused by hardware and fluctuations in NDs concentrations used for measurements.

4. Acknowledgements

This work was supported by H2020 RISE DiSeTCom (No 823728) and H2020 RISE Graphene 3D (No 734164)

Temperature-dependent fluorescence of SiV and NV color centers in micron-sized single crystal diamond needles

Yaraslau Padrez¹, Lena Golubewa¹, Sergei Malykhin³, Tatsiana Kulahava², Renata Karpicz¹, Alexander Obraztsov³, Yuri Svirko³ and Polina Kuzhir³

¹State research institute Center for Physical Sciences and Technology, Sauletekio Av. 3, Vilnius, LT-10257, Lithuania

²Institute for nuclear problems of Belarusian state university, Bobruiskaya str. 11, BY-220006 Minsk

³University of Eastern Finland, Yliopistokatu 7, Joensuu, 80101, Finland

yaraslau.padrez@ftmc.lt

1. Introduction

Micro-diamonds with color centers are promising objects for various applications spreading from micro-electronics to quantum optics due to their remarkable mechanical, thermal, and optical properties. Photoluminescence (PL) of color centers in diamonds can be also applied for precise temperature sensing at the micro- and nano-scales. Micro-diamonds are chemically inert and biocompatible, widening their application to biophotonics.

Synthesis of micro-crystallites with specific needle shape, controlled localization of color centers and enriched with SiVs may allow increasing accuracy and reliability of all-optical temperature determination and sensitivity of the method.

2. Result and Discussion

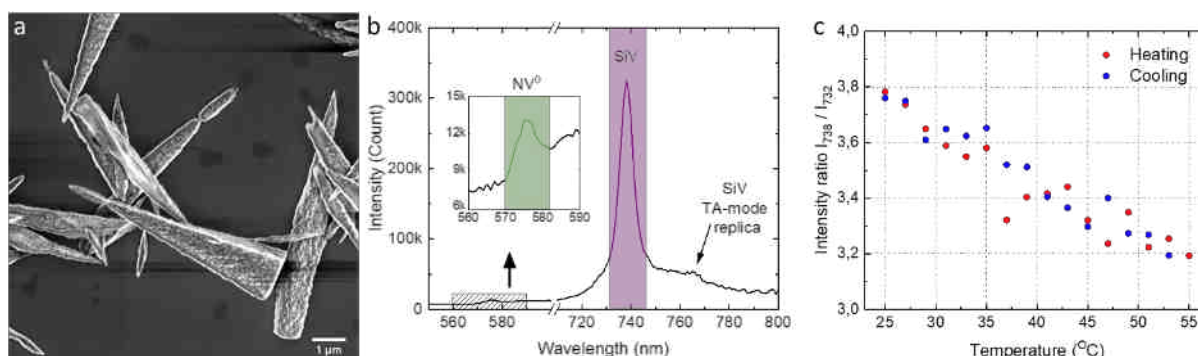


Fig. 1: a) SEM micrographs of D-SCDNs; b) PL spectra of them at room temperature at $\lambda_{ex}=470$ nm; c) temperature dependence of the I_{738}/I_{732} fluorescence intensity ratio during heating and cooling.

Dart-like micron-sized single crystal diamonds needles (D-SCDNs) were obtained by CVD-synthesis as described in [1]. D-SCDNs have a pronounced tip (see Fig.1a) and are enriched with both nitrogen-vacancy (NV) and silicon-vacancy (SiV) color centers, which follows from the presence characteristic PL of these centers in spectra (see Fig.1b). However, intensity of zero-phonon line (ZPL) of SiV color centers is several orders of magnitude higher than NVs. The major part of SiVs is concentrated in the tip.

All-optical thermometry was performed in the following way: The PL spectra of SiV color centers of DSCDNs were measured with excitation at 470 nm wavelength during uniform heating followed by cooling in the physiologically significant range (25-55 °C). The dependencies of lifetime, FWHM and peak position of SiV ZPL and its intensity on temperature were investigated. In order to reduce the errors caused by equipment and laser intensity fluctuations and to increase the measurement accuracy, we applied the normalizing of PL intensity measured at the maximum peak position of SiVs' ZPL ($\lambda_{em}=738$ nm) on the intensity at the wavelength where it is temperature independent ($\lambda_{em}=732$ nm) (see Fig. 1c).

3. Conclusions

Our results open a way towards accurate, non-invasive, precise, and real-time monitoring of temperature variations accompanying endothermic/exothermic processes on the sub-micro-scale, covering possible applications from quantum bioimaging to lab-on-a-chip systems.

4. Acknowledgement

This work was supported by Horizon 2020 RISE DiSeTCom (Project No 823728) and Academy of Finland (Flagship Programme PREIN, decision 320166, and research project, decision 343393).

5. References

[1] S. Malykhin, Y. Mindarava, R. Ismagilov, F. Jelezko, and A. Obraztsov, *Diamond and Related Materials*, **125**, 109007 (2022)

Using Nanomaterials and Machine Learning for Advanced Sensing Applications

Antonio Maffucci

Dept. of Electrical and Information Engineering, Univ. of Cassino and Southern Lazio, Cassino, Italy
maffucci@unicas.it

1. Nanomaterials and deep transfer learning for improved sensing platforms

Reliable real-time monitoring pollutants is a major need in industrial and residential areas, to ensure health and safety [1]. Traditional techniques, such as chromatography [2], are not suitable for a real time in-situ detection, hence effort is currently addressed to assess monitoring and sensing technologies suitable for: i) in-situ monitoring (through compact sensing platforms); ii) smart distributed systems (collective data processing).

The first concept is addressed through alternative electrical and electrochemical techniques, such as Voltammetry, VA [3-4] or Electrical Impedance Spectroscopy, EIS [5-7]. Indeed, both techniques can be implemented by means of compact systems with hand-held sensing platforms connected to portable instrumentation. For instance, disposable Screen-Printed Electrodes (SPEs) can be used as sensing platforms. However, the limits of conventional SPEs (i.e., made by graphite, carbon, etc.) related to their sluggish surface kinetics severely affect the sensor performance indicators (such as sensitivity, selectivity, responsivity, etc.. [4]).

To overcome these limits, the SPEs can be modified by enhanced materials, such as the promising Carbon Nano-Materials (CNMs), that can improve surface kinetics and enhance electroactive surface area [4-5]. More in general, CNMs are abundant and span a wide range of physical and chemical properties that can be tailored according to the purposes. Graphene, Carbon Nanotubes (CNTs), Nano-Diamond (ND) and their derivatives have been widely employed for electrochemical sensing in recent years [8-9].

Despite the high improvement in SPEs' performance after their modification, a reliable technology for in-situ real-time monitoring based on these platforms and the above-mentioned techniques is still far to be assessed. Indeed, major limits still need to be overcome: (i) high sensitivity of the platforms to uncertainties of the fabrication process, environmental conditions, and ageing effects; (ii) complicated time- and resource-consuming calibration procedures, needed for in-situ measurements; (iii) difficult classification of substances with similar electrical and electrochemical footprint.

Many of the above issues can be faced by moving from conventional solutions to IoT paradigms [10]. This is the second concept mentioned above: the sensing platforms becomes nodes of a smart distributed sensing system, where the data are processed both locally and collectively (e.g., in Cloud), eventually by means of Artificial Intelligence (AI) algorithms. This approach can strongly improve the monitoring performance also in presence of the above-mentioned uncertainties, see for instance [11], where IoT-based real-time frameworks are proposed to perform water quality monitoring, by using machine learning approaches and cloud computing.

The talk will present some recent results related to the detection and classification of organic pollutants (quinones) in water performed by means of EIS and VA techniques. Improved sensing platforms will be shown, where the sensing membranes for EIS and working electrodes for VA are modified by means of 2D nanomaterials. Examples of AI-based post-process will be also discussed, with the possibility of classifying the pollutants starting from VA results, transformed into equivalent images via GAF transformations and finally processed by pre-trained convolutional neural networks.

2. Acknowledgement.

This work was supported by the Project "2DSENSE", funded by NATO under the SPS Programme, grant # G5777, and by the Project "TERASSE", funded by EU under H2020-MSCA-RISE Programme, grant # 823878.

3. References

- [1] H. Nakamura (2010) *Anal. Methods*, 2, 430-444
- [2] A. M. Meyer, et al. (2019) *Science of the Total Environment*, 651, 2323-2333.
- [3] N.-B. Mincu, et al. (2020) *Diagnostics*, 10, 517
- [4] R. Cancelliere, A.D. Tinno, et al., (2021) *Biosensors*, 12, 2.
- [5] M. Baah, et al., (2022) *Nanotechnology*, 33, 075207.
- [6] G. Miele, et al. (2021) *IEEE Trans. on Instrum. and Measur.*, 70, 503912.
- [7] L. Ferrigno, et al. (2020), *Nanotechnology*, 31, 075701
- [8] H. Beitollahi, et al., (2020) *Anal. Methods*, 12, 1547-1560.
- [9] R. Kour, et al., (2020) *J. Electrochem. Soc.*, 167, 037555
- [10] G. Mois, S. Folea, and T. Sanislav (2017) *IEEE Trans. Instrum. Meas.*, 66, 2056-2064
- [11] A. Bhardwaj, et al. (2022) *Environ Sci Pollut Res* (DOI: 10.1007/s11356-022-19014-3).

Scientific publishing within the new “*Open Science*” world: how to write for high-impact factor journals

Gaia Tomasello, Associate Editor

Materials Science and Physics Department at Wiley-VCH

Abstract

Open science and open access (OA) have become main drivers for the current transformation of the scientific publication process. Wiley is leading this transition with a broad range of initiatives: from corresponding agreements with institutions supporting gold and green OA policies to launching new premier Gold OA titles within materials science and physics. In the talk entitled “*Scientific publishing within the new “Open Science” world: how to write for high-impact factor journals*” Gaia Tomasello, (peer review editor for the journals: *Advanced Functional Materials*, *Advanced Electronic Materials* and *Physica Status Solidi* family) will provide an overview of the journal portfolio and publication opportunities in materials science physics within the Advanced family at Wiley, from including precious insights on how to prepare a scientific manuscript for high impact factor journals to emphasizing both hybrid and pure OA models within the prestigious *Advanced X Research* brand.

Advanced Physics Research

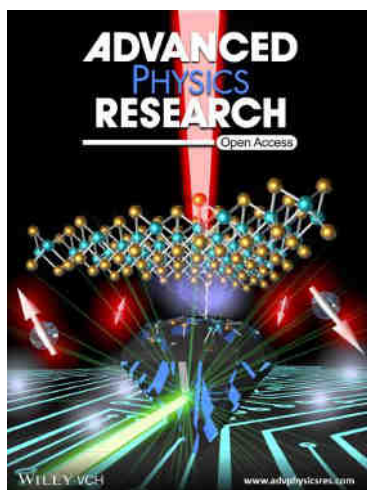


Figure 1. Front cover of the new pure OA title : *Advanced Physics Research* (<http://www.advphysicsres.com>), the new open-access journal covering the whole gamut of physics, from applied to fundamental, however, with a strong emphasis on important and relevant current topics. This includes, but is not restricted to atomic and molecular physics, computational physics, condensed matter physics, cosmology, ferroelectrics, magnetism, nuclear and particle physics, optics, physics of complex systems, physics of soft matter, quantum physics, spintronics, superconductivity, surface physics, thermodynamics, etc.

Graphene 3D project Symposium



Biopolymer-graphene nanocomposites: properties, applications and safety issues

R. Kotsilkova¹, E. Ivanov^{1,2}, T. Batakliiev^{1,2}, V. Georgiev^{1,2}, D. Menseidov¹, S. Kotsilkov¹

¹Institute of Mechanics, Bulgarian Academy of Sciences, Acad. G. Bonchev Str. Block 4, Sofia 1113

²NanoTechLab Ltd., Acad. G. Bonchev Str. Block 4, Sofia 1113, Bulgaria
kotsilkova@yahoo.com

Introduction

Based on the superior properties of graphene, the polymer nanocomposites offer enhanced mechanical properties and functionality, which make them attractive for variety of applications. However, many factors are found to govern the final nanocomposite properties and due to the complexity of the factors, contradicting properties may be obtained [1]. The present study addresses the role of the dispersion and the loading of graphene nanoplatelets (GNPs) in the polylactic acid (PLA) biopolymer for the enhancement of mechanical, electrical and thermal properties of nanocomposites (NCs), towards 3D printing and packaging applications.

Results and Discussion

The PLA composites of varying GNP contents from 1.5 to 12 wt.% are prepared by melt extrusion using a masterbatch approach. By increasing the filler loading, GNP/PLA nanocomposites demonstrate a significant enhancement of Young's modulus, and scratch resistance, but the tensile strength and elongation slightly decrease (Fig.1). The coefficient of friction in wear is strongly decreased by increasing the GNP contents if compared to the neat PLA, demonstrating the self-lubricating properties of GNP/PLA nanocomposites. The electrical percolation threshold was determined between 3-6 wt.% GNP content, while the thermal conductivity gradually increases by increasing the amount of filler. The highest values of the conductivities is observed for the 12 wt.% GNP/PLA nanocomposites, with dc-conductivity of 1.3 S/m and thermal conductivity of about 1.0 W/mK, while the matrix polymer is an electrical and thermal insulator.

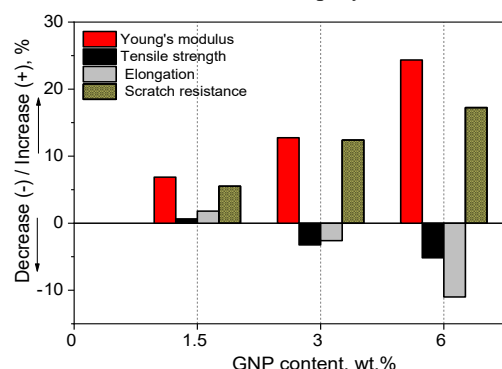


Fig. 1. Mechanical properties of GNP/PLA NCs

The highly improved mechanical properties (tensile, bending and friction), as well as the strongly enhanced electrical and thermal conductivity of the PLA-based nanocomposites at GNP loading above the percolation threshold, allowed us to propose the 6-12 wt.% GNP/PLA as a novel multifunctional material for 3D printing application (FDM/FFF). The good printability is due to the lubricant effect of graphene nanoplatelets during the flow, which is associated with sliding of the GNPs one over another and hydrodynamic slip at the filler-polymer interfaces. The slip-sliding effects of GNPs increase significantly by increasing the filler content, which makes printable the highly filled GNP/PLA nanocomposites [2].

At low filler loading around the percolation threshold (3 - 6 wt.% GNPs), the improved tensile properties, the enhanced scratch resistance with 12-15%, dc-conductivity in the range 10^{-6} - 10^{-2} S/m and 2 to 3-folds enhanced thermal conductivity compared to the neat PLA, make the biodegradable GNP/PLA nanocomposite films a good candidate for packaging applications. However, our study on safety showed that the graphene platelets may release from the films into the food simulants if a high temperature treatment (4 hours at 90°C) is applied [3]. Although the nanoparticles are tightly bound in the matrix polymer, the release of GNPs mostly due to the swelling and partial degradation of the PLA polymer in alcohol and acetic acid media at high temperatures. Therefore, if the GNP/PLA nanocomposite films are used for food packaging application the potential hazard of graphene associated with the high temperature treatment of the packaged food needs of further investigations.

Acknowledgements

The authors thank to the support of H2020MSCA-RISE 734164 Graphene 3D project for the present work.

References

- [1] R. Kotsilkova, E. Ivanov, V. Georgiev, R. Ivanova, D. Menseidov, T. Batakliiev, V. Angelov, H. Xia, Y. Chen, D. Bychanok, P. Kuzhir, R. Di Maio, C. Silvestre, S. Cimmino, *Polymers* **12**, 1208 (2020).
- [2] R. Kotsilkova, S. Tabakova, S. and R. Ivanova, *R. Mechanics of Time-Dependent Material* (2021)
- [3] S. Kotsilkov, *Safety and risk assessment of polymer nanocomposites for packaging applications: technological aspects and regulations*. PhD Thesis (2018)

3D printing for Terahertz absorbers

Polina Kuzhir

*Institute of Photonics, Department of Physics and Mathematics, University of Eastern Finland
polina.kuzhir@uef.fi*

A brief overview of the work done within Horizon 2020 Graphene 3D project towards THz perfect absorbers made of carbon-based 3D printed architectures is given. A number of strategies are discussed.

High broadband absorption can be achieved by 3D-printed by FDM or stereolithography cellular structures made of a moderately conductive ($1\text{--}30\text{ S m}^{-1}$) skeleton. The interplay between characteristic geometrical features (cell size) of those meshes and their conductivity allows to get very good results in very broad ranges of wavelengths [1,2].

Another option is deposition of a thin metal layer onto 3D printed regular array of polymer hemispheres covered with graphene [3]. Tailoring the electromagnetic responses of such metasurfaces could be done by changing the diameter of hemisphere and / or period of the overall structure. Another pattern rather than hemispheres could be also applied successfully, e.g. pillar-type structure.

Perfect tuneable resonant absorption could be obtained by 3D meshes made of highly conductive ($1200\text{--}2000\text{ S m}^{-1}$) glassy carbon scaffold.

Probably the most interesting case is an array of multi-layered graphene hemispheres made through the combination of 3D ink-jet printing, electroplating and chemical vapor deposition processes. These very thin metasurfaces demonstrate almost perfect absorption, $> 95\%$, in very broad frequency range ($100\text{ GHz} - 10\text{ THz}$). They are also robust against macroscopic structural defects, i.e. their electromagnetic properties remain the same when structure comprises up to 40% of randomly distributed holes and other geometrical imperfectness [4,5].

Acknowledgement

This research is supported by H2020 RISE 734164 Graphene 3D project.

References

- [1] Polina Kuzhir, et al, Carbon **171**, 484 (2021).
- [2] Dmitry Bychanok, et al, Materials **13**, 5208 (2020).
- [3] Alesia Paddubskaya, et al, Nanomaterials **11**, 2494 (2021).
- [4] Marian Baah, et al, Carbon **185**, 709 (2021).
- [5] Andrey Novitsky, et al, Phys. Rev. Applied **17**, 044041 (2022).

Innovative nanocomposites for 3D printing: the effect of carbonaceous fillers segregated morphology on structural and functional properties

M. Lavorgna^{a,e}, C. Santillo^a, A.P. Godoy^b, A. Ronca^{a,e}, G. Rollo^{a,e}, R.J. Espanhol Andrade^b, R.K. Donato^c, G. Fei^d, G.G. Buonocore^a, H. Xia^{d,a}

^aInstitute for Polymers, Composites and Biomaterials-CNR, 80155 Portici, Italy

^bMackGraphe, Mackenzie University, Rua da Consolação, 930, São Paulo, SP, Brazil

^cCentre for Advanced 2D Materials, National University of Singapore, 117546 Singapore

^dPolymer research Institute, Sichuan University, 610065 Chengdu, China

^eInstitute for Polymers, Composites and Biomaterials-CNR, 23900 Lecco, Italy)

Corresponding author Marino Lavorgna marino.lavorgna@cnr.it

The development of polymer-based nanocomposites for 3D printing application based on graphene and its derivatives and/or carbon nanotubes is addressed to the tailoring and optimization of functional properties of printed manufacts, such as thermal dissipation and EMI shielding [1]. It is well known that in the preparation of nanocomposite filaments for Fused Deposition Modeling (FDM) technology, the dispersion of fillers into the polymeric matrix plays a key role in determining the processability and final properties of the printed object. On the other side, in the preparation of powder for Selective Laser Sintering (SLS) technology, is the homogenous deposition of conductive filler onto the particle surface which is essential to enhance the functional properties of printed objects, due to the formation of a percolating 3D structure during laser sintering [2]. In this study new competitive conductive nanocomposite materials for FDM and SLS 3D printing, based respectively on modified polyvinyl alcohol (HAVOH) and thermoplastic polyurethane (TPU), carbon nanotubes (MWCNTs) and graphene derivatives (GE) as filler and Benzyl Imidazole Chloride (BenzImCl) as IL, have been designed, prepared and characterized in terms of printability and final properties.

The results demonstrate that both HAVOH-MWCNTs filament and TPU/GE powder are suitable for the production of FDM and SLS printed structures. The developed materials exhibit a filler segregated morphology, ascribed both to the confinement of filler at the interface of sintered particles (TPU, SLS) and the effect of ILs to promote π - π interaction between carbonaceous fillers (HAVOH, FDM). This peculiar filler morphology enables the obtainment of a right balance between mechanical and functional properties of the printed structures, which in turns hold great potential to be used as highly sensitive piezoresistive sensors in wearable devices.

Acknowledgement.

This research was funded by Marie Skłodowska-Curie Actions (MSCA) Research and Innovation Staff Exchange (RISE) H2020-MSCA-RISE-2016, Project Acronym: Graphene 3D-Grant Number: 734164.

References

- [1] Gnanasekaran K., Heijmans T., van Bennekom S., Woldhuis H., Wijnia S., de With a G., Friedrich H. *Applied Materials Today* 9, 21–28 (2017).
- [2] Li, Z.; Wang, Z.; Gan, X.; Fu, D.; Fei, G.; Xia, H.; *Macromol. Mater. Eng.* 1700211 (2017).
- [3] Santillo C., Godoy A.P., Donato R., Espanhol Andrade R.J., Buonocore G.G., Xia H., Lavorgna M., Sorrentino A., *Comp. Sci. Tech.*, 207, 108742 (2021).

Robust Design of Multifunctional Nanocomposites suitable for Additive Manufacturing of Electrical Devices

P. Lamberti^{1,*}, M. La Mura¹, V. Tucci¹

¹Dept. of Information and Electrical Eng. and Applied Math., University of Salerno, via Giovanni Paolo II 132, Fisciano (SA) – ITALY
*plamberti@unisa.it

1. Summary

A robust design approach for the selection of the best nanofilled polylactic acid (PLA) filament for the Fused Deposition Modeling (FDM) additive manufacturing of electrical devices will be reported. The use of two nanofillers to modify the electrical and thermal properties of the hosting material has been considered in order to realize a three phase nanocomposite, i.e. PLA matrix, electrically conductive multiwall carbon nanotubes (CNT) and graphene-based nanoparticles (GNP), expecting to have different effects [1-3]. According to the customer requirements, the PLA filament with the best combination of fillers amount respecting the physical constraints is selected among those realized following a Design of Experiment (DoE) pre-planning-phase.

2. Description of the problem and proposed approaches

The production and use of conductive polymeric composites is in continuous development due to the opportunity to combine the advantages of plastic materials (low cost, low weight, easy workability) with the possibility of modulating the thermal and electrical conductivity as the filler concentration varies [4-6]. It has been demonstrated that the electrical behaviour of a nanocomposite changes from insulator to conductor following the addition of electrically conductive nanoparticles, such as CNT and GNP, when their concentration reaches the percolation threshold [7,8]. Moreover, the introduction of nanoparticles influences also the mechanical and thermal properties. In case of multiphase nanocomposites, it is crucial to define the amount of a specific filler and to understand the role of each one on specific features. In order to reduce the samples and to exploit as much as possible the experimental measurements, specific points in the parameter space have been

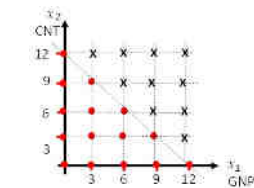


Figure 1. Discretized 5 level parameter space used to define the required experimental samples according to the constraint.

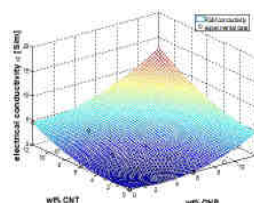


Figure 2. RSM interpolation of σ as a function of fillers percentage (colour-map) together with the experimental data (black circles).

selected, avoiding the classical trial and error experimental analysis. By expressing the material formulation in terms of two parameters, i.e. the GNP wt% concentration, x_1 , and the CNT wt% concentration, x_2 , the array of the input parameters to use in the analysis is $\mathbf{x} = (x_1, x_2) \in \mathbb{R}^2$. The values considered for both parameters are chosen by uniformly discretizing the interval $x_1, x_2 \in [0, 12]$, defined according to possible percolation threshold, with the constraint on the total wt% concentration of $0 \leq x_1 + x_2 \leq 12$ addressed for rheological constraint. The last constraint reduces the region of variation of the parameter space, the x_1 - x_2 plane, to the triangle described by the red dots in Figure 1, sampled with 15 sets in the 5-level full-factorial design.

The experimental analyses are then performed on these selected configurations. The same points are used to derive an interpolation of the experimental data, with Response Surface Methodology (RSM), and exploited in the optimization procedure. For example, if the main goal is the maximization of the electrical conductivity σ , the optimization algorithm is applied to the RSM interpolation of the measured DC conductivity $f_1(x_1, x_2)$, suggesting the solution $x_1=0$ and $x_2=12$.

3. Acknowledgement.

The H2020-MSCA-RISE-734164-Graphene 3D project is acknowledged for the funding of the research.

4. References

- [1] G. Spinelli, P. Lamberti, V. Tucci, et al. *Morphological, Rheological and Electromagnetic Properties of Nanocarbon/Poly(lactic) Acid for 3D Printing: Solution Blending vs. Melt Mixing*, *Materials*, **11**, 2256 (2018).
- [2] P. Lamberti, G. Spinelli, P. Kuzhir, et al. *Evaluation of Thermal and Electrical Conductivity of Carbon-based PLA Nanocomposites for 3D Printing*, *AIP Conference Proceedings*, **1981**, 020158 (2018).
- [3] G. Spinelli, P. Lamberti, V. Tucci, et al. *Nanocarbon/Poly(Lactic) Acid for 3D Printing: Effect of Fillers Content on Electromagnetic and Thermal Properties*, *Materials*, **12**, 2369 (2019).
- [4] G. Spinelli, P. Lamberti, V. Tucci, et al. *Experimental and theoretical study on piezoresistive properties of a structural resin reinforced with carbon nanotubes for strain sensing and damage monitoring*, *Composites Part B: Engineering*, **145**, 90-99 (2018).
- [5] D. Bychanok, G. Gorokhov, A. Plyushch, et al. *Terahertz Optics of Materials with Spatially Harmonically Distributed Refractive Index*, *Materials*, **13**(22), 5208 (2020).
- [6] A.V. Kukhta, A.G. Paddubskaya, T. Kulahava, et al. *Conductive Luminescent Material Based on Polymer-Functionalized Graphene Composite*, *Phys. Status Solidi A*, 2100492 (2022).
- [7] A. Plyushch, P. Lamberti, G. Spinelli, et al. *Numerical Simulation of the Percolation Threshold in Non-Overlapping Ellipsoid Composites: Toward Bottom-Up Approach for Carbon Based Electromagnetic Components Realization*, *Appl. Sci.*, **8**, 882 (2018).
- [8] A. Plyushch, D. Lyakhov, M. Simenas, et al. *Percolation and Transport Properties in The Mechanically Deformed Composites Filled with Carbon Nanotubes*, *Applied Sciences*, **10**(4), 1315 (2020).

Influence of annealing-induced phase separation on the shape memory effect of graphene-based thermoplastic polyurethane nanocomposites

Fernanda Cabrera Flores Valim^{a,d}; Gustavo Peixoto Oliveira^a; Gibran da Cunha Vasconcelos^b; Leice Gonçalves Amurin^c; Lucilene Betega de Paiva^d; Chiara Santillo^e, Marino Lavorgna^e, Ricardo Jorge Espanhol Andrade^a

^aMackgraphe - Mackenzie Institute for Research in Graphene and Nanotechnologies, Mackenzie Presbyterian Institute, São Paulo, Brazil

^bInstitute for Technological Research (IPT) – Lightweight Structures Laboratory (LEL), São Paulo, Brazil

^cCenter of Technology in Nanomaterials (CTNano) at Federal University of Minas Gerais (UFMG), Belo Horizonte, Minas Gerais, Brazil

^dInstitute for Technological Research (IPT) – Laboratory of Chemical Processes and Particle Technology, Group for Bionanomanufacturing (BIONANO), São Paulo, Brazil

^eInstitute of Polymers, Composites and Biomaterials (IPCB-CNR), Portici (NA), Italy

ricardo.andrade@mackenzie.br

Shape memory polymers (SMPs) is an emerging class of smart materials, which are of special interest due to their ability to return to their original shape after being subjected to an external stimulus, such as mechanical stress, electric or magnetic fields, temperature, among others [1]. Among the shape memory polymers, thermoplastic polyurethane (TPU) stands out for its easy processability and versatility, which raises its range of final shapes and applications, including membranes, medical implants, smart stents and artificial muscles [2].

TPU is a multiblock copolymer and its morphology is composed by rigid and elastomeric immiscible segments highly dependent on thermodynamic parameters, leading to a phase separation and forming domains[3]. The elastomeric segment (soft domain) is associated with a polyol or a long chain diol, while the hard domain refers to the intercalation of a diisocyanate and a chain extender. However, the low stiffness, tensile strength, thermal and electrical conductivity are still some of TPU limitations. In addition, the use of temperature as the main type of stimulus for the returning into the original shape narrows its application. In this scenario, the incorporation of nanomaterials is widely explored in the literature in order to obtain composites with superior final properties.

In this study, 0.1 wt.% of graphene nanoplatelets (GNP) and multilayers graphene oxide (mGO) are incorporated into TPU by polymer solution casting, and a contribution on the phase separation of these domains is observed. This phenomenon is even more pronounced when these graphene-based nanocomposites are submitted to annealing at 110 °C for 24 hours, suggesting a good interaction between the fillers with both soft and hard domains. To elucidate the relationship between the hard and soft phase separation and the shape memory properties, the samples were characterized within a rheometer, by selecting well defined thermal cycles. As consequence, after annealing, both nanocomposites (TPU+GNP and TPU+mGO) presented better performance in SME regarding the increase on shape recovery ratio (Rrec) in more than 3%. All nanocomposites maintained a high strain during SME programming, even higher than that presented by pure TPU, before and after annealing, indicating a direct influence of the graphene-based nanostructures on the shape memory effect.

Acknowledgment

The authors would like to acknowledge the Coordenação de Aperfeiçoamento de Pessoal de Nível Superior (CAPES) for the grants PROSUC - 88887.154374/2017-00, and PRINT 88887.310339/2018-00. The authors also acknowledge the Fundação de Amparo à Pesquisa do Estado de São Paulo (FAPESP) through grants 2012/50259-8, 2018/08035-1, and 2018/10910-8, as well as the Mackenzie Research Fund (MackPesquisa, Project nr. 181009) and the Institute for Technological Research Foundation (FIPT) for the New Talents Program grant. The work was also partially supported by European Commission, within the framework of the H2020-MSCA-RISE-2016-734164 Graphene 3D project. The authors also thank Delmac do Brasil for supplying the polymer.

References

- [1] N. Meinzer, *Nat. Rev. Mater.*, **2**, 2017, (2017)
- [2] F. Pilate, A. Toncheva, P. Dubois and J. Raquez, *Eur. Polym. J.*, **80**, 268–294, (2016)
- [3] F. C. F. Valim, G. P. Oliveira, G. da Cunha Vasconcelos, L. B. de Paiva, C. Santillo, M. Lavorgna and R. J. E. Andrade, *J. Appl. Polym. Sci.*, **139**, 1–13, (2022)

Influence of the type and combination of carbon nanofillers on the nanomechanical properties of PLA-based nanocomposites

Evgeni Ivanov^{1,2*}, Todor Batakliov^{1,2}, Rumiana Kotsilkova¹

¹ Open Laboratory on Experimental Micro and Nano Mechanics (OLEM), Institute of Mechanics, Bulgarian Academy of Sciences, Acad. G. Bonchev Str. Block 4, 1113 Sofia

² Research and Development of Nanomaterials and Nanotechnologies (NanoTech Lab Ltd.), Acad. G. Bonchev Str. Block 4, 1113 Sofia, Bulgaria

The polymer used in this study for the compounding formulation was Ingeo™ Biopolymer PLA-3D850 (Nature Works, Minnetonka, MN, USA). Four types of carbon nanofiller were chosen to manufacture the nanocomposites: (1) industrial graphene TNIGNP (Times Nano, Chengdu, China); (2) industrial MWCNTs – TNIMH4 (Times Nano, Chengdu, China); (3) graphene – TNGNP (Times Nano, Chengdu, China); and (4) MWCNTs – N7000 (NC7000™ series, Nanocyl® SA, Sambreville, Belgium). The four types of nanofillers, with different size, shape, aspect ratio and specific surface area, were used in order to estimate the influence of their characteristics on the nanomechanical properties of the obtained mono-filler (PLA/MWCNT and PLA/GNP) and bi-filler (PLA/MWCNT/GNP) nanocomposites up to 6 wt%. The mono and bi-filler nanocomposites were processed, using the melt extrusion method through preparation of masterbatches and further dilutions. In order to prepare films, pellets were dried, followed by hot pressing. The obtained samples were with around 150 microns of thickness. Nanoindentation and nanoscratch tests were performed on Hysitron TI 980 instrument (Bruker, MN, USA). The nanoindentation measurements were done to minimum five selected areas of each composite film, with size of each indented area of 70 μm x 70 μm , grid of 7 \times 7 indents and spacing of 10 μm . The maximum force of 1500 μN and spacing were carefully selected so that individual indents did not affect each other. The results show that the sample filled with 6 wt% of MWCNTs have a maximum improvement for the hardness and Young's modulus, in comparison with the PLA. The samples with hybrid combination of both nanofillers MWCNTs and GNP (1:3, 1:1 and 3:1), also show improvement, but no synergistic effect is observed. Coefficient of friction at scratch (COF) is calculated from the ratio of the exerted lateral force during material plowing to the constant normal force set in load function and it could measure the surface resistance of a composite against scratch. Figure 1 presents 3D SPM topography image of nanoscratch test trace, made on the surface of 3 wt.% MWCNT/3 wt.% GNP/PLA composite sample. The maximum improvement is reached for the COF at scratch for two bi-filler composite films containing 1.5 wt.% MWCNT/4.5 wt.% GNP/PLA and 4.5 wt.% MWCNT/1.5 wt.% GNP/PLA. Synergy effect with combining GNPs and MWCNTs is found pointing out higher scratch resistance of the bi-filler composites compared to mono-filler composites, with same carbon loading.

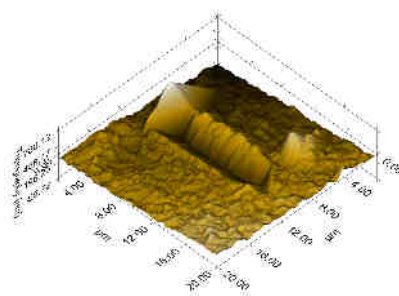


Figure 1. 3D SPM topography image of nanoscratch test trace, made on the surface of 3 wt.% MWCNT/3 wt.% GNP/PLA composite sample

Acknowledgement

This study has been accomplished with the financial support by the European Union's Horizon 2020-MSCA-RISE-734164 Graphene 3D Project. This work was also financed by the Grant No BG05M2OP001- 1.002-0011, financed by the Science and Education for Smart Growth Operational Program (2014-2020) and co-financed by the European Union through the European structural and Investment funds.

Fragmented graphene on dielectric substrate for THz applications

Hamza Rehman¹, Lena Golubewa², Alexey Basharin¹, Andzej Urbanovic²,
Erkki Lahderanta³, Ekaterina Soboleva³, Ieva Matulaitiene², Marija Jankunec⁴, Yuri Svirko¹, Polina Kuzhir¹

¹Institute of Photonics, University of Eastern Finland, Yliopistokatu 2, FI-80100 Joensuu, Finland,

²Center for Physical Sciences and Technology, Saulėtekio av. 3, LT-10257 Vilnius, Lithuania

³Lappeenranta-Lahti University of Technology LUT, Yliopistonkatu 34, 53850, Lappeenranta, Finland

⁴Institute of Biochemistry, Life Sciences Center, Vilnius University, Saulėtekio al. 7, LT-10257, Vilnius, Lithuania
hamza.rehman@uef.fi

Fragmented multi-layered graphene films were directly synthesized via chemical vapor deposition (CVD) on dielectric substrates with pre-deposited copper catalyst. We demonstrated that the thickness of the sacrificial copper film, process temperature and growth time essentially influence the integrity, quality, and disorder of the synthesized graphene.

Atomic Force and Kelvin Probe Force Microscopy measurements revealed the presence of nano-agglomerates and charge puddles. The potential gradients measured over the sample surface confirmed that the deposited graphene film possesses a multilayered structure, which was modelled as an ensemble of randomly oriented conductive prolate ellipsoids (see Fig.1). THz time domain spectroscopy measurements gave ac conductivity of graphene flakes and homogenized graphitic films of around 1200 S/cm and 1000 S/cm (see Fig.2), respectively. Our approach offers a scalable fabrication of the graphene structures composed of graphene flakes and having effective conductivity sufficient for a wide variety of THz applications[1,2].

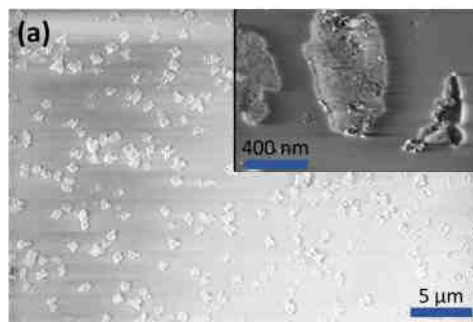


Fig. 1. Top view SEM image of CVD Graphene islands on dielectric.

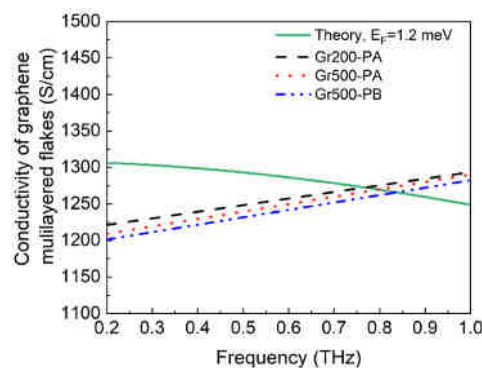


Fig. 2. Calculated conductivity of the graphene flakes and theoretical conductivity obtained by Kubo formulas at chemical potential 1.2 meV.

Acknowledgement

This work was financially supported by H2020 RISE 734164 Graphene 3D.

References

- [1] J. Leng *et al.*, "Investigation of terahertz high Q-factor of all-dielectric metamaterials," *Opt. Laser Technol.*, vol. 146, no. October 2021, p. 107570, 2022, doi: 10.1016/j.optlastec.2021.107570.
- [2] X. He, F. Lin, F. Liu, and W. Shi, "Tunable terahertz Dirac-semimetal hybrid plasmonic waveguides," *Opt. Mater. Express*, vol. 12, no. 1, p. 73, 2022, doi: 10.1364/ome.445362.

Electromagnetic Wave Absorber RGO/PDMS Polymer Nanocomposite

Natia Jalagonia^{1,2}, Tinatin Kuchukhidze¹, Nino Darakhvelidze¹, Ekaterine Sanaia¹, Guram Bokuchava¹, Badri Khvitia¹

¹*Ilia Vekua Sukhumi Institute of Physics and Technologies, Tbilisi, Georgia*

²*Institute of Macromolecular Chemistry and Polymeric Materials, Ivane Javakhishvili Tbilisi State University, University street. 13, Tbilisi 0186, Georgia*

*Corresponding author's e-mail: nati.jalagonia@gmail.com

Recently, electromagnetic interference (EMI) has become a critical problem for electric devices, medical systems, high quality information and safety technologies, etc. EMI can degrade the performance of a system or an equipment and in order to solve this problem the development of EMI shielding materials received increasing attention. Due to the wide impact of telecommunications, several economically heavy industrial sectors are likewise eager on the progress of EMI shielding materials. These technological fields demand not only efficient shields, but also properties of materials. For example, chemical and corrosion resistance, lightweight, flexibility, tunable morphology, processing easiness, and inexpensiveness are requirements that materials must fulfill in order to be applicable in flexible electronics or in aerospace and automotive industries [1-2].

Graphite, carbon black and carbon fibers were the first to combine with polymers for the fabrication of EMI shields. After discovery of the unique properties of graphene, new possibilities for research and development of polymer nanocomposites have been opened up. The sphere of application of the innovative polymer nanocomposites produced by using other graphene and carbon nanostructures is enormous, since such nanocomposites can be characterized by extraordinary multifunctional properties [3], which further increases the number of products applied in innovative technologies. Based on the composition and processing complexity, a serious question for mass production of such nanocomposites is how control over the structure, dispersion degree, and morphology will be exercised, so that a material with best properties is produced. In our research, we have synthesized reduced graphene oxide (with good mechanical and electrical properties) for well distribution into matrix.

Polymer nanocomposites obtained by mixing the calculated amounts of Polydimethylsiloxane (PDMS) and reduced graphene oxide (RGO) (Figure 1). The mixture evaporated and dried. Then obtained solid composites used for further research.

As studies show, RGO/Polymer composite absorb energy particularly efficiently in the range of 0.5-6 GHz (Figure 1) which includes: TV broadcasting, GSM, WIFI, 3G, 4G, and 5G irradiation ranges. It is advisable to continue studies to increase the absorption coefficient in the relatively low-frequency range (50 MHz-1 GHz).

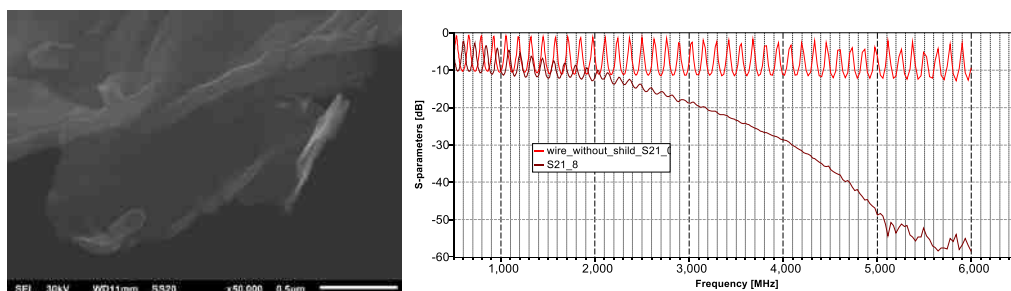


Fig. 1. Micrographs of reduced graphene oxide

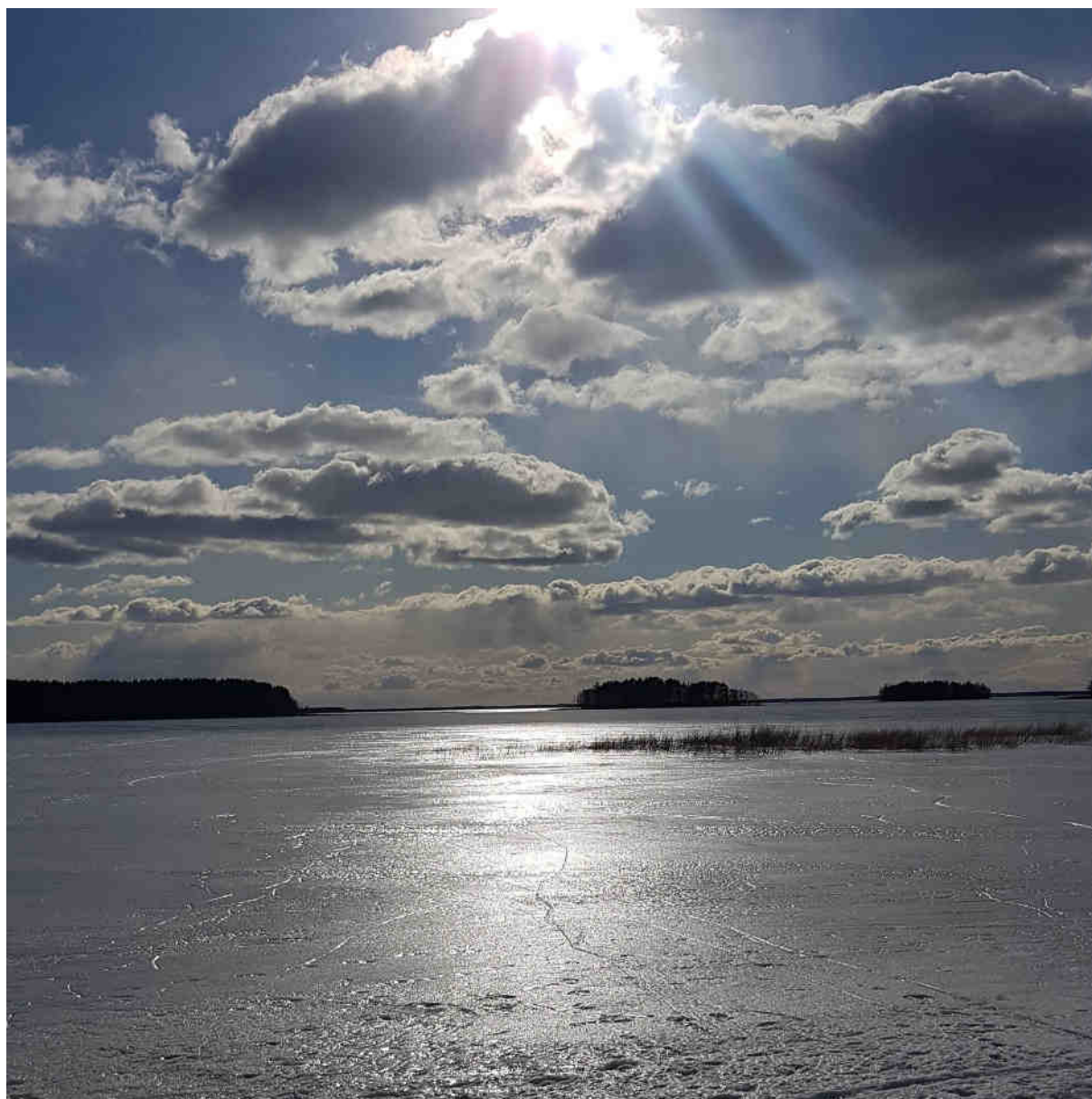
Acknowledgement.

The financial support of the H2020 MCA RISE project "Graphene-3D", Grant No. 734164, is gratefully acknowledged.

References

1. Jian, B. Wu, Y. Wei, S. X. Dou, X. Wang, W. He and N. Mahmood, *ACS Appl. Mater. Interfaces*, 2016, **8**, 6101–6109;
2. 2.A. Gupta and R. K. Jha, „A survey of 5G network: Architecture and emerging technologies“, *IEEE Access*, vol. 3, pp. 1206, 1232, 2015;
3. Dhand V., Rhee K.Y., Kim H.J., Jung D.H. A Comprehensive Review of Graphene Nanocomposites: Research Status and Trends. *J of Nanomaterials* (2013) (763953):14;

Graphene 3D project Symposium Poster Session



Graphene electro-optic modulators on silicon nitride waveguides

I. Reduto¹, M. Roussey¹, P. Mustonen², Z. Sun², H. Lipsanen², and S. Honkanen¹

¹ Institute of Photonics, University of Eastern Finland, FI-80101 Joensuu, Finland

² Department of Electronics and Nanoengineering, Aalto University, FI-00076 Aalto, Finland

Corresponding author e-mail igor.reduto@uef.fi

1. Abstract

Graphene is an attractive material for optoelectronics due to its broadband absorption and high carrier mobility [1]. With only an atomic layer of material, graphene offers the possibility for extremely fast and broadband electro-optical devices. Two graphene layers separated with a few nanometers-thin dielectric layer create a capacitor, which has been successfully demonstrated for signal modulation of tens of Gb/s [2]. For doped Si-waveguides, it is enough to have one graphene layer since the waveguide can act as a second capacitor plate [3]. Spectral filtering on Si can be obtained by a Bragg grating located along the waveguide [4]. Another spectral filtering approach is based on arrayed waveguide grating [5]. They are of special interest due to their flexibility in parameter choices and the possibility of fabrication with the same step as the waveguide, and no additional space is required on the chip. The interest in silicon nitride as an optical material has increased recently. Especially, Si_3N_4 waveguides feature broadband transparency and low losses compared to conventionally used Si waveguides. This allows silicon nitride to be used in nonlinear and quantum systems. However, the process of graphene transfer or growth on top of silicon nitride can still be improved. This work is devoted to research on nanostructured silicon nitride waveguides (Fig. 1) combined with graphene for electro-optical modulation.

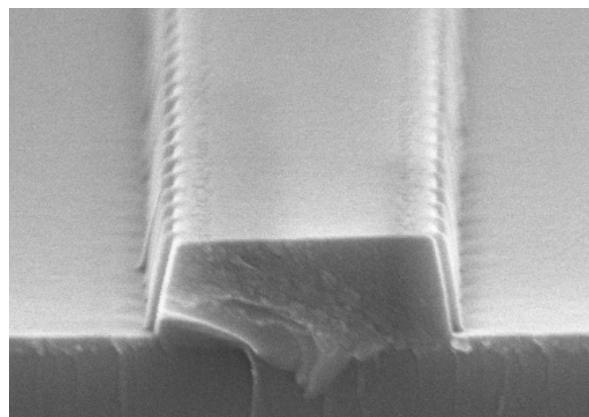


Fig. 1. Cross section SEM image of the nanostructured Si_3N_4 waveguide.

2. Acknowledgement.

Authors acknowledge the support from Business Finland grant #28416, Academy of Finland Flagship PREIN #320166, and MSCA RISE H2020-MSCA-RISE-2016 Project Graphene 3D (Grant Number: 734164).

3. References

- [1] F. Bonaccorso, Z. Sun, T. Hasan & A. C. Ferrari, *Nature Photonics*, **4**, 611-622 (2010).
- [2] V. Sorianello, G. Contestabile, and M. Romagnoli, *Journal of Lightwave Technology*, **38**, 10 (2020).
- [3] Yingtao Hu, Marianna Pantouvaki, Joris Van Campenhout, Steven Brems, Inge Asselberghs, Cedric Huyghebaert, Philippe Absil, and Dries Van Thourhout, *Laser Photonics Reviews*, **10**, 2, 307–316 (2016).
- [4] D. T. H. Tan, K. Ikeda, and Y. Fainman, *Optics Letters*, **34**, 9, 1357-1359 (2009).
- [5] P. Dumon, W. Bogaerts, D. Van. Thourhout, D. Taillart, R. Baets, J. Wouters, S. Beckx, and P. Jaenen, *Optics Express*, **14**, 2, 664–669 (2006).

Electrical properties of composites of poly (lactic) acid and polyvinylidene difluoride with carbon fillers

Dzhihan Menseidov

Institute of Mechanics at the Bulgarian Academy of Sciences, Sofia, Bulgaria
menseidov@gmail.com

1. Introduction

In this study, we consider polymer composites based on two different matrices with the same fillers in terms of electrical conductivity. The study does not aim at a comparison between the two polymers, the focus is on the effect of the fillers on different polymer matrices. Unconventional polymer nanocomposites based on PLA and PVDF, made of multi-walled carbon nanotubes (MWCNT), graphene nanoplates (GNP), and a combination of the two fillers (MWCNTs / GNPs) have been developed.

The method chosen to obtain the nanocomposites is by melt extrusion. Monofill nanocomposites (GNP / polymer and MWCNT / polymer) with 6% by weight of filler content as basic mixtures are produced. Composites with bi-fillers with a total filler content of 6% by weight are prepared by mixing the two fatty mixtures with a mono-filler in a suitable ratio. The resulting composites were extruded on a Thermo Scientific Process 11 Parallel Twin-Screw Extruder. The radar temperatures in the extrusion of composites with PLA matrix were in the range of 170–180 °C, and in the extrusion of PVDF in the range of 160–170 °C.

2. Results and Discussion

Figure 1 shows the DC electrical conductivity for PLA and PVDF fibers reinforced with various combinations of thread-shaped carbon fillers used. It should be noted the more pronounced influence of MWCNT in increasing electrical conductivity.[1] The difference in the conductivity of pure polymers and composite materials is several orders of magnitude higher. This can be explained by obtaining functioning electrically conductive paths between the individual nanoparticles, thus changing the insulator to a conductor, making the passage of electrons.[2] From the graphs we notice that the two groups are differently influenced by the fillers. While in the group with the PVDF matrix we report better conductivity in monofillers, in the case of PLA-based composites the bi-fillers clearly achieve better conductivity.[3]

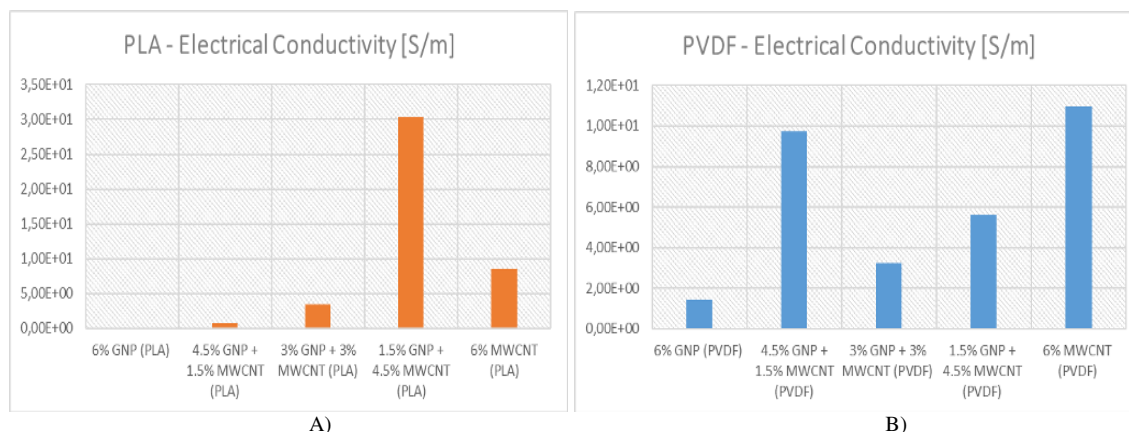


Fig. 1 Presented in DC the conductivity of shaped fibers at 6% by weight concentration of the filler with PLA and PVDF matrices.

3. Acknowledgement.

H2020-MSCA-RISE-734164-Graphene 3D project

4. References

- [1] Spinelli, G.; Kotsilkova, R.; Ivanov, E.; Georgiev, V.; Ivanova, R.; Naddeo, C.; Romano, V. Dielectric Spectroscopy and Thermal Properties of Poly(lactic) Acid Reinforced with Carbon-Based Particles: Experimental Study and Design Theory. *Polymers*(2020)
- [2] Spinelli, G.; Lamberti, P.; Tucci, V.; Kotsilkova, R.; Ivanov, E.; Menseidov, D.; Naddeo, C.; Romano, V.; Guadagno, L.; Adami, R.; Meisak, D.; Bychanok, D.; Kuzhir, P. Nanocarbon/Poly(Lactic) Acid for 3D Printing: Effect of Fillers Content on Electromagnetic and Thermal Properties. *Materials* (2019)
- [3] Gonçalves, J.; Lima, P.; Krause, B.; Pötschke, P.; Lafont, U.; Gomes, J.R.; Abreu, C.S.; Paiva, M.C.; Covas, J.A. Electrically conductive polyetheretherketone nanocomposite filaments: From production to fused deposition modeling, *Polymers* (2018)

Back to the future with nanocarbon composite polymers

Paolo Ciambelli^{1,2}, Giuseppe De Filippis¹, Antonio Di Grazia¹

¹Narrando, via Giovanni Paolo II, 132, 84084 Fisciano, Italia

²University of Salerno, via Giovanni Paolo II, 132, 84084 Fisciano, Italia

1. Introduction

Polymer nanocomposites are produced by using nanomaterials, mostly nanoclays, carbon nanotubes, nanofibers, nano-oxides, and polymers, mostly epoxy resin, polyamide, light polyolefin. The relevant market size was valued at around USD 8.66 billion in 2021 and will exhibit a growth rate of over 19.1% CAGR from 2022 to 2028 [1]. Main driving forces are still the packaging and automotive industrial sectors.

Inside this big market, a growing interest is addressed towards graphene as alternative to carbon nanotubes, towards biodegradable polymers, and to provide specific properties for more sophisticated application. In parallel, with respect to technological advances, the 3D printability of these composites is a major objective. The above systems are the object of the Horizon RISE project Graphene 3D [2]. Moving from the imminent conclusion of this project, we will try to bring some considerations up for discussion on the world of nanocarbon filled polymer composites.

2. Nanocarbon polymer composites

Even if limited to this class of composites, the academic literature is overflowing in terms of papers dealing with this subject. Really, if changing a single filler or coupling two of them, or changing the polymer matrix, or the manufacturing technique allow to write a new publication, it's not surprising.

However, it seems to us that, despite this huge amount of papers, less attention is devoted to profit from the specificity of nanocarbon fillers, i.e. the fact that, differently from chemical substances, you can change their size and shape and look for the effect of this change on the properties of the manufactured composite. We still need systematic studies comparing, for instance, the effect of aspect ratio or purity of the nanocarbon filling the polymer. It has been demonstrated that the aspect ratio of graphene strongly affects mechanical properties [3].

Moreover, playing with carbon nanotubes you can change length, diameter, thickness to find the best geometric parameters providing the best features for each application.

2. Future outlook

The world of nanocarbons is really unlimited. Carbide Derived Carbon allows a hierarchial control of porosity, the preparation of tridimensional carbon aerogel is very versatile, microporous template nanocarbons [4] show extremely high surface area. On the other hand, cheaper nanocarbon (carbon black, active carbon graphite, char) could substitute expensive high aspect ratio carbon nanotubes and graphene platelets, by controlling the morphology and excluded volume of the polymer network, instead of the morphology of the filler. The potentiality of fullerene was perhaps underestimated. We should come back to reconsider these potential nanofillers.

Bio-char, a low cost carbon based material obtained by pyrolysis of different cellulosic matrices could substitute much expensive carbon nanofillers to improve mechanical and electrical properties [5], but also reducing the relevant negative waste impact. Moreover, carbon nanotubes and graphene may be integrated into natural-fibre-reinforced polymer composites and wood-plastic composites [6].

4. Conclusion

Examples of future challenges for nanocarbon polymer composites will be collected and discussed in the poster which this abstract is relevant to. Future challenges will be also the footprint of a Joint lab on nanocarbon filled composite materials to be established by the Consortium Graphene 3D as a fallout of the mentioned project [2].

5. Acknowledgement.

Narrando acknowledges the H2020-MSCA-RISE-734164-Graphene 3D project for financial support.

6. References

- [1] Global Polymer Nanocomposite Market, GMI3892 Report (Global Market Insights, 2022) <https://www.gminsights.com>
- [2] Graphene 3D RISE project, <http://graphene3d.imbm.bas.bg>
- [3] P. May, U. Khan, A. O'Neill, J.N. Coleman, J. Materials Chemistry, **22**, 1278 (2012).
- [4] P. Ciambelli, D. Sannino, M. Sarno, A. Fonseca, J.B. Nagy, Carbon **43**, 631 (2005)
- [5] M. Bartoli, M. Giorcelli, C. Rosso, M. Rovere, P. Jagdale and A. Tagliaferro, Applied Sciences, **9**, 3109 (2019).
- [6] D. Łukawski, P. Hochmanska-Kaniewska, D. Janiszewska, G. Wróblewski, J. Patmore and A. Lekawa-Raus, Polymers, **14**, 745 (2022).

Effect of carbon nanofillers on the permeability, conductive and nanomechanical properties of PLA-based composites films

C. Santillo¹, G.G. Buonocore¹, R. Di Maio¹, M. Lavorgna¹, E. Ivanov^{2,3}, T. Batakaliyev², R. Kotsilkova²

¹National Research Council of Italy, Institute for Polymers, Composites and Biomaterials, P.le E. Fermi 1, Portici, Naples 80155, Italy

²Open Laboratory on Experimental Micro and Nano Mechanics (OLEM), Institute of Mechanics, Bulgarian Academy of Sciences, Acad. G. Bonchev Str. Block 4, 1113 Sofia, Bulgaria

³Research and Development of Nanomaterials and Nanotechnologies (NanoTech Lab Ltd.), Acad. G. Bonchev Str. Block 4, 1113 Sofia, Bulgaria

Corresponding author Rosa Di Maio: rosa.dimaio@ipcb.cnr.it

Poly(lactic acid) (PLA) is one of the most widely used polymers during the last years which finds versatile applications in packaging, pharmaceutical, textiles, engineering, chemical industries, automotive composites, biomedical and tissue engineering fields. However, the low mechanical properties limit the number of its applications. In this context, carbon-based nanomaterials, offer the potential to combine PLA properties with several of their unique features, such as high mechanical strength, electrical conductivity, thermal stability and bioactivity and a significant research has dealt with the use of fillers for improving the properties of PLA [1-3]. In the present work, two- and three-component PLA-based nanocomposites with carbon nanotubes and graphene have been developed by the method of melting carbon fillers into the polymer matrix suitable for FDM 3D printing. In particular, the effect of nanoparticles, such as two different types of carbon nanotubes, graphene and their combination, on nanomechanical, permeability and conductive properties of PLA nanocomposites prepared by the melt blending method was investigated. Results show a remarkable improvement in the thermal conductivity of graphene-based composite. RX analysis show that in presence of GNPs and at low concentration of MWCNTs an increase of the size of the bundles (d1) is observed. Moreover, q2 and d2 values suggest an increase of the distance between MWCNTs in the PLA matrix, as decreasing the content of MWCNTs and increasing the content of GNPs. Water permeability tests of the developed films show a good improvement in water barrier properties, mainly due to the effect of GNPs which reduce the diffusion of water molecules through the polymer matrix. Results of conductivity tests suggest that a combination of conductive carbon fillers (MWCNT and GNP) in an equal weight ratio leads to the formation of a more effective percolation path: a conductive network can be formed thanks to the flexible MWCNTs rods that are bridged between the planar GNP nanoplatelets

Nano-indentation tests performed with a new rapid type of nanoindentation show that a synergistic effect was found on the combination of graphene with carbon nanotubes on the mechanical properties of nanocomposites based on PLA. This mechanical reinforcement of the nanocomposites is probably related to the specific structure and geometry of the particles of the hybrid fillers, the interactions between the fillers, the effect of the concentration of carbon nanoparticles and the processing method.

Acknowledgement.

Authors acknowledge the support from MSCA RISE H2020-MSCA-RISE-2016 Project Graphene 3D (Grant Number: 734164), H2020-SGS-FET-Graphene Flagship-881603 Graphene Core 3, Bilateral collaboration between BAS-CNR (2019-2021) and Project MIRACle № BG05M2OP001-1.002-0011.

References

- [1] Ivanov, E.; Kotsilkova, R.; Xia, H.; Chen, Y.; Donato, R.K.; Donato, K.; Godoy, A.P.; Di Maio, R.; Silvestre, C.; Cimmino, S.; Angelov, V.. *Appl. Sci.*, 9, 1209 (2019).
- [2] Kotsilkova, R.; Ivanov, E.; Georgiev, V.; Ivanova, R.; Menseidov, D.; Batakaliyev, T.; Angelov, V.; Xia, H.; Chen, Y.; Bychanok, D.; Kuzhir, P.; Di Maio, R.; Silvestre, C.; Cimmino, S.. *Polymers*, 12, 1208 (2020).
- [3] Spinelli, G.; Kotsilkova, R.; Ivanov, E.; Georgiev, V.; Ivanova, R.; Naddeo, C.; Romano, V. *Polymers*, 12, 2414. (2020).

Multifunctional porous conductive TPU/carbon-based system 3D printed for piezoresistive sensors

G. Rollo^{1,2}, R. Di Maio¹, A. T. Silvestri^{1,3}, A. Ronca^{1,2}, H. Xia^{4,1}, M. Lavgorgna^{1,2}

¹National Research Council of Italy, Institute for Polymers, Composites and Biomaterials, P.le E. Fermi 1, Portici, Naples 80155, Italy

²National Research Council of Italy, Institute for Polymers, Composites and Biomaterials, Via Previati 1, Lecco, Italy

³University of Naples Federico II, DICMAPI, Naples, Italy

⁴State Key Laboratory of Polymer Materials Engineering, Polymer Research Institute, Sichuan University, Chengdu, 610065, China

Corresponding author Alessia Teresa Silvestri: alessiateresa.silvestri@unina.it

During the last forty years, which increased significantly with the advent of nanostructured carbon-based conductive materials, light, highly conductive and easy-to-obtain fillers have broadened the spectrum of materials that had been used up to that time, opening up the possibility of greater development of multifunctional materials. In particular, the carbonaceous fillers, homogeneously dispersed within a polymer matrix, immediately represented a valid alternative to the metals used in the field of piezoresistive systems. A significant challenge for the scientific community is represented by the achievement of an effective percolation pathway, which allows the passage of an electric current at the lowest percentage of filler (percolation threshold). Generally, a conductive composite can be obtained by exploiting the concept of segregation of filler in the polymeric matrix.

Selective Laser Sintering (SLS) 3D printing is one of the most interesting technology, able to build up easily the segregated filler network, starting from polymeric powder adequately prepared. It is focused on the sintering of polymeric particles by a laser in the classic layer-by-layer mode. In this work it was investigated the possibility of obtaining piezoresistive materials printed with 3D SLS using thermoplastic polyurethane (TPU) as a polymer matrix and graphene nanoparticles (GE) and multiwalled carbon nanotubes (MWCNTs) as conductive filler, evaluating the effect of different geometries and porosities (from 20% to 80%) and different shape of the conductive filler (i.e. 1D filler and 2D filler). Porous systems were printed using TPU modified with 1wt% of GE and starting from Diamond (D), Gyroid (G) and Schwarz (S) geometries for the building up of systems with regular porosity.

3D printed TPU products with MWCNTs and a mixture of the two fillers, again at 1wt% but with a proportion of 70/30 wt/wt MWCNTs/GE with geometries D and G, in order to investigate a possible synergistic effect of the two conductive fillers. The results showed that the porous structures based on TPU with 1wt% MWCNTs/GE exhibit excellent electrical conductivity and mechanical strength. In particular, all the porous structures show a robust negative piezoresistive behavior, with a GF values of about -13 at 8% deformation. Moreover, the G20 porous structures (20% porosity) show microwave absorption coefficients ranging from 0.70 to 0.91 in the 12-18 GHz region and close 1 in the THz (300 GHz - 1 THz) frequency region. The results show that the simultaneous presence of MWCNT and GE brings about a significant improvement in the multifunctional properties of porous structures, which are piezoresistive actuators for potential application in the field of prosthetic devices.

Acknowledgement.

Authors acknowledge the support from MSCA RISE H2020-MSCA-RISE-2016 Project Graphene 3D (Grant Number: 734164) and from the National Key R&D Program of China (2017YFE01115000)

References

- [1] Rollo G., Ronca A., Cerruti P., Gan X.P., Fei G., Xia H., Gorokhov G., Bychanok D., Kuzhir P., Lavgorgna M., Ambrosio L. *Polymers*, 12, 1841 (2020).
- [3] Ronca A., Rollo G., Cerruti P., Fei G., Gan X., Buonocore G.G., Lavgorgna M., Xia H., Silvestre C., Ambrosio L., *Applied Science*, 9, 864, 2414 (2019).

Production of Reduced Graphene Oxide for potential industrial graphene nanocomposite manufacture

Natia Jalagonia^{1,2}, Tinatin Kuchukhidze¹, Nino Darakhvelidze¹, Ekaterine Sanaia¹, Guram Bokuchava¹, Badri Khvitia¹, Leila Kalatozishvili^{1,2}

¹*Ilia Vekua Sukhumi Institute of Physics and Technologies, Tbilisi, Georgia*

²*Institute of Macromolecular Chemistry and Polymeric Materials, Ivane Javakhishvili Tbilisi State University, University street. 13, Tbilisi 0186, Georgia*

Carbon nanostructures possess the unique properties, such as low density, high conductivity, high chemical, thermal and mechanical stability, because of which an interest towards them is constantly increasing. These materials can be used for producing diverse novel materials with perfect optical, electric, mechanical and magnetic properties.

Graphene has a great attention in the recent research innovations mainly due to its unique properties, which is composed of one-atom thick sheet of hexagonally arrayed sp^2 carbon atoms [1]. The synthesis of perfect graphene is complicated process that is why pure graphene is very expensive. Therefore, graphene is often replaced by graphene oxide or reduced graphene oxide. The work focuses on a method of synthesis of reduced graphene oxide granules, which can use as nanofiller in polymer matrix. It is known that polymer nanocomposites reinforced with graphene nanofillers have better mechanical, thermal and electrical properties than pure polymer materials [2]. According to the aim, some corrugated spherical structures/granules of reduced graphene oxide were produced by a dispersion/drying method. The reduced graphene oxide suspension produced by an improved Hummers's method (figure 1), was mixed on a magnetic stirring and delivered by a peristaltic pump to the granulation zone at a speed 10-20 ml/min. The granulation zone temperature is kept within 40-150°C. The suspension was dispersed by compressed air up to 3 atmospheres. The produced granules were accumulated in a receiver, and for the purpose of final removal of the solvent was additionally dried in the vacuum oven. The engineered reduced Graphene oxide were analyzed and the materials identification and structural-morphological characterized by XRD, TGA, UV, Raman and SEM.



Fig. 1. Illustration of the preparation of GO

Acknowledgement.

The financial support of the H2020 MCA RISE project "Graphene-3D", Grant No. 734164, is gratefully acknowledged.

References

1. Novoselov, K. S. et al. Electric field effect in atomically thin carbon films. *Science* 306, 666–669, 2004;
2. Andrew T. Smith, Anna Marie LaChance, Songshan Zeng, Bin Liu, Luyi Sun. Synthesis, properties, and applications of graphene oxide/reduced graphene oxide and their nanocomposites. *J. Nano materials Science*, 1 (1), 31-47, 2019;

Synthesis of highly amorphous polyvinyl alcohol/reduced graphene oxide nanocomposite with promising electrical percolation threshold

R. Adami^{1*}, P. Lamberti^{2,3}, M. Casa⁴, N. D'Avanzo², M. Sarno^{1,3}, D. Bychanok⁶, P. Kuzhir⁷, C. Yu⁸, H. Xia⁸, P. Ciambelli⁴

¹Department of Physics, University of Salerno.

²Department of Information and Electrical Engineering and Applied Mathematics, University of Salerno.

³Centre NANO_MATES, University of Salerno.

⁴Narrando srl, Via Giovanni Paolo II, 132, 84084 Fisciano (SA), Italy

⁶Research Institute for Nuclear Problems Belarusian State University (Belarus)

⁷Dept. of Physics and Mathematics, University of Eastern Finland (Finland)

⁸State Key Lab of Polymer Material Engineering, Sichuan University, Chengdu, 610065, Sichuan, P.R. China

*radami@unisa.it

1. Introduction

The novel high amorphous polyvinyl alcohol (HAVOH) is water soluble, biodegradable polymer and has good compatibility with most inorganic/organic fillers. It has excellent extrusion processability, ease of use in coating, and oxygen barrier properties and has been patented and commercialized with the trade name G-Polymer. It has been studied in a blend with chemically-modified organoclays [1] and as modified matrix loaded with multiwalled nanotubes [2]. HAVOH/rGO composites can be considered commercially competitive compared to benchmarks in several fields, as electrically conductive composite materials, electromagnetic shielding and additive manufacturing, therefore it is interesting to study G-Polymer/reduced graphene oxide (rGO) nanocomposite obtained by solution blending process of HAVOH and Graphene Oxide (GO) water solutions and a subsequent 'in situ' reduction of GO.

2. Results and discussions

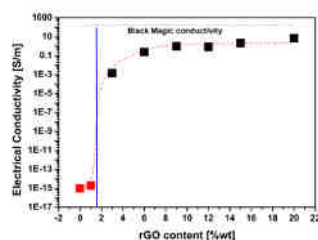


Fig. 1. Percolation curve for HAVOH/rGO nanocomposite

The HAVOH/rGO nanocomposite was prepared by mixing of two water solutions, containing GO and G-Polymer respectively, in order to obtain 20%wt of GO. The solid composites, then, underwent thermal treatment for 'in situ' GO reduction for different times [3]. After the optimization of the reduction time, HAVOH/rGO composites with different concentrations in order to evaluate the electrical conductivity of the materials. The materials obtained were mechanically grinded and hot pressed, then bone-like samples were modeled in order to evaluate mechanical properties of the nanocomposites. The obtained nanocomposite presents low percolation threshold ($\sim 1.7\%$) and high electrical conductivity (~ 1 S/m, Fig. 1) due to the uniform dispersion in the polymer matrix as a result of the solution

blending process and the good reduction level of GO. Already at 9 wt% of rGO the conductivity of the nanocomposite is 1 S/m, 3 order of magnitude higher than the reference value of PVA/rGO system [4] and not far from the conductivity of Black Magic filament, that is a traded system composed by poly lactic acid, graphene and nanotubes. For higher percentages a random value of conductivity is showed, probably for the degradation of samples.

3. Conclusions

In consideration of the processability of G-Polymer, the conductivity obtained by using rGO as filler and the low percolation threshold, the nanocomposite produced is a good candidate for 3D-printing of conductive structure, that can be used for packaging and electromagnetic shielding.

4. Acknowledgement

The H2020-MSCA-RISE-734164-Graphene 3D project is acknowledged for the funding of the research.

5. References

- [1] P. Russo, V. Speranza, A. Vignali, F. Tescione, G. G. Buonocore, and M. Lavorgna, 'Structure and physical properties of high amorphous polyvinyl alcohol/clay composites', AIP Conf. Proc., vol. 1695, no. 1, p. 020035, Dec. 2015.
- [2] C. Santillo, A.P. Godoy, R.K. Donato, R.J. Espanhol Andrade, G.G. Buonocore, H. Xia, M. Lavorgna, A. Sorrentino, 'Tuning the structural and functional properties of HAVOH-based composites via ionic liquid tailoring of MWCNTs distribution' Composites Science and Technology, vol. 207, 2021
- [3] S. Pei and H.-M. Cheng, 'The reduction of graphene oxide', Carbon, vol. 50, no. 9, pp. 3210–3228, Aug. 2012.
- [4] H. J. Salavagione, G. Martínez, and M. A. Gómez, 'Synthesis of poly(vinyl alcohol)/reduced graphite oxide nanocomposites with improved thermal and electrical properties', J. Mater. Chem., vol. 19, no. 28, pp. 5027–5032, Jul. 2009.

Graphene enhanced free-standing silicon anapole-type metasurface

I. Appiah Otoo¹, A. Basharin¹, P. Karvinen¹, D. Pashnev², I. Kasalynas², H. Rehman^{1*}, Y. Svirko¹, and P. Kuzhir¹

¹Institute of Photonics, University of Eastern Finland, Joensuu, Finland

²Terahertz photonics laboratory, Center for Physical Sciences and Technology (FTMC), Vilnius, Lithuania

Corresponding author: isaac.appiah.otoo@uef.fi, *presenting author: hamza.rehman@uef.fi

In recent times, the concept of anapole has gain significant consideration in the area of photonics due to its ability as a non-radiating state of light which is induced by interference of the electric and toroidal dipole moment [1]. These electric and toroidal dipoles have identical energy but oscillate out of phase and cancel each other. Being able to produce/tune a meta-atom lattice of a metasurfaces for it to have a high-Q resonances will potentially increase the improvement of the interactions between light and matter in both microwave and terahertz regions of the meta-atoms for sensing applications [2,3].

We present metamaterial structure comprises of a periodic array of anapole-type metasurface of free-standing membrane of Si and patterned with a doped layer of graphene as a novel sensing principle in the THz range as shown in Fig.1.

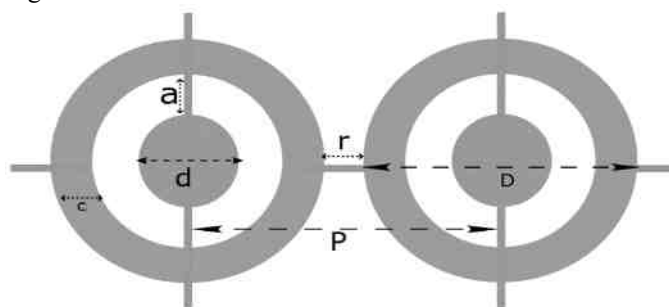


Figure 1: 2D view of metasurface of free-standing Si membrane with dimensions. a is the distance between meta-atom and unit structure, d diameter of the meta-atom, c is the width of big ring, D is diameter of unit cell, p is the period between the unit cell, r is inter-unit cell distance.

The spectral position of anapole modes shaped of a periodic-spherical silicon meta-atom is first investigated without graphene layered and when patterned with highly doped graphene sheet with THz-TDS in both transmission and reflection mode. Our simulations and experimental data reveal that our modeled transmission and reflection spectra of the structure at the normal incident angle up to 1THz structure has very high Q-factor, anapole-type behavior, and resonances of absorption in THz range. Higher resonances were observed at frequencies up to 1 THz range in a normal incidence of THz beam for both with and without graphene. However, there was enhancement when graphene was transferred on the structure.

This shows that our anapole metamaterial spectra do not depend on the angle of the incident reflection measurements and dependence on incidence angle. However, changing the chemical potential of graphene or conductivity of silicon, produces hysteresis of resonant frequency because of hybridization of mode of particles and graphene impedance.

Acknowledgement

This work is supported by the Academy of Finland via Flagship Programme Photonics Research and Innovation (PREIN) decision 320166 and grant 343393, and by the Horizon 2020 RISE 734164 Graphene 3D project.

References

1. E. Takou, A. C. Tasolamprou, O. Tsilipakos, Z. Viskadourakis, M. Kafesaki, G. Kenanakis, and E. N. Economou "Anapole Tolerance to Dissipation Losses in Thermally Tunable Water-Based Metasurfaces" *Physical review applied* 15, 014043-17 2021
2. K. Du, P. Li, Q. Miao, K. Gao, H. Wang, L. Sun, W Zhang, and T. Mei "Optical Characteristics of Metasurfaces at Meta-Atom Anapole" *IEEE Photonics Journal* 13 (3) 2021
3. E. Zanganeh, M. Song, A. Evlyukhin, and P. Kapitanova "Electromagnetic Anapole States of Nano-disks" 5th International Conference on Metamaterials and Nanophotonics METANANO 020138-1–020138-4, 2020

Author index

- Aamir, A. bin, 21
Adami, R., 75
Alexeeva, N., 33, 37, 48
Andrade, R. J. E., 61, 63
- Barnes, W. L., 46
Basharin, A., 44, 65, 78
Bataliev, T., 72
Bataliev, T., 59, 64
Bokuchava, G., 66, 74
Bukin, V. V., 38
Buonocore, G. G., 61, 72
Bychanok, D., 75
- Campion, J., 41
Casa, M., 75
Chizhov, P. A., 38
Ciambelli, P., 71, 75
- Darakhvelidze, N., 66, 74
Donato, R. K., 61
Drozd, P. A., 41
- Eremin, T. V., 39
Eremina, V. A., 34
- Faella, E., 20
Fedorov, G., 40
Fei, G., 61
Ferrari, A., 3
Filippis, G. De, 71
- Ganichev, S., 40
Gayduchenko, D. B. I., 40
Georgiev, V., 59
Gets, D. S., 38
Giubileo, F., 20
Godoy, A. P., 61
Golberg, D. V., 5
Goltsman, G., 40
Golubewa, L., 9, 17, 31, 53, 54, 65
Grazia, A. Di, 71
- Hartmann, R. R., 4, 7
Honkanen, S., 69
Horsley, S. A. R., 46
- Ignatjev, I., 48
Ilday, S., 6, 21
- Ismagilov, R. R., 52
Ivanov, E., 59, 64, 72
- Jalagonia, N., 66, 74
Jankunec, M., 65
Jelezko, F., 51
Jokubauskis, D., 33, 37
Jorudasa, J., 48
- Kafesaki, M., 43
Kalatozishvili, B. K. L., 74
Karpicz, R., 9, 29, 31, 53, 54
Karvinen, P., 78
Kasalynas, I., 78
Kawano, Y., 27, 28, 42
Kazansky, P. G., 22
Khvitia, B., 66
Kinoshita, Y., 27
Konishi, K., 10
Kotsilkov, S., 59
Kotsilkova, R., 59, 64, 72
Krajewska, A., 41
Kuchukhidze, T., 66, 74
Kulahava, T., 9, 31, 53, 54
Kuzhir, P., 9, 30–33, 53, 54, 60, 65, 75, 76
- Lahderanta, E., 65
Lamberti, P., 47, 62, 75
Lavorgna, M., 61, 63, 72, 73
Lazareva, M. D., 52
Levinson, O., 9, 31, 53
Li, K., 27
Li, Kou, 28, 42
Lioubtchenko, D., 41
Lipsanen, H., 69
- Maffucci, A., 55
Maio, R. Di, 72, 73
Makarov, S. V., 38
Makey, G., 6
Malykhin, S. A., 30, 52, 54
Mann, C. -R., 46
Mariani, E., 8, 46
Matulaitiene, I., 65
Matyushkin, Y., 40
Menseidov, D., 59, 70
Moskotin, M., 40
Mura, M. La, 47, 62

- Mustonen, P., 69
- Nasibulin, A., 41
- Nasibulino, A. G., 18
- Niaurab, G., 48
- Norrman, A., 12
- Novitsky, A., 32
- Oberhammer, J., 41
- Obraztsov, A. N., 52, 54
- Obraztsov, P. A., 34, 38, 39
- Obraztsova, E. D., 34, 39
- Ogrin, F. Y., 11
- Ospanova, A., 45
- Otoo, I. A., 32, 78
- Özer, Y., 6
- Paddubskaya, A., 32, 33
- Padrez, Y., 9, 31, 53, 54
- Pashnev, D., 78
- Pashneva, D., 48
- Pekkarinen, M., 32
- Pelella, A., 20
- Portnoi, M. E., 4, 7, 8
- Quarshie, M., 30
- Reduto, I., 69
- Rehman, H., 17, 65, 78
- Rollo, G., 73
- Ronca, A., 61, 73
- Roussey, M., 69
- Sakai, D., 28
- Sanaia, E., 66, 74
- Santillo, C., 61, 72
- Sarno, M., 75
- Saroka, V. A., 7
- Seliuta, D., 33
- Semenova, O. I., 38
- Silvestri, A. T., 73
- Smirnov, S., 41
- Soboleva, E., 65
- Sturges, T., 46
- Sun, Z., 16, 69
- Svintsov, D., 40
- Svirko, Y. P., 32, 34, 54, 65, 76
- Tasolamprou, A. C., 43
- Tomasello, G., 56
- Tucci, V., 47, 62
- Urbanovic, A., 33, 37, 65
- Vahabli, D., 6
- Valkūnas, L. V., 29
- Weick, G., 46
- Wild, A., 8
- Xenidis, N., 41
- Xia, H., 61, 73, 75
- Yamashita, S., 15
- Yasui, S., 28
- Yu, C., 75
- Yumoto, J., 23
- Zousman, B., 31



ISBN: 978-952-61-4586-0